Toward a Detailed Understanding of Base Excision Repair Enzymes: Transition State and Mechanistic Analyses of *N*-Glycoside Hydrolysis and *N*-Glycoside Transfer

Paul J. Berti*,†,‡ and Joe A. B. McCann‡

Department of Chemistry and Department of Biochemistry and Biomedical Sciences, McMaster University, 1280 Main Street West, Hamilton, Ontario L8S 4M1, Canada

Received July 26, 2005

Contents

* To whom correspondence should be addressed. Telephone: (905) 525-9140 ext 23479. Fax: (905) 522-2509. E-mail: berti@mcmaster.ca.
† Department of Chemistry.
‡ Department of Biochemistry and Biomedical Sciences.

10.1021/cr040461t CCC: $59.00
Published on Web 01/26/2006

1. Introduction

This review focuses on the chemistry performed by base excision repair (BER) enzymes, enzymes that remove nucleobases from DNA in the first step of the repair of many types of DNA damage. Monofunctional BER enzymes are DNA glycosylases that hydrolyze *N*-glycosidic bonds to create a common product from disparate types of DNA damage, namely an abasic (AP) site (Scheme 1). This site is

Scheme 1

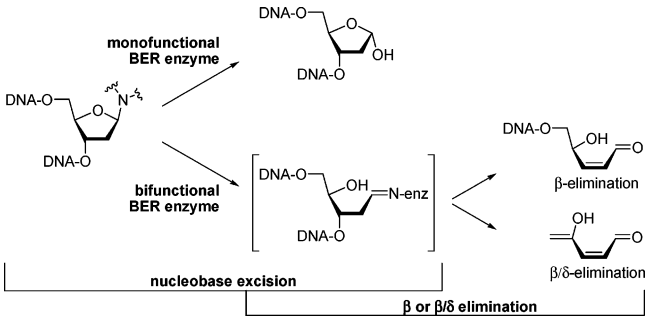

the substrate of an AP endonuclease that cleaves the DNA backbone on the 5′-side of the lesion. Bifunctional BER enzymes have both glycosylase and lyase activities. They remove the damaged nucleobase by glycosyl transfer, using an amine nucleophile from the enzyme (a Lys side chain or Nα of the N-terminal residue). The resulting Schiff base (imine) intermediate then undergoes β-elimination to cleave the DNA backbone on the 3′-side of the lesion. Some bifunctional BER enzymes also catalyze δ-elimination. Thus, BER enzymes channel many types of damage into three common products: (i) DNA with an AP site, (ii) AP-DNA with a nick on the 3′-side of the lesion, or (iii) DNA with the lesion removed and 3′- and 5′-phosphorylated ends at the gap. The challenge for BER enzymes is to recognize and remove multiple types of DNA damage while avoiding reactions with the millions-fold excess of normal DNA.

Most transition state (TS) analysis studies to date have involved *N*-glycoside hydrolyses and *N*-glycosyl transfers

Paul Berti was born and raised in Toronto, ON. He received a B.Sc. in Biology and Chemistry at the University of Waterloo (Ontario). He received M.Sc. (Ottawa) and Ph.D. (McGill) degrees in Biochemistry, studying the catalytic mechanism and protein inhibitors of cysteine proteases with Dr. Andrew Storer at the Biotechnology Research Institute. In 1993, he joined the laboratory of Professor Vern Schramm (Albert Einstein College of Medicine), where he was an NSERC postdoctoral fellow. He performed TS analysis of *N*-glycoside hydrolysis and *N*-glycosyl transfer reactions, and developed methods of determining TSs from KIEs. He joined McMaster University in the Department of Chemistry and the Department of Biochemistry and Biomedical Sciences in 1999, where was a CIHR New Investigator (2000–2005) and is now an Associate Professor. He is continuing to study enzyme mechanisms and methods of TS analysis. In addition to TS analysis of BER enzymes, his lab pursues studies in the catalytic mechanisms of antimicrobial targets, and new methods of KIE measurement.

Joe McCann obtained his B.Sc. degree in Biochemistry from the University of Guelph in 2001 and is currently completing his doctorate in Biochemistry at McMaster University. During his time at McMaster, Joe has been using isotopic methods to study the enzymatic mechanism and transition state of the *E. coli* DNA repair enzyme MutY.

with nucleosides. We will describe these studies and how that information, combined with other mechanistic studies, can be used to elucidate the chemistry of deoxynucleosides and BER enzymes. Previous reviews have examined the chemistry of BER enzymes[1−6] and *N*- and *O*-glycoside chemistry.[7−11] Other reviews on the methods[12−14] and the results[12,15−20] of TS analyses, especially with nucleoside hydrolases, phosphorylases, and phosphoribosyl transferases, are available.

1.1. Transition State Analysis

A variety of structural and kinetic techniques can be used to infer information about TSs, but kinetic isotope effect (KIE) analysis is the only experimental approach that probes TSs directly. The phrase "TS analysis" refers specifically to

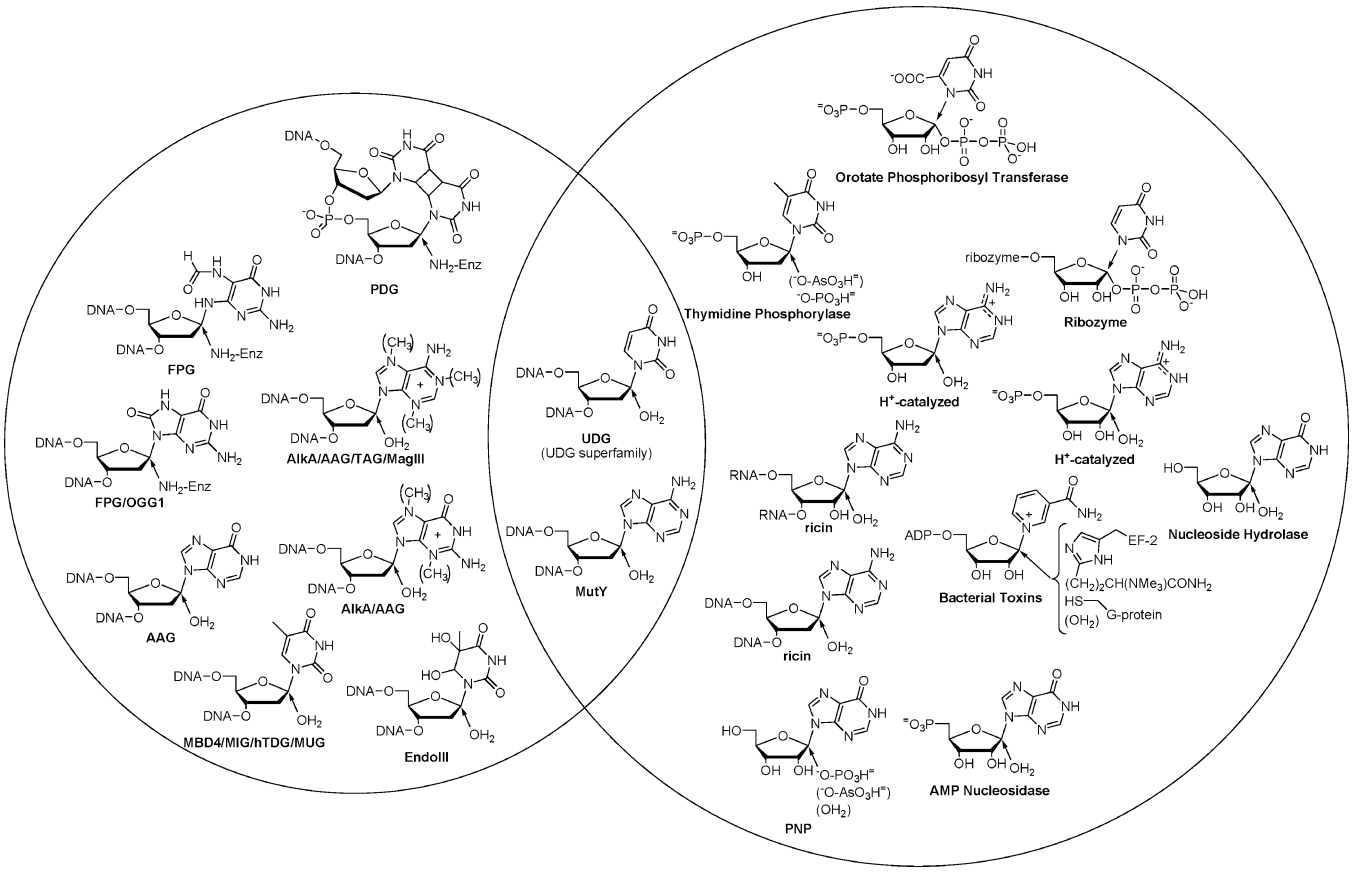

Figure 1. Venn diagram showing (left) reactions catalyzed by BER enzymes, and (right) relevant *N*-glycoside hydrolysis or transfer reactions which have been examined by TS analysis using KIEs. The intersection of the circles illustrates the BER reactions with TS analysis, UDG and MutY.

the use of multiple KIEs to determine TSs in atomic detail. TS analysis consists of (i) measuring kinetic isotope effects (KIEs) at multiple labeled positions in the substrate and then (ii) analyzing the KIEs computationally to give the TS. In the best cases, TS analysis can yield the structure of the TS, a species that exists for less than a single bond vibration (*ca.* 10^{-13} s^{-1}), with accuracy that rivals that of X-ray crystallographic structures of stable molecules. It is capable of providing information directly on each labeled atom at the TS. Enzymes work by binding to and stabilizing TSs in preference to any other molecular species; thus, understanding the TS is a key to understanding catalysis.

As powerful as TS analysis is, it is also experimentally challenging. There are only two published TS analysis studies of DNA glycosylase reactions. One was of the monofunctional BER enzyme uracil DNA glycosylase (UDG),[21] and the other was of the ricin-catalyzed adenine hydrolysis of a DNA substrate.[22] Ricin is a plant toxin that normally acts on 28S ribosomal RNA but is also active against DNA substrates *in vitro*. TS analysis is underway on the BER enzyme MutY from *Escherichia coli*.[23] Because TS analysis is challenging, the rate of TS analyses is unlikely to increase in the foreseeable future. Thus, it is important to apply as much knowledge as possible from TS analyses of related reactions to understand the chemistry of DNA repair.

Fortunately, a number of TS analyses of related *N*-glycoside hydrolysis and transfer reactions have been published which shed light on DNA chemistry, including enzymatic rA hydrolysis from RNA,[24] nucleoside phosphorylation,[25,26] nucleo(s/t)ide hydrolysis,[27−31] ADP−ribose transfer,[32−34] NAD^+ hydrolysis,[35−37] nucleotide synthesis,[38] RNAzyme-catalyzed nucleotide synthesis,[39] and nonenzymatic reactions, acid-catalyzed AMP hydrolysis,[27,40] dAMP hydrolysis,[23] and uncatalyzed NAD^+ hydrolysis[41] (Figure 1).

1.2. Chemistry of Nucleobase Removal

Mechanistic studies of *N*-glycoside hydrolysis and *N*-glycosyl transfer reactions reveal a number of common themes which are also shared with *O*-glycoside (polysaccharide) hydrolyses. A unifying theme is the accumulation of positive charge on the sugar ring at the TS. Glycoside chemistry is largely the chemistry of the oxacarbenium ion.[42]

Most glycoside hydrolases and transferases proceed through highly oxacarbenium ion-like TSs. Stabilizing a positively charged oxacarbenium ion is therefore a potential catalytic strategy, and some enzymes appear to act primarily by directly stabilizing the oxcarbenium ion. However, there is increasing evidence that at least some enzymes provide little direct stabilization of the oxacarbenium ion itself. Rather, they stabilize the TS mostly by activating the leaving group through protonation or stabilizing the anionic form and/or by activating the nucleophile. One of the important questions with any BER enzyme is whether it stabilizes the TS through interactions with the oxacarbenium ion, the leaving group, and/or the nucleophile.

2. Transition State Analysis—The Power and Limitations of the Approach

2.1. Reaction Space—The Field of Play

Plots of "reaction space", based on More O'Ferrall-Jencks style diagrams, help describe mechanisms and TS structures

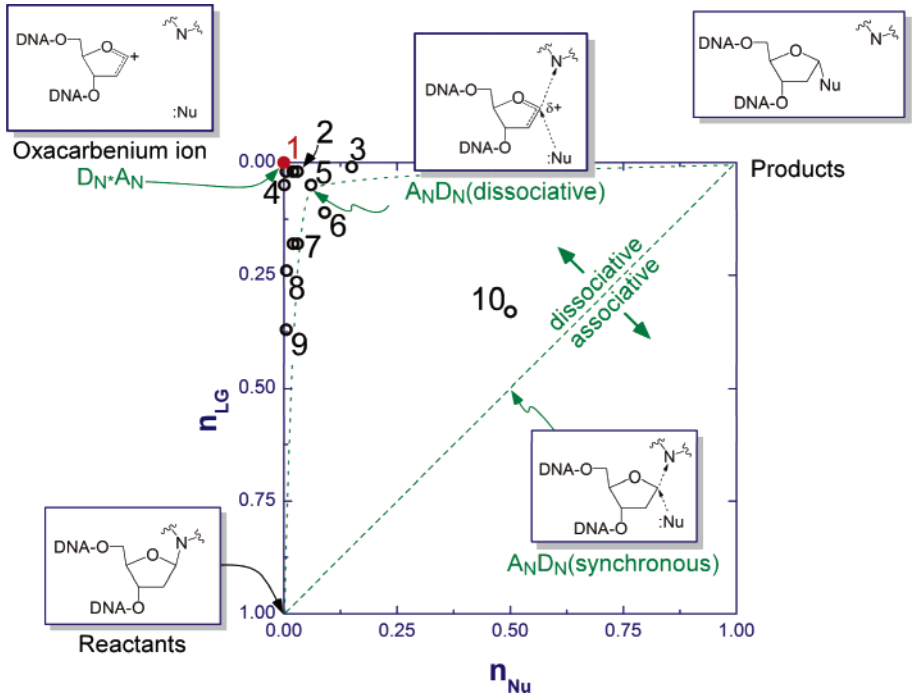

Figure 2. Reaction space for *N*-glycoside hydrolysis and transfer. The axes are the bond orders from C1′, the anomeric carbon, to the leaving group (n_{LG}) and the nucleophile (n_{Nu}). The reactant (bottom left) and products (top right) are shown. In a stepwise D_N*A_N (S_N1) mechanism, an oxacarbenium ion intermediate is formed (top left) by dissociation of the leaving group. The nucleophile attacks C1′ in a separate step. A concerted, synchronous A_ND_N (S_N2) mechanism would follow the dashed diagonal line. A dissociative (asynchronous) A_ND_N mechanism would pass through a TS closer to the top left corner. Selected experimentally determined TSs are plotted in reaction space. D_N*A_N mechanisms: (1) UDG,[21] ricin (RNA[24] and DNA[22]), hPNP,[26] and mPNP.[26] A_ND_N mechanisms: (2) cholera toxin hydrolysis,[36] diphtheria toxin hydrolysis,[35] and NAD^+ nonenzymatic hydrolysis;[41] (3) NH GI;[17] (4) pertussis toxin hydrolysis;[37] (5) NH IU;[12,31] (6) pertussis toxin ADP-ribosylation;[32,33] (7) NH IAG[17] and diphtheria toxin ADP-ribosylation;[34] (8) bPNP hydrolysis;[30] (9) bPNP arsenolysis;[25] (10) hTP arsenolysis.[46] (Adapted from ref 17.)

(Figure 2).[43] For nucleophilic substitutions, the axes are the Pauling bond orders[44] to the leaving group (n_{LG}) and nucleophile (n_{Nu}). In a classic A_ND_N (S_N2) mechanism (diagonal line), nucleophile approach and leaving group departure are precisely synchronous, while, in a D_N*A_N (S_N1) mechanism, a discrete intermediate is formed (top left) after leaving group departure and before nucleophile approach. A_ND_N indicates concerted nucleophile approach (A_N) and leaving group departure (D_N), while the "*" in D_N*A_N indicates a discrete intermediate.[45] In practice, a continuum of TSs are possible. Most *N*-glycoside reactions proceed through highly dissociative A_ND_N TSs or through stepwise D_N*A_N mechanisms. In describing A_ND_N TSs, we will list the values of n_{LG} and n_{Nu}.

2.2. An Introduction to KIEs

Isotope effects are *defined* as the ratio of rate constants (KIE = $^{light}k/^{heavy}k$) or equilibrium constants (EIE = $^{light}K/^{heavy}K$) observed upon isotopic substitution. Isotope effects are *interpreted* to reveal the changes in structure between reactant and TS (or reactant and product for EIEs). KIEs also contain information on the reaction coordinate motion, which is reflected in the primary KIEs, *i.e.*, KIEs on the atoms undergoing bond making and breaking in the reaction. Secondary KIEs are those at any position not directly involved in the chemical step(s).

A KIE > 1.0 means the light isotopologue reacts faster than the heavy one. This indicates a "looser" vibrational environment in the TS than in the reactant, and is called a "normal" KIE. For example, in acid-catalyzed AMP hydrolysis, N9 is a normal aromatic nitrogen in the reactant, forming a total of three bonds to neighboring atoms (Scheme 2).[28] At the TS in this highly dissociative A_ND_N mechanism, the C1′−N9 bond is almost completely broken. Protonation at N7 results in increased C8−N9 π-bonding, compensating somewhat for the loss of C1′−N9 bond order, but the overall bonding to N9 is decreased, and a normal 9-^{15}N KIE is observed. In contrast, the ring oxygen, O4′, experiences a "tighter" vibrational environment at the TS. With the leaving group largely departed and with the bond to the nucleophile water, C1′−O, still very weak, the ribosyl ring carries almost a full positive charge; that is, it has high oxacarbenium ion character. The charge on C1′ is stabilized by π-bonding with the lone pair electrons on O4′, with the C1′−O4′ bond changing from a single C−O bond in the reactant to a bond order of 1.7 at the TS. Thus, the overall vibrational environment for O4′ becomes tighter in the TS than the reactant, and an inverse 4′-^{18}O KIE is expected. It is useful to remember that "light isotopes prefer weak bonds".

Scheme 2

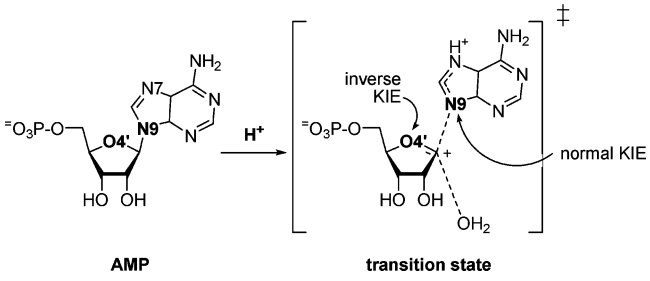

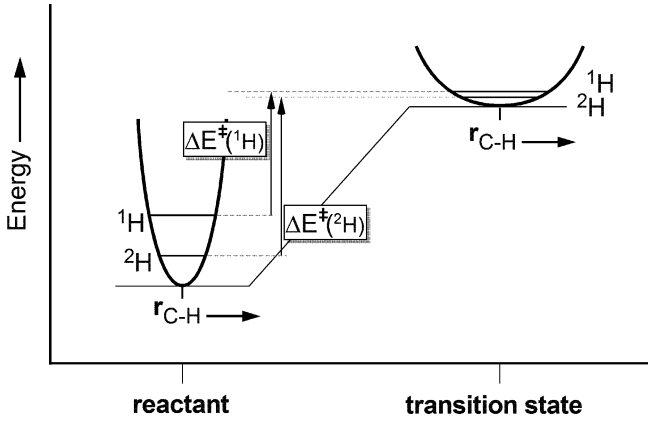

Figure 3. Vibrational origin of isotope effects (IEs). Each inset shows the energy of stretching/compressing a C−H bond from its equilibrium length in the reactant and the TS. The zero point energies for ^{1}H and ^{2}H (horizontal lines) depend on the mass and the bond stretching force constant. For a normal IE, the zero point energy decreases more for the light isotope (^{1}H) than for the heavy isotope (^{2}H) when the bond stretching force constant decreases at the TS. This leads to a difference in activation energies ($\Delta\Delta E^{\ddagger} = \Delta E^{\ddagger}_{2H} - \Delta E^{\ddagger}_{1H}$), which is the source of the ZPE contribution to the IE. This illustration is valid for vibrational modes except the reaction coordinate. The reaction coordinate has no zero point energy at the TS because it has an imaginary frequency and, therefore, no restoring force. For a primary KIE, $\Delta\Delta E^{\ddagger} = E_{2H,reactant} - E_{1H,reactant}$.

2.3. The Origin and Meaning of Isotope Effects

The physical origins of IEs have been described thoroughly[13,47−51] and will not be covered in detail here. Isotope effects are primarily a vibrational phenomenon, in the same sense as infrared and Raman spectroscopies. They reflect the change in vibrational environment of atoms between the reactant and TS. Like vibrational spectroscopies, KIEs are interpreted by treating molecules as balls-and-springs models, with bonds acting as ideal harmonic oscillators. The mass of the ball represents the atomic mass, and spring strength represents the strength of each bond stretch, angle bend, or torsion. Changes in molecular structure correspond to changing the strengths of the springs, which changes vibrational frequencies and causes KIEs. Mathematically, three factors contribute to KIEs, with the contribution from zero point energies (ZPE) usually being dominant (eq 1):[47,48]

$$\mathrm{KIE} = \mathrm{MMI} \times \mathrm{ZPE} \times \mathrm{EXC} \qquad (1)$$

MMI results from the increased mass and moments of inertia in labeled molecules leading to slightly slower overall translation and rotations of the molecule. EXC is a contribution from molecules that are vibrationally excited in the reactant. The MMI and EXC terms are generally small compared to ZPE, so qualitative interpretation of KIEs tends to focus on ZPE, though all three terms are included in computational analyses.

2.3.1. ZPE

The ZPE contribution reflects changes in zero point energies upon isotopic substitution. The ZPE contribution arises from the fact that bonds have vibrational energy, even at 0 K, which is a function of the atomic masses and the strength of the bond (Figure 3). Zero point energies decrease as bonds becomes weaker, and they decrease more for light atoms than for heavy ones. This results in changes in activation energy ($\Delta\Delta E^{\ddagger}$), which leads to KIEs. Figure 3 illustrates a bond stretching motion, but angle bending and out-of-plane motions also contribute to KIEs. Torsions also contribute to KIEs but are generally negligible. The example shown is valid for all vibrational modes except the reaction coordinate (see below).

2.3.2. Reaction Coordinate

Making the distinction between A_ND_N and $D_N{*}A_N$ mechanisms is important both from the point of view of understanding how BER enzymes catalyze nucleobase displacement and for understanding what enzyme·substrate interactions are possible in the TS. In a $D_N{*}A_N$ mechanism the relative positions of the sugar ring and the nucleobase ring are poorly defined. They may be distant from each other and the nucleobase ring may reorient significantly before the second step. In contrast, in an A_ND_N mechanism the relative locations of the nucleophile, the anomeric carbon (C1′), and the leaving group are prescribed by the TS bond orders. This has implications for defining structures and interactions at the TS, especially in reactions where one catalytic group is proposed to have different roles in different steps of the reaction.

The contribution of reaction coordinate motion to KIEs is $^{light}\nu{*}/^{heavy}\nu{*}$, where $\nu{*}$ is the imaginary frequency for each isotopologue. For our purposes, the reaction coordinate is defined as the vibrational mode in a TS structure with an imaginary frequency. It represents motion across the top of the energetic barrier, with forward motion leading to products and reverse motion returning to reactants. There is no restoring force in the reaction coordinate because any movement away from the TS leads to lower energies. This leads, in turn, to the reaction coordinate having an imaginary frequency (often reported by software as a negative frequency).

For A_ND_N reactions, the reaction coordinate motion is the concerted motion of the leaving group and the nucleophile in an asymmetric stretch, with one group approaching C1′ while the other retreats (Figure 4). The symmetric stretch,

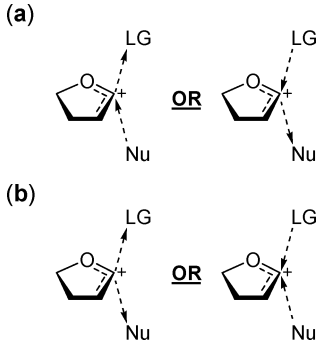

Figure 4. (a) The reaction coordinate motion (asymmetric stretch) for an A_ND_N reaction showing simultaneous approach and retreat of the leaving group and nucleophile. There is no restoring force, and this vibrational mode has an imaginary frequency. (b) The symmetric stretch motion is a regular harmonic oscillator with a real frequency.

with both groups approaching or retreating simultaneously, is a "regular" normal mode with a restoring force. For $D_N{*}A_N$ reactions there are two TSs. The reaction coordinate motion is departure of the leaving group in the first step and approach of the nucleophile in the second.

The reaction coordinate motion allows us to unambiguously distinguish between highly dissociative A_ND_N and

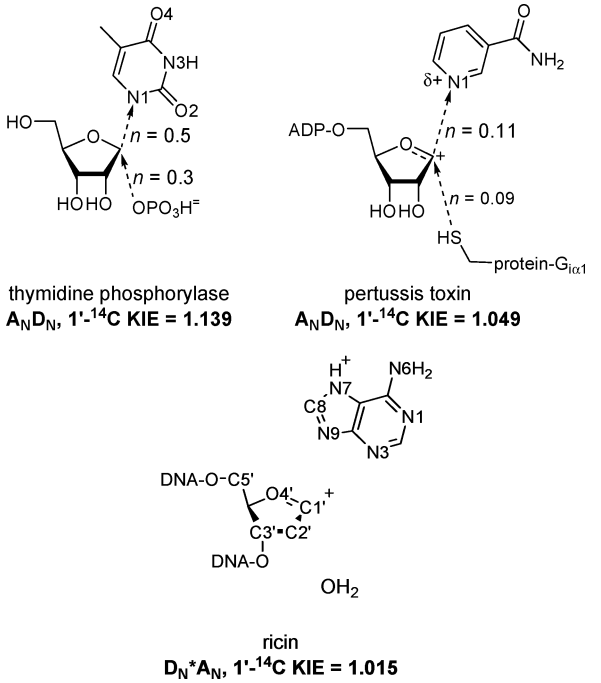

Figure 5. TS structures of thymidine phosphorylase,[46] a pertussis toxin,[33] and ricin[22] catalyzed reactions.

$D_N{*}A_N$ mechanisms, something that is difficult or impossible by conventional physical organic chemistry methods. Some highly dissociative A_ND_N TSs have values of n_{LG} and n_{Nu} that are so low (<0.05) that the question could arise whether they are present at all in the TS. The reaction coordinate motion makes a normal contribution to the primary carbon KIE that is larger than the combined ZPE and EXC contributions and ensures a normal KIE. The practical upshot is that it is possible to distinguish highly dissociative A_ND_N TSs from stepwise $D_N{*}A_N$ TSs that are structurally very similar but which have different mechanisms.

The reaction coordinate contribution leads to the seemingly paradoxical result that more synchronous A_ND_N TSs have larger primary ^{14}C (or ^{13}C) KIEs despite higher total bond order to C1′ at the TS. Comparing three experimental TSs, we see that the TS structure with the highest total bond order to C1′ has the highest 1′-^{14}C KIE, rather than the lowest, as would be expected based on the ZPE contributions alone (Figure 5). Typical values are discussed below.

2.3.3. Swain–Schaad Relationship—^{2}H versus ^{3}H, and ^{13}C versus ^{14}C KIEs

^{2}H and ^{3}H are commonly used in TS analyses, as are ^{13}C and ^{14}C (and occasionally ^{11}C). When comparing reactions, it is helpful to be able to convert between KIE values for different isotopic labels. The Swain−Schaad relationship[52−54] gives the expected relationship between KIEs with different nuclei:

$$^3\text{H KIE} = (^2\text{H KIE})^{1.44} \quad (2)$$

$$^{14}\text{C KIE} = (^{13}\text{C KIE})^{1.89} \quad (3)$$

In the absence of quantum tunneling, the Swain−Schaad relationship usually holds well for hydrogen isotopes, though it was recently shown not to hold for KIEs near unity.[53,54] Thus, the Swain−Schaad relationship should be applied with caution.

2.4. Typical KIEs for *N*-Glycoside Hydrolysis or Transfer

2.4.1. KIEs near the Reactive Site

Typical values of KIEs for labels close to the reactive site, and their significance, are summarized in Table 1.

Primary ^{13}C/^{14}C KIEs. A_ND_N reactions give primary carbon KIEs in the range of ^{13}C KIE = 1.013−1.08 or ^{14}C KIE = 1.025−1.16, with the size of the KIE correlating inversely with the dissociative character of the TS. Highly dissociative, asynchronous TSs have KIEs near the lower limit while synchronous mechanisms give high KIEs. $D_N{*}A_N$ mechanisms give ^{13}C KIE = 0.995−1.01 or ^{14}C KIE = 0.99−1.02.[55,56] In reactions where only the chemical steps are kinetically significant, *i.e.*, leaving group departure and nucleophile approach, KIEs will be near the upper limit. If oxacarbenium ion formation is reversible, *i.e.*, the C−N bond is repeatedly broken and reformed, and there is an irreversible nonchemical step before nucleophilic attack, such as a protein conformational change or diffusion away of the leaving group, then the experimental KIE will equal the equilibrium IE for breaking the C−N bond, near the lower end of the range. This was observed with ricin-catalyzed RNA hydrolysis[24] and with malarial and human PNPs (mPNP, hPNP).[26]

Primary ^{15}N KIEs. The leaving group ^{15}N KIE is (usually) directly proportional to the extent of bond cleavage, reaching a maximum of 9-^{15}N KIE ∼ 1.03 for purine leaving groups. There is no good experimental estimate of the maximum for pyrimidine 1-^{15}N KIEs, though it would be expected to be broadly similar to that for purines. In some cases, such as the bovine purine nucleoside phosphorylase (bPNP)-catalyzed arsenolysis and hydrolysis, the 9-^{15}N KIEs were anomalously low for reasons that are still not clear (section 4.7).

1′-^{3}H/1′-^{2}H KIEs. α-Secondary hydron KIEs (a hydron is any of ^{1}H, ^{2}H, or ^{3}H) are expected to be large and normal for dissociative A_ND_N and for $D_N{*}A_N$ reactions, and inverse for synchronous A_ND_N reactions.[57−60] Rehybridization of the anomeric carbon toward sp^2 and decreased steric crowding by the leaving group increase the out-of-plane bending freedom of H1′. In contrast, synchronous A_ND_N TSs give inverse 1′-^{3}H KIEs because of the increased steric crowding from the presence of both the leaving group and nucleophile at the TS. More detailed interpretation is often confounded by poor correlations between TS structure and 1′-^{2}H/^{3}H KIEs.[12]

2′-^{3}H/2′-^{2}H KIEs. Hyperconjugation between the 2′-hydrons of (deoxy)nucleosides and the cationic center at C1′ in oxacarbenium ions helps to stabilize the TS and leads to large, normal 2′-hydron KIEs.[57,61] Hyperconjugation can be described as donation of electron density from the C2′−H2′ σ-bond(s) into the empty p-orbital at C1′, forming a C2′−C1′ π-bond. Weakened C2′−H2′ bonds give large, normal β-secondary ^{2}H or ^{3}H KIEs. Because hyperconjugation is strongly angle dependent, 2′-hydron KIEs can give the ring conformation at the TS.[31,61,62] These KIEs have demonstrated how enzymes can manipulate the ring conformation to stabilize the TS, or, in rare cases, fail to use hyperconjugation.[24,26,63]

Hyperconjugation depends on the dihedral angle between the C2′−H2′ bond and the developing empty p-orbital on C1′ (Figure 6),[61] being maximal at 0° or 180°, and zero at 90°. Hyperconjugation in ribosyl oxacarbenium ions is strongly conformation dependent because there is only one

Table 1. Approximate Ranges of KIEs Measured in TS Analyses

position	type	approximate range	interpretation
C1′	primary, electrophile	1′-^{14}C ≥ 1.13 1′-^{13}C ≥ 1.07	synchronous A_ND_N mechanism[46] large KIE due to contribution from reaction coordinate
		1′-^{14}C = 1.025−1.06 1′-^{13}C = 1.013−1.03	dissociative A_ND_N mechanism[25,28−37,40,112,158] large KIE due to contribution from reaction coordinate
		1′-^{14}C = 1.01−1.02 1′-^{13}C = 1.005−1.01	stepwise D_N*A_N mechanism with a discrete oxacarbenium ion intermediate[21,22,112]
		1′-^{14}C = 0.99−1.00 1′-^{13}C = 0.995−1.00	nonchemical step as the second step in a stepwise D_N*A_N mechanism[24,26,63] observable KIE equals EIE for oxacarbenium ion formation
N9	primary, leaving group	9-^{15}N = 1.00−1.03	KIE is directly proportional to C−N bond cleavage; larger KIEs indicate greater breakage[22,24−26,28−37,40,41,46,63,112,158]
H1′	α-secondary	1′-^{3}H = 1.15−1.34 1′-^{2}H = 1.08−1.20	dissociative A_ND_N or $D_{N*}A_N$ mechanism[21,22,24−26,28,30−37,40,41,63,158] detailed interpretation difficult because of poor correlation between TS structure and KIE
		1′-^{2}H < 1.0	synchronous A_ND_N mechanism[46]
H2′	β-secondary	2′-^{3}H > 1.1 2′-^{2}H > 1.07	large KIEs indicate both high oxacarbenium ion character *and* hyperconjugation; likely a 3′-*exo* ring conformation[21,22,24−26,28−37,40,41,63,112] 2′-^{2}H >1.065[21,158]
		2′-^{3}H < 1.05 2′-^{2}H < 1.035	small KIEs indicate either low oxacarbenium ion character *or* lack of hyperconjugation; likely a 3′-*endo* ring conformation[24,26,46,63]
N7	β-secondary (purines only)	7-^{15}N = 0.980−0.985	inverse KIE indicates protonation at N7 of purine reactants, promoting purine departure[24]
O4′	α-secondary (ring oxygen)	4′-^{18}O ≈ 0.98	indicates increased π-bonding to C1′ in oxacarbenium ion-like transition state[35,41] not often measured with *N*-glycosides[35,41]

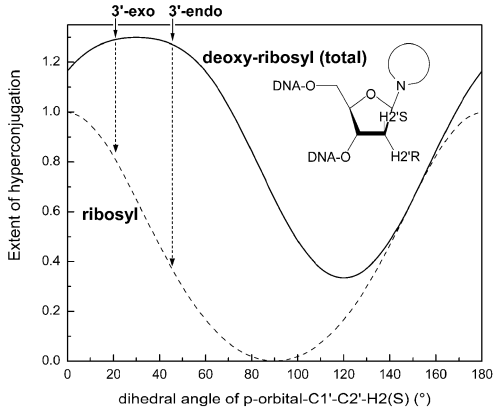

Figure 6. Hyperconjugation in oxacarbenium ions. The total hyperconjugative stabilization is shown for deoxyribsoyl (solid line) and ribosyl (dashed line) oxacarbenium ions as a function of θ, the dihedral angle between the C2′−H2′(S) bond and the p-orbital on C1′. The curves were derived from the angular dependence of hyperconjugation, which is proportional to $\exp(\cos^2\theta)$.[61]

H2′. In deoxyribosyl oxacarbenium ions, both H2′ hydrogens can contribute, lessening the angular dependence. The strong π-bonding in the C1′−O4′ bond forces the five-membered ring into one of two envelope conformations, 3′-*endo* or 3′-*exo* (**1**). The 3′-*exo* conformer of the ribosyl oxacarbenium

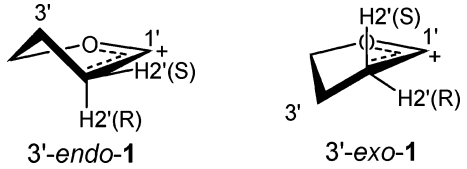

has the C2′−H2′ bond at a 20° dihedral angle with the p-orbital on C1′,[22] allowing strong hyperconjugation. In the 3′-*endo* conformer, the angle is 52°, resulting in lower hyperconjugation.[57,61] Thus, a large β-secondary hydron KIE in riboside reactions implies both (i) a highly oxacarbenium ion-like structure and (ii) a 3′-*exo* ring conformation. In the majority of riboside reactions examined, the β-secondary hydron KIE has been large, >1.1 for ^{3}H and >1.07 for ^{2}H, indicating that a majority of reactions pass through the TS in a 3′-*exo* conformation.

In deoxynucleosides, both C2′−H2′ bonds are capable of hyperconjugation, and maximal total hyperconjugation is achieved when both C2′−H2′ bonds are at an angle of ∼30°, corresponding to a flattened 3′-*exo* conformation (Figure 6).

2.4.2. Remote KIEs

Enzyme binding at remote sites is reflected in remote KIEs. In enzymatic reactions involving *N*-glycosides, there is usually a large, normal 5′-^{3}H KIE,[22,25,26,30−33,35−37,46,64] though inverse[24,34] or small[28] 5′-^{3}H KIEs have been observed. 4′-^{3}H KIEs for enzymatic reactions are generally nonunity, with both inverse[24,31−33,35−37] and normal[25,26,30,34,46,64] KIEs observed. The corresponding KIEs in nonenzymatic reactions are near unity,[28,40,41] demonstrating that these KIEs are enzyme-induced, not intrinsic to the reactions. It is not common to assign a specific cause to the 5′-^{3}H KIEs because several different factors are possible. Conformational changes,[31,65] bond angle bends,[35] protonation of an adjacent phosphate,[35] or hydrogen bonding[66] can all cause normal KIEs. As a rule, it is only possible to conclude that the enzyme is interacting at remote sites to promote catalysis. Interestingly, the large 5′-^{3}H KIE on thymidine arsenolysis catalyzed by human thymidine phosphorylase (hTP)[46] also occurred in the EIE for thymidine binding,[64] demonstrating that whatever interactions caused the 5′-^{3}H IEs were present in both the Michaelis complex and the TS.

2.5. Computational Analysis of IEs

There is no algorithm to simply calculate a TS from experimental KIEs. The general approach is to search for a TS structure for which the calculated KIEs match the experimental KIEs. More accurately, it is a pair of structures

because KIEs reflect the *change* between the reactant and the TS; they both contribute equally to the calculated KIEs.Reactant structures, being stable molecules with crystal structures and other structural information available, are easier to define, so the focus is on finding a TS structure that gives the correct KIEs.

2.5.1. Electronic Structure Methods

Using electronic structure (quantum mechanical) calculations, it is possible to calculate the structures and vibrational frequencies of reactant and TS molecules. An electronic structure program, *e.g.*, Gaussian, is used to optimize reactant and TS structures and calculate the vibrational frequencies. IEs are then generated from the frequencies with the programs QUIVER[67] or ISOEFF98.[68] Only frequencies calculated at post-Hartree−Fock levels of theory are suitable for IE analysis.[69,70] The computationally "cheapest" methods are DFT or MP2. Vibrational frequencies calculated at this level are generally quite accurate for a given structure,[71] so it is safe to assume that if calculated and experimental KIEs agree, then the calculated TS structure is accurate and can be taken as the experimental TS.

The factor limiting the accuracy of computed IEs is the accuracy of the structure itself. Calculated TS structures for solution reactions are often not accurate, partly because of limitations in the computational models, but largely because solvents and enzymes change TSs. If the calculated and experimental KIEs do not match, there is nothing more that can be done with IEs from electronic structure methods. Frequency calculations on quantum mechanical models are valid only at stationary points, *i.e.* energetic minima or saddle points. Vibrational frequencies for unoptimized structures, or structures optimized with constraints, have no physical meaning. If IEs from electronic structure models do not match the experimental KIEs, other methods such as bond order vibrational analysis (BOVA) or "quantum BOVA" must be used to find the TS.

2.5.2. Bond Order Vibrational Analysis (BOVA) and Structure Interpolation

KIEs can be calculated for any pair of reactant and TS structures using BOVA.[72−75] A vibrational model is created that treats the reactant and TS molecules as perfect harmonic oscillators with atoms (point masses) connected together with bonds (massless springs) with defined force constants. If the vibrational model and the structure of the reactant are accurate, then the TS model that gives calculated KIEs matching the experimental ones is considered the experimental TS. Vibrational models and KIE calculation have been discussed in detail elsewhere.[13,72−74] The programs available for BOVA are BEBOVIB,[73,76] VIBIE,[77,78] and ISOEFF98.[68]

In the past, BOVA analysis involved varying putative TS structures in an *ad hoc* way, that is, adjusting bond lengths and angles iteratively until the calculated KIEs matched the experimental ones. To systematize the process and avoid some of its shortcomings, the "structure interpolation" approach to BOVA was created.[13,41] Structure interpolation involves creating an algorithm that describes the structure of a molecule as a function of its position in reaction space (Figure 2) and generates trial TS structures throughout reaction space. KIEs are then calculated using BOVA. The area in reaction space where the calculated and experimental KIEs match for all isotopic labels is the experimental TS structure.

Using structure interpolation, a "unified model" of a reaction can be created.[13] A unified model differs from any other TS analysis only in that a single vibrational model and structure interpolation model is used to determine TS structures for several different reactions of a given type. The TSs of four hydrolytic and two ADP-ribosylation reactions of NAD^+ were determined using a unified model (section 4.9). The fact that this model worked for all these different reactions lent support to the correctness of each step in the process.

2.5.3. Quantum BOVA

TS analyses have recently been published which used quantum BOVA for finding TS structures in situations where electronic structure calculations did not match the experimental KIEs.[26,34,46] The program ISOEFF98[68] is capable of calculating KIEs using frequencies derived from quantum mechanical calculations, as well as directly manipulating the Hessian matrices to allow matching of experimental to calculated IEs.

2.6. Which Step(s) Do KIEs Reflect? Irreversible and Rate-Limiting Steps

KIEs for TS analysis are usually measured by the competitive method; that is, labeled and unlabeled reactants are combined in a single reaction mixture and allowed to act as competitive substrates. If there is an isotope effect at the labeled position, the ratio of light to heavy isotopes will change during the reaction. For example, a ^{2}H KIE is measured with a mixture of ^{1}H and ^{2}H at the position of interest. With a normal KIE, the product is enriched in ^{1}H and the residual substrate becomes enriched in ^{2}H. Isotope ratios can be measured in either the product (compared with a reaction taken to 100%) or residual substrate (compared with unreacted substrate).

Competitive KIEs reflect the specificity constant, k_{cat}/K_M,[79] with KIE $= [^{light}(k_{cat}/K_M)/^{heavy}(k_{cat}/K_M)]$. As k_{cat}/K_M reflects the change going from free enzyme and free substrate in solution (E + S) to the TS for the *first irreversible* step of the reaction ($E{\cdot}S^{\ddagger}$), competitive KIEs reflect the same step. As discussed in detail previously,[12] the *first irreversible* step and the *rate-limiting* step are often not the same. This is commonly the case with BER enzymes, where nucleobase excision is effectively irreversible, but product release is slower than the chemistry, making it rate limiting. Once the first irreversible step has been passed, the reaction is committed to proceed forward and there is no longer any discrimination between the isotopic labels.[80] Thus, rate-limiting product release has no effect on the KIEs of the irreversible chemical steps.

Reactions may have more than one partially irreversible step. One example is $D_N{*}A_N$ reactions, where a transient oxacarbenium ion intermediate is formed (**I** in Figure 7a). The oxacarbenium ion can partition both forward (k_5) and backward (k_4). In the example shown, **I** formation (k_3) is rate limiting and partially irreversible, while its breakdown (k_5) is the first fully irreversible step. The degree of irreversibility is determined by the ratio k_5/k_4.[22,75] If $k_5 \gg k_4$, then **I** partitions completely forward, and the mechanism is $D_N^{\ddagger}{*}A_N$, with the KIEs reflecting the TS for **I** formation (leaving group departure). If $k_5 \ll k_4$, then the intermediate is in equilibrium with the reactant, the mechanism is $D_N{*}A_N^{\ddagger}$, and the KIEs will be the EIEs for intermediate formation

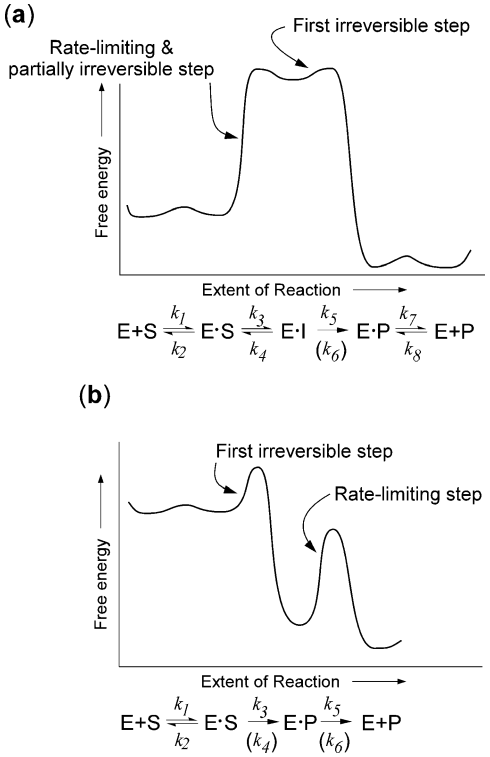

Figure 7. Reaction profiles illustrating irreversible and rate-limiting steps. (a) A $D_N{*}A_N$ reaction with formation of a discrete, enzyme-bound oxacarbenium ion intermediate (E·I) that is rate limiting and partially irreversible. Breakdown of the intermediate is the first fully irreversible step. The energetic barriers to intermediate breakdown are the same in the forward and reverse directions, so $k_4 = k_5$. (b) A "typical" BER enzyme reaction where the chemical step, k_3, is the first irreversible step (which is reflected in the KIEs) and the rate-limiting step is product release (k_5).

multiplied by the KIEs for nucleophile attack on **I** (k_5). For intermediate values of k_5/k_4, the experimental KIEs vary monotonically between the extremes. For (deoxy)nucleoside hydrolysis, the calculated KIEs for $D_N{}^{\ddagger}{*}A_N$ and $D_N{*}A_N{}^{\ddagger}$ mechanisms are similar enough that is often difficult to distinguish between them.

An additional complication is if **I** is sufficiently long-lived that some nonchemical step becomes the first irreversible step. In a nonenzymatic reaction, if the oxacarbenium ion intermediate is long-lived enough for it to diffuse away from the nucleobase leaving group, the mechanism becomes $D_N{+}A_N$. The KIEs on diffusion will be negligible, so the experimental KIEs will equal the EIEs for intermediate formation. In ricin-catalyzed rA hydrolysis, the experimental KIEs were close to the calculated EIEs for oxacarbenium ion intermediate formation, indicating formation of the oxacarbenium ion intermediate, followed by a nonchemical irreversible step, such as a conformational change, or simply diffusion of the water nucleophile into position to perform nucleophilic attack.[24]

In order for experimental KIEs to be interpretable, it is necessary to ensure that they reflect the chemical steps. Some enzymes are so effective that nearly every molecule of substrate that binds proceeds forward to products ($k_3 \gg k_2$ in Figure 7). The first irreversible step becomes substrate binding, and competitive KIEs will reflect only substrate binding, with no contribution from the chemical steps. This situation is called "commitment to catalysis". It is necessary in TS analysis to ensure that commitment to catalysis is small so that the experimental KIEs reflect the chemical step(s).[81−83] In all the studies discussed here, the commitment to catalysis was negligible, or occasionally the observed KIEs were corrected for a modest amount of commitment to yield the intrinsic KIEs on the chemical steps.

Noncompetitive KIEs, where reaction rates are measured for each isotope in separate reactions and the ratio of rates is used to calculate the KIE, are not normally precise enough for TS analysis. Recently, methods have been reported for measuring noncompetitive KIEs precisely, though the measurements require large amounts of material.[84,85]

2.7. Combining TS Analysis with Other Experimental Approaches

TS analysis, as a direct probe of catalysis, is most powerful when combined with other experimental techniques, particularly structural and inhibition studies. PNP[86] represents a case study in the integration of experimental approaches, including TS analysis[25,30] and protein dynamic,[87] structural,[88] and functional analyses[89−91] that have yielded profound insights into the catalytic mechanism.[17,18] TS analysis combined with structural studies resulted in convincing evidence for an "electrophile migration" mechanism (section 3.6.3). Cycles of inhibitor design and testing resulted in a PNP inhibitor, immucillin H, with a dissociation constant of 23 pM, that is in clinical trials for treating T-cell lymphoma. These analyses have made it possible to create nanomolar inhibitors that differentiate human and malarial PNPs even though they use very similar mechanisms.[92]

3. N-Glycoside Hydrolysis

3.1. Catalytic Imperative

Enzymes are made up of the same kinds of functional groups as their substrates; they are not infinitely powerful to protonate, deprotonate, or distort their substrates. Rather, they take advantage of the intrinsic reactivities of their substrates to promote catalysis. Thus, in discussing enzyme mechanisms, it is important to understand the intrinsic reactivities of their substrates. The half-life of the natural purine nucleobases in DNA is 400 years at physiological pH and temperature, and it is 11 000 years for the natural pyrimidine bases (see below). Thus, the catalytic imperative for BER enzymes is to supply up to 19 kcal/mol of TS stabilization in order to accelerate bond cleavage 10^{14}-fold. The catalytic imperative for the more labile alkylated bases may be as low as 2 kcal/mol for 3-methyladenine residues, which have a half-life of 35 min under physiological conditions.[93] Nonenzymatic β-elimination is much faster than *N*-glycoside hydrolysis, with half-times of hours to days, rather than years.[3,23] Thus, the greater catalytic imperative for bifunctional BER enzymes is by far *N*-glycoside cleavage. The fact that the rate-limiting chemical step for most or all bifunctional enzymes is elimination[4,94−106] indicates that they devote much less catalytic power to the elimination reactions than nucleobase excision. In this section, we examine the intrinsic reactivities of *N*-glycosides.

3.2. Concerted versus Stepwise Reactions

Glycoside hydrolyses tread the borderline between concerted and stepwise reactions, and almost invariably proceed through either stepwise $D_N{*}A_N$ (S_N1) reactions or highly dissociative A_ND_N (S_N2) mechanisms (Figure 8).[7,12,107,108] (The sole known exception[46,64] is discussed below.) Thus,

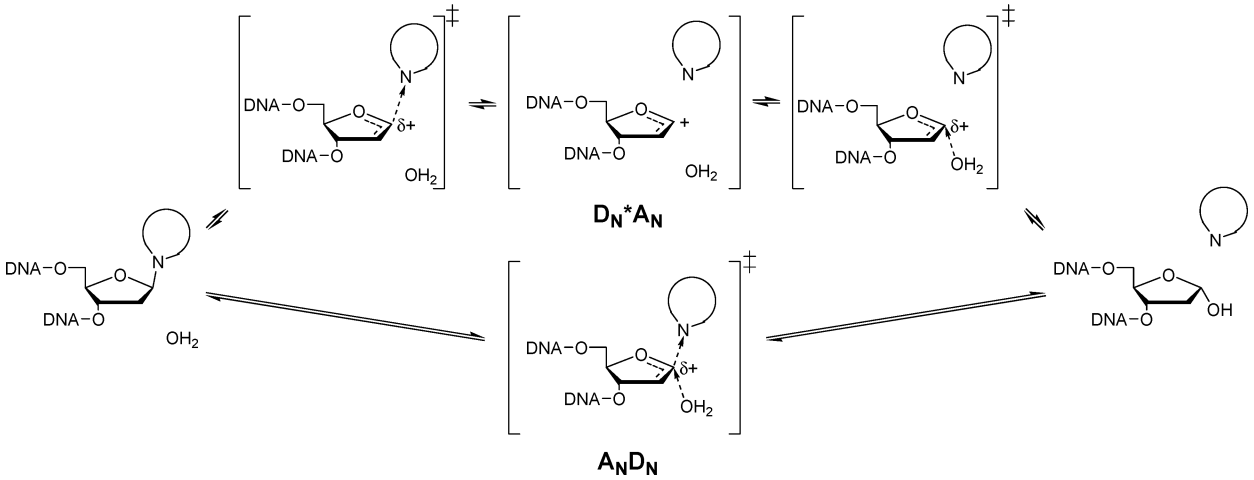

Figure 8. Possible mechanisms of nucleobase hydrolysis from DNA. (top) A D_N*A_N (S_N1) mechanism passing through a discrete oxacarbenium ion intermediate. There are two TSs in this reaction, one for leaving group departure to form the oxacarbenium ion, and one for nucleophile approach, forming the deoxyribosyl product. (bottom) An A_ND_N (S_N2) mechanism has a single TS, with leaving group departure being concerted with, though in advance of, nucleophile approach.

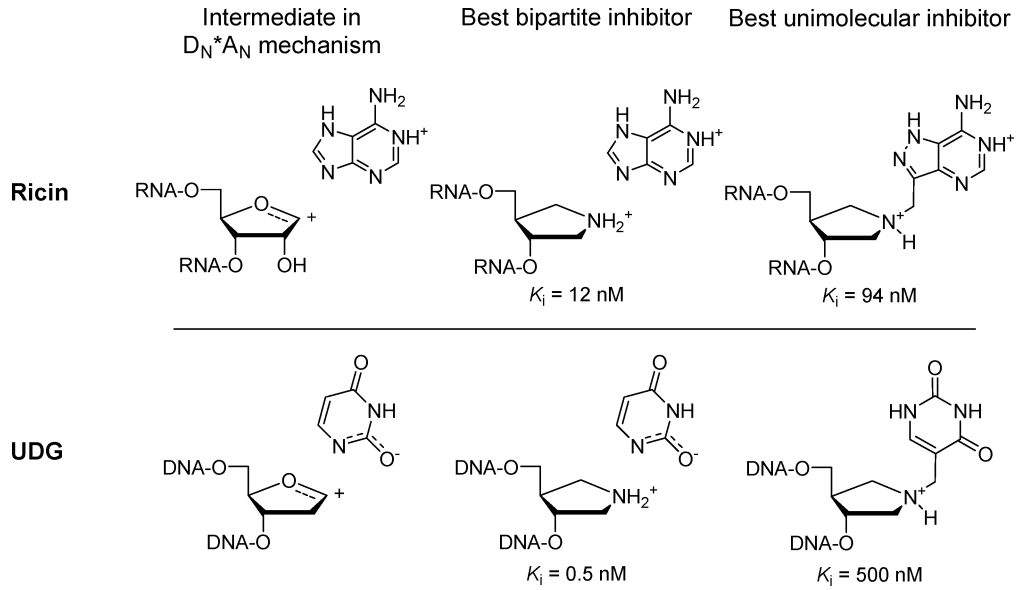

Figure 9. Unimolecular and bipartite inhibitors of ricin and UDG, enzymes with D_N*A_N mechanisms. For ricin ligands, the protonation states at pH4.0 are shown.

these reactions form either a discrete oxacarbenium ion intermediate or an oxacarbenium ion-*like*[109] TS where leaving group departure is far advanced over nucleophile approach, and positive charge accumulates on the sugar ring.

TS analyses have revealed examples of both A_ND_N[27−38,110−114] and D_N*A_N[21,22,24,113,115] mechanisms for enzymatic *O*- and *N*-glycoside reactions. Similarly, nonenzymatic reactions tread the borderline. Among *O*-glycosides, glucosides have been observed to hydrolyze through either D_N*A_N (leaving group = OMe,[113,116] arylamines[114]) or A_ND_N mechanisms (leaving group = F[117]), depending on the leaving group. The ribofuranosyl oxacarbenium ion is expected to be more stable than the glucopyranosyl oxacarbenium ion, based on the higher reactivity of *O*-ribosides[7] and sugar 1-phosphates,[118] and therefore more prone to proceed through D_N*A_N mechanisms. Nonetheless, the nonenzymatic hydrolyses of the AMP[27] and NAD^+[41] had A_ND_N mechanisms, though hydrolysis of dAMP appears to be stepwise.[23]

The distinction between A_ND_N and D_N*A_N is important (i) from the point of view of understanding how *N*-glycosylases function and (ii) for designing enzyme inhibitors (where that seems desirable). An A_ND_N TS has well-defined distances and orientations between the leaving group, the sugar, and the nucleophile, even if the bonds are extremely long. In a stepwise mechanism, where the oxacarbenium ion has a finite lifetime, it is possible for the leaving group to reorient within the active site, potentially forming interactions that are not possible in the substrate. Interestingly, with UDG and ricin, two enzymes that employ stepwise mechanisms, the best inhibitors to date are "bipartite",[119−122] consisting of an oxacarbenium ion mimic and a nucleobase that form a ternary complex with the enzyme (Figure 9). The inability to find single molecules that bind as well as bipartite inhibitors, despite the large entropic advantage inherent to a unimolecular inhibitor,[123−125] may indicate that none of the unimolecular inhibitors tested were capable of simultaneously effectively mimicking the oxacarbenium ion and the nucleobase simultaneously in the active site.

The observation of concerted versus stepwise mechanisms also has implications for the order and simultaneity of acid/base catalytic steps. In some proposed mechanisms, the same enzymatic side chain is proposed to act in sequential steps

of the reaction, which will be possible only if the reaction is stepwise. For example, with *Bacillus stearothermophilus* MutY (bMutY), residue Glu43 was proposed to act as a general acid catalyst to promote leaving group departure, followed by acting as a general base catalyst to activate the water nucleophile (section 5.3.2). Human Ogg1 (hOGG1) was proposed to employ product-assisted catalysis, with the 8-oxoguanine leaving group deprotonating the nucleophile amine, which could only occur in a stepwise reaction (section 5.3.8).

3.3. Leaving Groups and Leaving Group Stabilization

The strategies that are available for catalysis of leaving group departure depend on the nature of the nucleobase. Purines are susceptible to acid catalysis by *N*-protonation (Figure 10). Pyrimidine cleavage can also be acid-catalyzed,

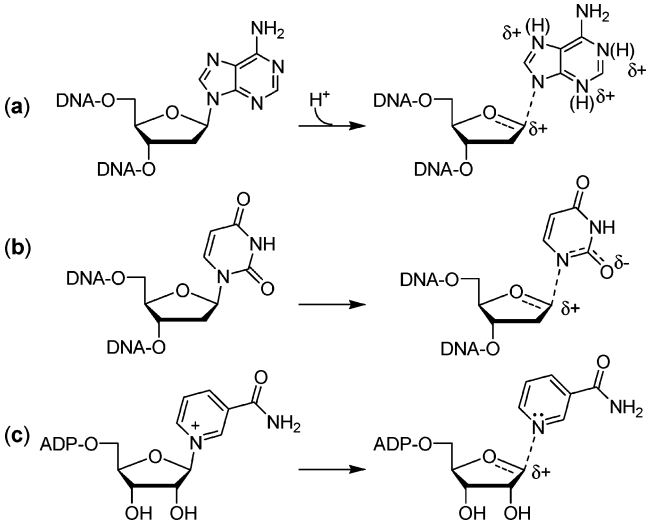

Figure 10. Leaving group activation in glycoside hydrolysis. (a) Purine ring departure is acid-catalyzed by protonating ring nitrogens (not N1 for G, Hx). (b) Pyrimidine ring departure is not (necessarily) acid-catalyzed; it can depart as the anion. (c) The cationic nicotinamide ring in NAD^+ leaves as the neutral form.

though the only well-characterized example, UDG, catalyzes departure of the uracil anion. Cationic, alkylated purines may depart in the neutral or protonated, doubly cationic, forms. ADP-ribosylating toxins catalyze nicotinamide departure, a cationic leaving group that cannot be protonated, in the neutral form.

3.3.1. Lessons from Nonenzymatic Hydrolyses

Studies of nonenzymatic nucleoside hydrolysis demonstrate (i) how much TS stabilization is necessary to achieve the observed catalytic rates and (ii) what catalytic strategies may be effective.

DNA was ~10-fold more stable to depurination than nucleosides, and native DNA was 4-fold more stable than denatured DNA.[126] Similarly, the cationic, alkylated nucleobase *N7*-methyl-2′-deoxyguanosine, 7MeG, was 25-fold more

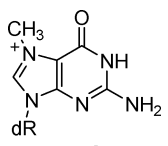

7MeG

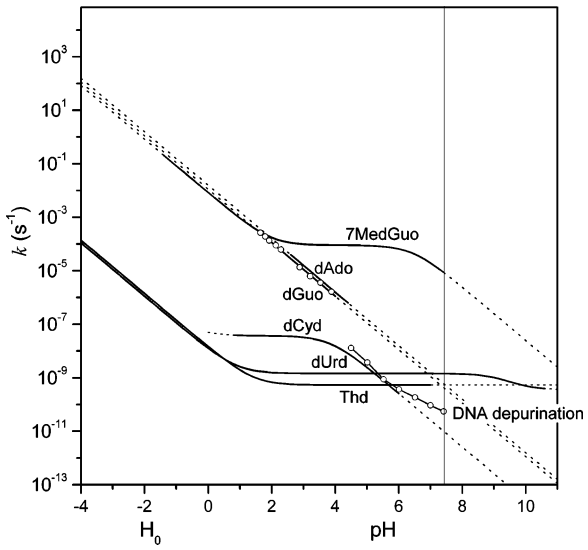

Figure 11. pH dependence of nonenzymatic hydrolysis of deoxynucleosides, at 37 °C. Solid lines represent pH values for which there are experimental rates; the dashed lines are extrapolations of fitted curves. Curves were fitted to experimental rate versus pH data (or H_0 below 0) derived from the original publications. DNA depurination data points (○) are simply joined by straight lines (see text). Rates at 37 °C were extrapolated from the original rates (usually at >75 °C) using the reported thermodynamic parameters, except for 7MedGuo, where the values for dGuo were used. Data were taken from the following references: Thd,[135,136] dUrd,[135,136] dCyd,[136] dAdo,[130] dGuo,[130] 7MedGuo,[130] and DNA purination.[126,159] (Adapted from ref 135.)

stable in DNA than it was as the nucleoside.[127] Depyrimidination was ~20-fold slower than depurination in DNA.[128] It was also slower in DNA than in nucleosides and slower in native than denatured DNA by a factor of 2 to 6.[128] Interestingly, T and C were hydrolyzed with almost equal rates from DNA at pH 7.4 (extrapolated to $k = 2 \times 10^{-12}$ s^{-1} at 37 °C), in contrast to the corresponding nucleosides (Figure 11). This may be related to the fact that thymine (and uracil) will depart as an anion, which would be unfavorable when surrounded by the negative phosphodiester backbone, while cytosine will depart in the neutral form. Thus, T hydrolysis was slowed 270-fold in DNA, while C hydrolysis was only slowed 5-fold. One consequence of these observations is that the act of flipping the target nucleobase out of the DNA helix is, in itself, catalytic because it makes the *N*-glycosidic bond more reactive by 0.4−3.3 kcal/mol.

Nonenzymatic mechanisms of purine and pyrimidine hydrolysis have been studied extensively.[7,93,126−138] Many of the essential features are shown (Figures 11 and 12, Table 2), including the relative reactivities as a function of pH, extrapolated to 37 °C.

As hydrolysis can be acid-catalyzed for any nucleobase, understanding the sites of protonation and their pK_a's are important in analyzing enzymatic reactions (Figure 12). Protonation makes nucleobases electron deficient and less stable. Breaking the *N*-glycosidic bond relieves that electron deficiency. Expressing the same idea in different terms, protonation stabilizes the leaving group. Departure of purine or pyrimidine as an anion is unfavorable because it is unstable in solution and a good nucleophile.

Pyrimidine Nucleobases. The rate versus pH profiles for dUrd and Thd show a pH-independent region between pH 1 and 9 (Figure 11). The reaction is not acid-catalyzed in this region, and uracil leaves as an anion. Of the natural

Table 2. Nonenzymatic *N*-Glycoside Hydrolyses at pH 7.4 and 37 °C[a]

	k (s^{-1})	$t_{1/2}$
2′-deoxyadenosine (dAdo)	6×10^{-10}	35 y
2′-deoxyguanosine (dGuo)	4×10^{-10}	49 y
thymidine (Thd)	5×10^{-10}	41 y
2′-deoxycytidine (dCyd)	1×10^{-11}	2100 y
DNA depurination	5×10^{-11}	400 y
DNA depyrimidination	2×10^{-12}	11000 y
2′-deoxyuridine (dUrd)	1×10^{-9}	15 y
7-methyl-2′-deoxyguanosine (7MedGuo)	6×10^{-5}	3 h

[a] Rates were extrapolated from the same data as in Figure 11.

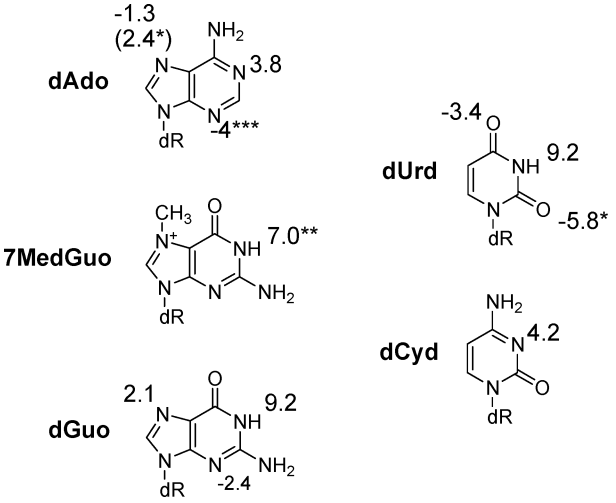

Figure 12. Sites of protonation and pK_a's for nucleobases. Nucleobases are shown in the dominant protonation states at pH 7.4, and pK_a's are indicated near the relevant atoms. pK_a's are for deoxynucleosides where possible, and they are for nucleosides otherwise.[129,136,139,160−163] The differences in pK_a between deoxynucleosides and nucleosides is modest, 0.2−0.4 at most positions. (*) pK_a for monoprotonation at O2 or N7; (**) pK_a increases to >9.5 in double stranded DNA, presumably because of Watson−Crick hydrogen bonding;[164] (***) estimated value.

nucleobases, uracil forms the most stable anion because of extensive resonance stabilization/charge delocalization on O2 and O4. At pH > 9, N3 becomes deprotonated, making departure as a dianion even less favorable. At pH < 1, the reactions are acid-catalyzed, likely through protonation at O4, which has p$K_a = -3.4$ in dUrd.[136] The rate versus H_0 profile does not plateau even at $H_0 < -5$, suggesting that protonation at O2 also becomes important. Given an equilibrium constant of 30 between O4- and O2-monoprotonation[139] with pK_a(O4) = −3.4, we can estimate pK_a(O2) = −5.9. UDG catalyzes uracil departure in the anion form,[140−144] likely a reflection both of the relative stability of the anion and the very low pK_a of O4, which would make general acid catalysis difficult.

dCyd hydrolysis has a plateau at pH 0−4,[136] indicating that it is not acid-catalyzed in this region and that cytosine departs in the neutral form. The decreasing rate, with pK_a = 3.8 corresponds well with pK_a = 4.2 for deprotonating N3 under somewhat different conditions. This indicates that protonation of N3 would be catalytically effective, enhancing catalysis up to (3×10^4)-fold at pH 7.4. The slight upward curve at pH < 1 indicates that cytosine hydrolysis is likely acid-catalyzed through O2, with pK_a < 0. To our knowledge, there are no known well-characterized examples of enzymatic dCyd hydrolysis, though there is evidence for glycosylase activity against 5MeC (see ref 6). Protonation at N3 should be effective and would likely be observed. While general acid catalysis at O2 would be expected to be effective, the pK_a may be too low for effective enzymatic protonation at this site.

There is little difference in the reactivity or nitrogen pK_a's of dUrd and Thd, which only differ by a 5-methyl group. The 3-fold lower rate for Thd in the pH-independent region represents the effect of the electron-donating methyl on the anionic leaving group. Similarly, dCyd and 5MedCyd differ 2-fold in rate in the pH-independent region.[136] We will not generally distinguish between the reactivities of dUrd and Thd or of dCyd and 5MedCyd.

Purine Nucleobases. *pH Range of Acid Catalysis.* Purine hydrolysis is strongly acid-catalyzed. The experimental pH profiles with dAdo and dGuo do not extend to physiological pH, but they do for DNA depurination. DNA depurination was acid-catalyzed at pH 4.5−7.4. As expected, the plot of log(k) versus pH was linear with a slope of −1 between pH 4.5 and 5.5 (Figure 11). Between pH 6.0 and 7.4, the plot was still linear, but with slope = 0.6. The cause of this deviation is not known, but the curve did not plateau at pH > 6.0, and the deviation from the expected rate at pH 7.4 was only 5-fold. Thus, despite this deviation, depurination was acid-catalyzed even at pH 7.4, well above the pK_a's of the ring nitrogens. The pH dependence of acid catalyzed adenosine was determined, and like dAdo, it was linear in the range examined, from $H_0 = -1$ to pH 3.8.[145]

Catalytic Enhancements through N-Protonation. The lack of a plateau in the high-pH region indicates that purine hydrolysis was acid-catalyzed at pH 7.4. It is possible to estimate the catalytic enhancement at pH 7.4 due to protonation of the most basic purine nitrogen, dAdo N1 (pK_a = 3.8), as (4×10^3)-fold ($=10^{(7.4-3.8)}$). There is circumstantial evidence that ricin protonates N1 in the target A residue of 28S ribosomal RNA. In minimal RNA substrates, the maximum rate was around pH 4.[146] This was attributed to ricin being unable to protonate N1 in the nonoptimal substrate, and was supported by calculations which showed that N1 protonation significantly decreased the activation energy for C−N bond cleavage.[24]

After N1, the most basic proton in dAdo is N7. The fact that the pH profile is linear in the range where N1 becomes protonated allows us to estimate the rate enhancement of N7. Considering for a moment only N1, we would expect the pH profile to plateau below its pK_a, 3.8, as dCyd does. The fact that the log(k) versus pH plots are linear in this region indicates either (i) that protonation at N1 is not catalytic, which contradicts other lines of evidence and is therefore unlikely, or (ii) a mathematical accident.[130] This mathematical accident is simply that the difference in pK_a's is equal to the ratio of rate constants. Given the dAdo N7 p$K_a \sim -1.3$ and N1 p$K_a = 3.8$,[147] the ratio K_{aN7}/K_{aN1} is 2×10^5. If the ratio of rate constants for the diprotonated (N7H, N1H) versus monoprotonated (N1H) forms, k_{N7}/k_{N1}, is also 2×10^5, then the pH profile will be a straight line below pH 3.8. Thus, the straight line in the dAdo hydrolysis profile indicates that dAdo breakdown is enhanced by $\sim(2 \times 10^5)$-fold by protonation at N7. (It seems an unlikely coincidence that the ratio of rate constants and acidity constants would match exactly, but various fits to the experimental data show that the pH dependence would appear linear within experimental error even if the ratios differed by a factor of 5.)

Direct evidence of the effectiveness of N7 protonation comes from the KIEs for acid-catalyzed dAMP hydrolysis in 0.1 M HCl, where the 7-^{15}N KIE was inverse. The inverse KIE indicates a tighter vibrational environment at the TS, indicating that it was protonated before or at the TS.[23] The inverse 7-^{15}N KIE = 0.981 ± 0.008 in ricin-catalyzed adenosine hydrolysis from RNA demonstrated the ricin used N7 protonation to promote catalysis.[24]

By the same reasoning, catalytic enhancement at pH 7.4 from protonation of dGuo N7 (pK_a 2.3) is 1×10^5-fold. Alkylation mimics some of the effects of protonation by placing a permanent positive charge on the purine ring; 7MedGuo was 2×10^4-fold more reactive than dGuo.[130] The same arguments also apply for dGuo N3. The dGuo pH profile was also linear, which translates to a 5×10^4-fold effect for protonation at N3.[148] The catalytic enhancements described here should only be regarded as guidelines.

Microscopic pK_a's. The macroscopic pK_a for dAdo N7, −1.3, represents formation of the dication after protonation of N1. The N7 microscopic pK_a of 9-methyladenine, *i.e.* protonation of N7 to form the monocation form, was 3.0,[129] corresponding to ∼2.4 in dAdo. This is important for enzymatic mechanisms because one of the most important talents of enzymes is their ability to protonate substrates site-specifically. While the macroscopic pK_a of dAdo N7 makes it appear strongly acidic, the microscopic pK_a is only 1.4 pH units lower than that for N1 and amenable to enzymatic protonation. Although microscopic pK_a's have not been reported, similar considerations undoubtedly apply for adenine N3 and guanine N3.

Alkylated Nucleobases. The two alkylation lesions that are the most relevant to BER enzymes are 7MeG and *N3*-methyl-2′-deoxyadenosine, 3MeA. Nucleoside methylation

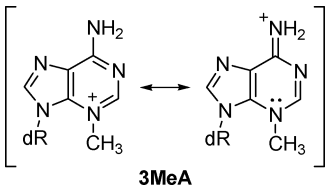

3MeA

has been extensively characterized.[149,150] 7MeG is relatively innocuous; however, the fact that cells effectively remove 7MeG with AlkA and AAG implies that it is not completely harmless.[150−152] 3MeA, 1MeA, and 3MeC all interfere with DNA replication. As well, the *N*-glycosidic bond of 3MeA is very unstable, with $t_{1/2} \sim 35$ min at pH 7 and 37 °C.[93] At least five BER enzymes can remove 3MeA, including TAG, MpgII, and MagIII, which are all 3MeA specific, and AlkA and AAG, which remove a variety of alkylated nucleobases.

The effect of alkylation is similar to protonation, creating a permanent positive charge on the nucleobase and increasing its reactivity dramatically. 7MedGuo undergoes nonenzymatic *N*-glycoside bond cleavage (2×10^4)-fold faster than dGuo (Figure 11). 3MedA is so extremely reactive because, based on the crystal structure of the 3-methyladenosine salt,[153] it exists in a quininoid-like form with N6 as an iminium ion and the double bonds localized within the ring. Cleaving the C1′−N9 bond restores aromaticity, making hydrolysis highly favorable. The effects of alkylation are reflected in the pK_a's of alkylated purines. In adenine, the N9 pK_a is 10.0, compared with 6.9 and 6.1 in 1-methyladenine and 3-methyladenine, respectively.[129,154,155] Decreased N9 pK_a's reflect the greater stability of the N9-unprotonated forms and improved leaving group ability.

Reactivity increases only if alkylation creates a positive charge on a formerly neutral nitrogen. 6-Methyladenosine (**2**) is only 2- to 3-fold more reactive than adenosine;[126] 1-methyldeoxyadenosine (**3**) is 3-fold less reactive than dAdo;[156] and 1,7-dimethylguanosine (**4**) is slightly less reactive than 7-methylguanosine.[130]

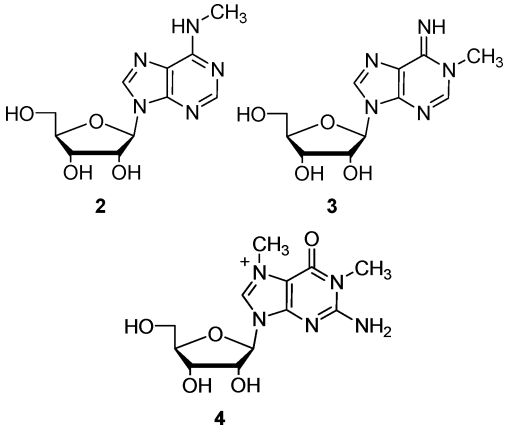

O-Alkylation is less common but more damaging. O2 alkylation of dCyd, dUrd, and Thd increased the rate of *N*-glycoside hydrolysis 10^4-fold.[157] The effect at O2 may be due to the same effect as N3-methylation of adenine, with the formation of a quininoid-like resonance form (dCyd) or a tautomer (dUrd, Thd). O4 alkylation of dUrd or Thd had little effect on reactivity, presumably because they can form neutral tautomers by N3 deprotonation.[157]

3.4. The Nature of Oxacarbenium Ions and Oxacarbenium Ion-like Transition States

O- and *N*-glycoside hydrolyses generally proceed through either oxacarbenium ion-*like* dissociative A_ND_N mechanisms or through stepwise D_N*A_N mechanisms with two oxacarbenium ion-*like* TSs, one for leaving group departure and one for nucleophile approach.[8,9,12] Interactions that stabilize an oxacarbenium ion will also stabilize an oxacarbenium ion-like TS. Thus, for simplicity we discuss interactions as stabilizing an oxacarbenium ion, even though the relevant species are the TSs.

Oxacarbenium ions are highly electrophilic, with essentially no barrier to nucleophilic attack.[165,166] The study of glycosylase mechanisms has often focused on understanding the nature of oxacarbenium ions and how their formation is stabilized by specific interactions with enzymes.

3.4.1. Geometry of Oxacarbenium Ions

Forming an oxacarbenium ion requires rehybridization of the anomeric carbon (C1′) from sp^3 to sp^2. There is increased π-bonding between C1′ and O4′, the ring oxygen, and between C1′ and C2′ to a lesser extent. The resonance forms imply a molecule that is somewhere between a carbocation, **5a**, and an oxonium ion, **5b**. A variety of experimental and

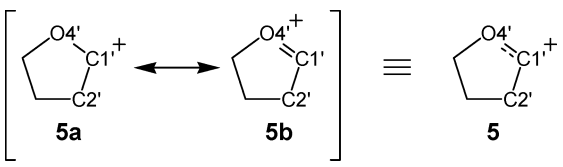

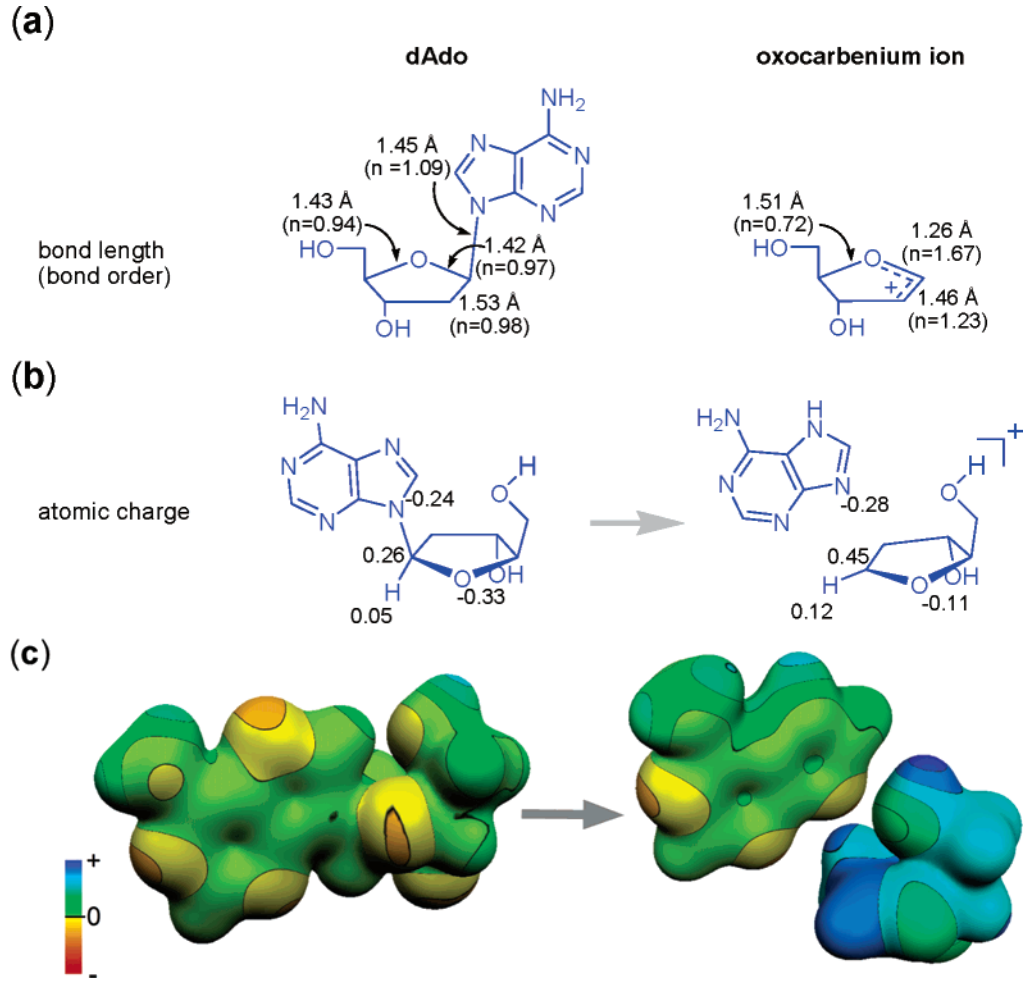

Figure 13. (a) Geometries of quantum mechanically optimized structures of dAdo and its oxacarbenium ion. Selected bond lengths and Pauling bond orders, *n*, are shown. The C1′−H1′ bonds were 1.096 Å ($n_{C1'-H1'} = 0.98$) and 1.091 Å ($n_{C1'-H1'} = 1.00$), respectively. (b) Selected atomic charges calculated by natural population analysis. (c) Electrostatic potential of dAdo and [oxacarbenium ion + adenine] in the same orientation as that in part b. The structures were optimized using a hybrid DFT method with Becke's exchange functional[177] and Perdew and Wang's correlation functional,[178] with the 6-31+G** basis set (RB3PW91/6-31+G**) using Gaussian 98.[179] Electrostatic potentials were mapped on isosurfaces at 0.01*e*/Å^3 and displayed using Molekel 4.3.[180]

computational approaches have demonstrated that the oxonium-like resonance form, **5b**, is predominant.[167−172] TS analysis supports this model; in TS structures derived from *ad hoc*,[25,27,29−32,36,37] structure interpolation,[33,35,41] and quantum mechanical approaches,[26,34] essentially all the loss in bond order upon leaving group departure is largely compensated by increases in the C1′−O4′ and C1′−C2′ bond orders. In the hydrolysis of nicotinamide from NAD^+, the sum of bond orders to C1′ ($\sum n_{C1'}$) was slightly higher in the TS than in the reactant. The loss of bond order to the leaving group was compensated by a larger increase in the bond orders between C1′ and the other ribosyl ring atoms, C2′, O4′, and H1′.

Similar effects are observed with deoxynucleosides. Comparing the computationally optimized structure of dAdo with its oxacarbenium ion, the C1′−O4′ and C1′−C2′ bond orders increase from 0.97 to 1.67 for $n_{C1'-O4'}$ and from 0.98 to 1.23 for $n_{C1'-C2'}$ (Figure 13). The total bond order to C1′, $\sum n_{C1'}$, decreases from 3.98 to 3.90, demonstrating again that leaving group departure is compensated by increased bonding within the deoxyribosyl ring. The extensive π-bonding around C1′ enforces a planar geometry.

While a number of deoxyribosyl ring conformations are possible in dAdo (predominantly 2′-*endo* in DNA), the oxacarbenium ion has two dominant ring conformations, 3′-*exo*-**1** and 3′-*endo*-**1**. In ribosyl oxacarbenium ions, 3′-*exo* is more stable because of hyperconjugation, but in deoxyribosyl oxacarbenium ions, both C2′−H2′ bonds can participate in hyperconjugation, lessening the angular dependence. With BER enzymes, the deoxyribosyl ring conformation will be strongly affected by the DNA backbone, which dictates the relative orientation of C3′ and C5′. Enzymes can control the ring conformation of the oxacarbenium ion.[22,24,26,173−175]

TS analyses have shown that all nonenzymatic *N*-glycoside hydrolyses and most enzymatic reactions form oxacarbenium ion-like TSs in the 3′-*exo* conformation. The 2′-^{2}H KIEs for UDG-catalyzed uracil hydrolysis were large and almost equal to each other, 2′S-^{2}H KIE = 1.10 and 2′R-^{2}H KIE = 1.11, indicating a dihedral angle around 30° for both hydrons, the maximal possible level of hyperconjugation.[21] These KIEs, combined with other studies, demonstrated that UDG enforces a conformational change on its target from the typical 2′-*endo* conformation in DNA to a flattened 3′-*exo* geometry in the oxacarbenium ion.

To date, small 2′-hydron KIEs have been observed with human thymidine phosphorylase (hTP),[46] ricin,[24] and human and malarial PNPs.[26] In hTP-catalyzed arsenolysis of thymidine, the 2′-^{3}H KIEs were small, (2′(R), 0.974; 2′(S), 1.036) because this reaction proceeded through a synchronous A_ND_N mechanism with little oxacarbenium ion character

(section 4.2). In ricin-catalyzed rA hydrolysis, 2′-^{3}H KIE = 1.01 due to a 3′-*endo* conformation enforced by the RNA backbone.[24] This agrees with the 2′-^{3}H KIEs measured for the ricin-catalyzed depurination of DNA, (2′(R), 1.146; 2′-(S), 1.117), which were consistent with a 3′-*endo* geometry at the TS.[22] Inosine arsenolysis reactions catalyzed by hPNP and mPNP proceeded through a stepwise D_N*A_N mechanism with a discrete oxacarbenium ion intermediate but had 2′-^{3}H KIEs of 1.031 and 1.036, respectively, which were in reasonable agreement with the calculated EIE for formation of the oxacarbenium ion in the 3′-*endo* conformation, 1.058, and much lower than that for the 3′-*exo* conformation, 1.21. Interestingly, bovine PNP, which shares 86% sequence identity with hPNP, had a 2′-^{3}H KIE = 1.13 for the same arsenolysis reaction. There is no compelling reason hPNP would not be able to stabilize the 3′-*exo* conformation, so the selection of a 3′-*endo* ring conformation is an interesting anomaly. The fact remains that most enzymes and all nonenzymatic hydrolyses to date proceed through a 3′-*exo* ring conformation which allows strong hyperconjugation between C2′−H2′ and C1′.

3.4.2. Charge Distribution in Oxacarbenium Ions

The +1 charge on an oxacarbenium ion is centered at the anomeric carbon, C1′, but is delocalized around the sugar ring (Figure 13). This is the site of the largest change in charge, where an enzyme can best stabilize an oxacarbenium ion electrostatically. Although the ring oxygen is formally trivalent in the dominant oxonium resonance form, **5b**, quantum mechanical calculations showed it still bears a negative charge in the oxacarbenium ion. As discussed recently,[12,176] electronic structure calculations demonstrate that the ring oxygen of an oxacarbenium ion is still negatively charged, and experimental evidence supports this conclusion.

When an oxacarbenium ion forms, π-bonding develops between C1′ and O4′, and the charge on O4′ increases but is only −0.11 in the deoxyribosyl oxacarbenium ion (Figure 13) compared with −0.33 in dAdo. Assigning atomic charges in molecules is somewhat arbitrary, but different charge calculation methods give essentially the same result. More importantly, electrostatic potential surfaces also demonstrate that the ring oxygen remains more electron rich than C1′. With a ribosyl oxacarbenium ion, the electrostatic potential around O4′ remained negative,[12] while, in a deoxyribosyl oxacarbenium ion, it is slightly positive because the charge at C1′ was not reduced by the electron-withdrawing 2′-hydroxyl substituent (Figure 13). Nonetheless, O4′ remained electron rich compared to C1′. Electrostatic potential surfaces present a true picture of the energetics of an external charge interacting with an oxacarbenium ion.

These computational results are supported by four lines of experimental evidence. (1) 1-Aza-sugar inhibitors such as isofagomine (**6**), where the nitrogen atom is situated in a position analogous to the anomeric carbon, are extremely potent inhibitors of β-glycosidases and often better inhibitors than the 5-aza inhibitors such as deoxynojirimycin (**7**), where the nitrogen atom is located at a position analogous to the ring oxygen.[181−186] (2) Some enzymes that bind deoxynojirimycin-type inhibitors also bind with similar inhibition constants to *N*-methylated inhibitors.[187,188] Undiminished binding despite the increased steric bulk around the ring nitrogen argues against tight, direct interactions between the enzyme and the positively charged amino group. (3) The X-ray crystallographic structures of enzymes complexed with 4-aza-sugar (also called iminoribitol or pyrrolidine) inhibitors do not show strong enzyme interactions with N4′. In the bPNP·immucillin H (**8**) crystal structure, the closest contacts with N4′ were Oβ of Ser33 at 3.7 Å and the backbone carbonyl oxygen of Ala116 at 4.0 Å, both distant interactions.[86] Similarly, nucleoside hydrolases, NH IU from *Crithidia fasciculata* (CfNH IU),[65] purine phosphoribosyl transferase,[189] and malarial PNP (mPNP)[92] all failed to form tight interactions with N4′. As the inhibitors were nearly isosteric with the substrates, this can be taken as evidence against stabilization of the oxacarbenium ion through contacts with the ring oxygen. Although 4-aza inhibitors of PNP bound most tightly when protonated at N4′, they initially bound in the neutral form and protonation was slower than catalysis, 0.1 s^{-1}, demonstrating that PNP was unable to deliver a proton to N4′.[190] In the BER enzyme context, in the hAAG·pyrrolodine crystal structure, the closest contact with N4′ was the hydroxyl of Tyr127 at 3.4 Å.[191] The crystal structure of hUDG with a 1-azadeoxyribose (**1**·aza-dR) inhibitor and uracil, hUDG·1-aza-dR·uracil, showed that the closest approaches to C4 (equivalent to O4′) were the backbone oxygens of Asp145 and Pro146, too distant at 3.6 Å to form strong interactions.[174] (4) A diphtheria toxin·TS model was created based on the diphtheria toxin·NAD^+ crystal structure.[35,192] The anomeric carbon in the TS model was located directly adjacent to the carboxylate of an invariant Glu. The nearest protein contact to O4′ was with the hydroxyl of Tyr65, with an oxygen−oxygen distance of 3.1 Å. There were no negative charges located near the ring oxygen. Taken together, these data suggest that the oxacarbenium ion intermediate or oxacarbenium ion-like TS has significant C=O double bond character from charge delocalization/resonance stabilization, but the positive charge remains on the anomeric carbon, C1′, despite the fact that the oxygen atom is formally trivalent (**5**). Because of extensive π-bonding stabilization from the ring oxygen, the positive charge on C1′ is less than it would be in an unstabilized carbocation.

The fact that 4-aza- and 5-aza-sugar compounds, such as deoxynojirimycin (**7**), an *O*-glycosidase inhibitor, are often effective glycosidase inhibitors[89,188,193−202] is likely a function of the positive charge being close enough to the site of the positive charge at C1′ to interact with whatever enzymic residues stabilize the oxacarbenium ion.

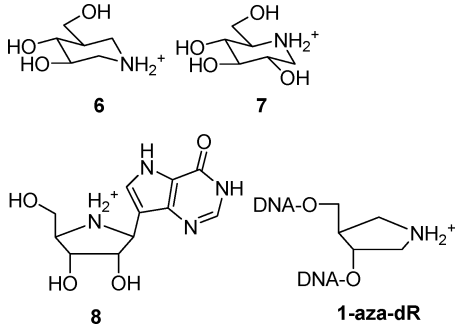

The presumed positive charge on the ring oxygen, O4′, in the oxacarbenium ion has been invoked to explain enzymatic oxacarbenium ion stabilization. In particular, carboxylate side chains positioned near O4′ have been postulated to stabilize the oxacarbenium ion by stabilizing the positive charge on the ring oxygen.[96,105,203] The evidence cited above argues that placing a negative charge adjacent to O4′ would not be catalytically effective.

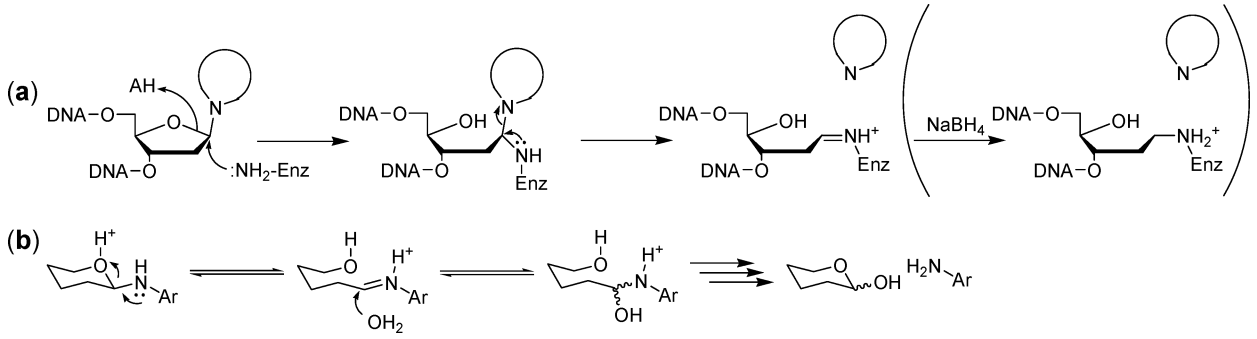

Figure 14. Proposed endocyclic mechanism for (a) enzymatic nucleoside cleavage and (b) nonenzymatic glycosylamine hydrolysis.

3.5. Endocyclic versus Exocyclic Hydrolysis

A number of BER enzymes have been proposed to catalyze *N*-glycoside cleavage through an endocyclic mechanism, *i.e.*, by first breaking the C1′−O4′ bond to open the sugar ring and then cleaving the C−N bond. Thus far, only bifunctional enzymes have been proposed to function through this mechanism, where the nucleophile is an enzyme-based amine, either a Lys side chain or the *N*-terminal α-amino group, Nα (Figure 14).

Nonenzymatic hydrolysis of nucleosides was initially believed to proceed through an endocyclic mechanism, but by the time of Capon's 1969 review, the consensus view had shifted toward direct C−N fission, the current model of nucleoside hydrolysis.[7] There was good evidence for a endocyclic hydrolysis of glycosylamines because mutorotation was faster than hydrolysis. Sugar ring fission is aided by resonance stabilization of the ring-open form by the amine forming an imine. Such stabilization is less likely with nucleosides because the aromatic nitrogens at N1 (pyrimidines) or N9 (purines) cannot donate lone pair electrons. There was some support for an endocyclic mechanism for Thd and dUrd (but not dCyd) hydrolysis in 2 M $HClO_4$ at 90 °C based on formation of the α-anomer and pentopyranosyl *N*-glycosides during hydrolysis.[132] However, even under these extreme conditions, these were minor products compared to those of direct C1′−N1 cleavage. In another study, dAdo anomerization was observed after γ-irradiation; however, this reaction involved free radicals and would not be relevant to acid- or enzyme-catalyzed heterolytic reactions.[204] Thus, the nonenzymatic precedent seems to favor direct C−N bond cleavage, with the endocyclic mechanism a minor pathway in some cases.

The exception to aromatic N9 atoms in purines is the formamidopyrimidine (Fapy) breakdown products of purines (*e.g.*, FapyA), which may have more accessible lone pair electrons in N9, depending on the amount of resonance stabilization into the pyrimidine ring. A FapyA derivative underwent facile α/β-anomerization with $t_{1/2} = 3.2$ h, a reaction that would proceed through a ring-opened Schiff base.[205] On the basis of the glycosamine precedent, these derivatives would be more prone to endocyclic cleavage than nucleobases with intact five-membered rings.

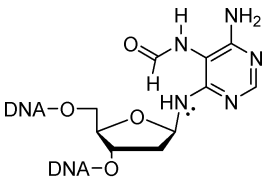

FapyA

The first proposal of an endocyclic mechanism for a BER reaction was for endonuclease III,[206,207] and this has since been proposed for several other bifunctional BER enzymes, including FPG,[98,207] Nei,[207,208] and PDG.[207] Any discussion of endocyclic mechanisms is complicated by the facts that, (i) to date, there has been little experimental evidence that addresses the question of enzymatic endocyclic versus direct fission mechanisms and (ii) the deoxyribosyl ring must be opened anyway for the β-elimination reaction (so it is not surprising to observe Glu or Asp residues poised to protonate O4′, and crystal structures with ring-opened product analogues).

In considering the likelihood of endocyclic mechanisms, it is worth considering that (i) many of the bifunctional BER enzymes belong to the same superfamilies as monofunctional BER enzymes, indicating that they have (or previously had) the ability to cleave *N*-glycosidic bonds by the "normal" direct fission route, and (ii) eMutY, a monofunctional glycosylase, was mutated to have β-elimination activity simply by adding a Lys residue to the active site (Ser120Lys).[209] This demonstrated both that β-elimination is not a catalytically demanding step and that bifunctional versus monofunctional activity is not a strongly conserved characteristic in BER enzyme superfamilies, in contrast to the glycosylase reaction. Many mutations that reduce or abolish glycosylase activity in bifunctional enzymes have modest or negligible effects on the lyase activities.[100,208,210−212]

Other evidence offered in favor of endocyclic mechanisms was the fact that a number of bifunctional enzymes could degrade urea nucleoside (**9**) and *N*-hydroxylamine compounds (**10**).[207] This evidence was not unambiguous, however, because (i) the reaction products were only characterized by band positions on gel electrophoresis and some reactions gave unexpected products, (ii) all the bifunctional enzymes degraded **9** and **10** at identical rates despite widely differing *N*-glycoside specificities, implying that, however they were degraded, it was not using the glycosylase catalytic machinery, and (iii) the mechanism of **10** breakdown was not characterized. It was only demonstrated that the enzymes were capable of acting on **10**, not that breakdown was relevant to the glycosylase mechanism.

Another piece of evidence advanced in favor of endocyclic cleavage[5] was that UDG, a monofunctional enzyme, was reported to be unable to cleave 4′-thiodU (**11**) substrates.[213] However, it was later reported to be a poor substrate.[173] In either case, it is known that thiosugars are not glycosylase substrates, or extremely poor ones, with isopropyl thiogalactoside (IPTG) being the best known example.[8] The weak activity of UDG against **11** is not evidence for an endocyclic mechanism.

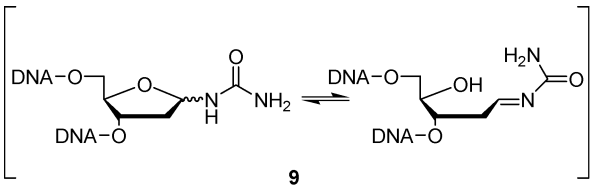

9

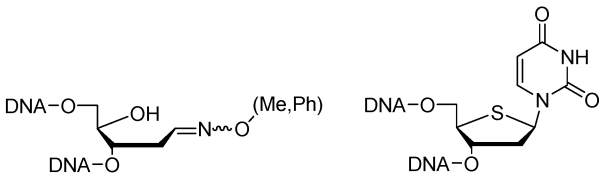

10 11

Given the lack of direct evidence for an endocyclic mechanism, the fact that bifunctional BER enzymes are extremely competent *N*-glycosylases which evolved from enzymes that use normal, direct cleavage mechanisms, and the overwhelming preponderance of evidence favoring direct C−N cleavage in other *N*-glycoside reactions, all BER enzymes likely follow a C−N direct cleavage model.

3.6. Catalytic Strategies

3.6.1. Enzymatic Strategies for Promoting Nucleobase Departure

The studies on nonenzymatic *N*-glycoside hydrolyses discussed above demonstrate that the strategies available to enzymes for promoting leaving group departure will depend on the identity of the leaving group.

Pyrimidine Departure. In principle, departure of uracil, thymine, and cytosine can be acid-catalyzed by protonation of O4 or O2. However, in the only clear precedent, UDG catalyzes uracil departure in the anion form.[140−144] This catalytic strategy may reflect the fact that uracil has a relatively stable anion form and that O4 has such a low pK_a that protonation would be difficult. UDG stabilizes the uracil anion by 4.6 kcal/mol relative to the neutral form, as evidenced by the change in the N1 pK_a from 9.8 in solution to 6.4 in the UDG active site.[214] The 5-methyl group of T has little effect on its reactivity, so similar catalytic strategies for T-hydrolyzing enzymes are possible. Cytosine has only one carbonyl oxygen to delocalize negative charge, making its anion less stable than uracil, as reflected by the pK_a of N1 = 12.2, compared with that of uracil, 9.5, and its slower nonenzymatic hydrolysis. In addition, O2 is very acidic, so it is not clear what catalytic strategies will be used by C-hydrolyzing enzymes. One possibility is that enzymes targeting C could proceed through synchronous A_ND_N TSs such as that observed for hTP,[46] avoiding large accumulation of charge on the cytosine ring at the TS.

Purine Departure. In the two enzymatic reactions and one nonenzymatic reaction where 7-^{15}N KIEs were measured, TS analyses demonstrated purine departure was acid-catalyzed by N7 protonation. The 7-^{15}N KIE was 0.981 for ricin-catalyzed rA hydrolysis.[24] It was also inverse for MutY-catalyzed A hydrolysis, and acid-catalyzed dAMP hydrolysis.[23] The inverse 7-^{15}N KIEs reflect protonation at or before the TS. There was also some kinetic evidence that ricin normally protonates N1 of adenine, placing two charges on the ring in the reactant.[146] While most purine *N*-glycosylases are expected to promote leaving group departure through protonation, important questions include the site(s) of protonation and the source of the proton. The microscopic pK_a's of adenine indicate that N7 is only 1.4 pH units less basic than N1, making it a reasonable candidate for enzymatic protonation.

Even in crystal structures with good substrate analogues, or TS mimic inhibitors, the source of the catalytic proton is not always obvious. A likely candidate, eMutY_Glu37, was identified in the eMutY·adenine crystal structure based on close contacts between N7 and Oϵ, with distances of 2.8 and 3.1 Å.[215] Almost identical contacts were observed when adenine was soaked into a crystal of a mutant *B. stearothermophilus* MutY, bMutY_Asp144Asn, with a reduced AP (RAP) site.[203] However, different contacts were observed with bMutYAsp144Asn cocrystallized with a substrate, OG:A DNA. Adenine was oriented differently, making only water-mediated contacts with bMutY_Glu43 (equivalent to eMutY_Glu37). Thus, it was not clear whether N7 protonation is directly from the catalytic Glu residue or indirectly via water (Figure 15).

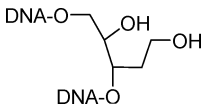

RAP

The source of N7 protonation with bPNP was also not obvious (Figure 16).[86,88] The 7-^{15}N KIEs have not been measured, but N7 protonation was supported by inhibitor and product complex structures where there was a hydrogen bond between bPNP_Asn243 Oδ and N7H. Hydrogen bonds to O6 and N1H of the hypoxanthine ring in the Michaelis complex became shorter with a TS mimic inhibitor, and the hydrogen bond to N7H was formed. The bPNP_Asn243Ala mutation decreased TS stabilization by 4 kcal/mol, demonstrating the importance of this interaction,[216] which persisted in the product complex. The enzyme can stabilize protonated

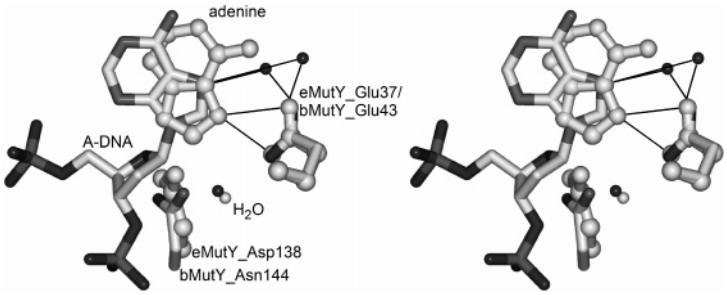

Figure 15. Stereoview of conserved Asp interactions with substrate and the presumed water nucleophile. The mutant structure, bMutY_Asp144Asn·(OG:A), is shown as the stick model with N and P atoms as gray and O atoms as black. eMutY_Lys20Ala·adenine is shown as the all white ball-and-stick model.

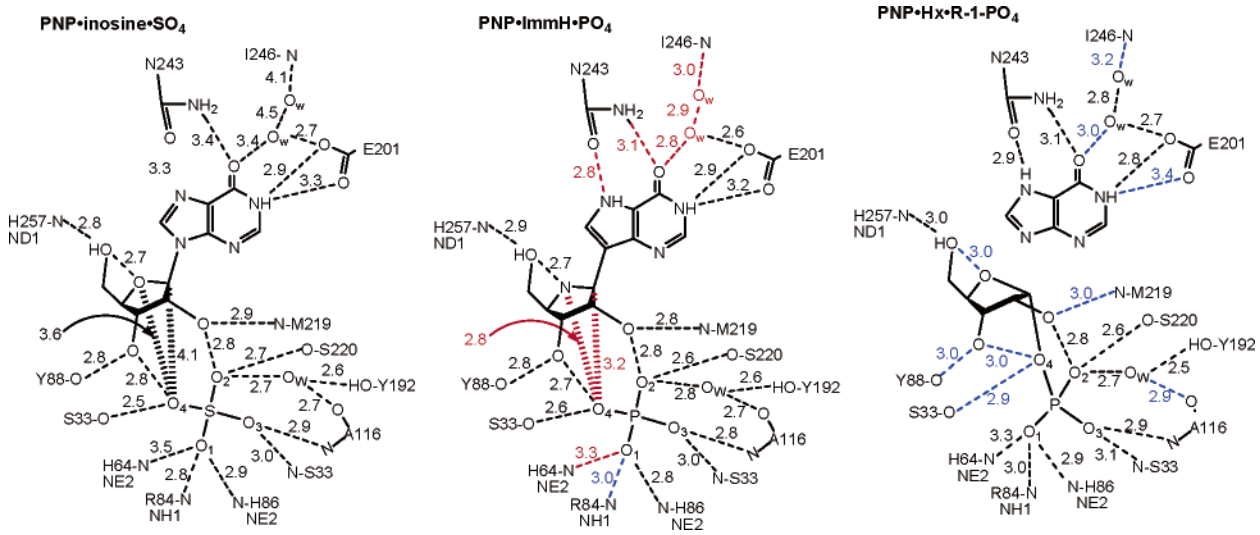

Figure 16. Catalytic contacts revealed by crystal structures of bPNP. (left) bPNP•inosine•SO4, which resembles the Michaelis complex; (center) bPNP•immucillin H•PO_4, a TS mimic inhibitor; (right) bPNP•ribose 1-phosphate•hypoxanthine, product complex. (red) Hydrogen bonds that become shorter in the TS mimic complex. (blue) Hydrogen bonds that become longer in the product complex. (Reprinted with permission from ref 17. Copyright 2003 American Chemical Society.)

N7, but it is not clear where proton comes from, as there are no acidic residues nearby. Protonation was proposed to be via two crystallographic waters, either directly or through the intermediacy of O6. These waters were in contact with bulk solvent. Thus, while there is good evidence for general acid catalysis through N7, the protonation route is nonintuitive.

Similar questions arose with AAG, a monofunctional BER enzyme.[217] pH profiles indicated general acid catalysis, but mutagenesis of the putative acid catalysts, hAAG_His136, hAAG_Tyr159, and hAAG_Tyr127, showed <40-fold decreases in rate. Alternatively, a water in the hAAG_Glu125Gln•(T:ϵA) crystal structure was close to N7 and part of a network that could pass a proton to N7 from bulk solvent. The driving force for protonation from bulk water was not obvious.[191] Identifying the source of N7 protonation with TvNH IAG was also problematic (see below).

Alkyl Nucleobases. A hypothetical mechanism that was proposed[1] for leaving group activation in alkylpurine BER enzymes has, in fact, been observed with diphtheria toxin, an ADP-ribosylating enzyme. The proposal was that binding cationic nucleobases in a hydrophobic site would activate them for departure because interaction of the positively charged nucleobase with the hydrophobic pocket would be less favorable than that of the neutral, aromatic nucleobase after C1′−N bond cleavage. TS analyses of diphtheria toxin reactions[34,35] and examination of diphtheria toxin•NAD^{+}[192] and diphtheria toxin•TS structures revealed that the positively charged nicotinamide ring of NAD^+ bound in a hydrophobic pocket. With the C1′−N1 bond largely broken at the TS, the nicotinamide ring becomes neutral, improving its binding in the hydrophobic pocket. This lowers the energy difference between the reactant and TSs by increasing the energy of the positively charged reactant relative to the neutral TS, an example of ground-state destabilization. The same mechanism for nucleobase activation is plausible for the cationic nucleobases and may be operative in enzymes such as TAG, AlkA, and AAG (sections 5.3.5, 5.3.6, and 5.5).

Other Mechanisms of Leaving Group Activation. Identifying the source of N7 protonation appears to be a common problem. There was no obvious candidate to protonate N7 in the structure of a purine-specific nucleoside hydrolase, NH IAG from *Trypanosoma vivax* (TvNH IAG).[218] A later mutagenesis and computational study presented evidence that aromatic face-to-face stacking of the purine ring with TvNH IAG_Trp260 could raise the N7 pK_a.[219] This interesting proposal is reasonable in the context of TvNH IAG, but it should be remembered that DNA depurination is 4-fold slower in native versus denatured DNA,[126] indicating that aromatic face-to-face interactions do not invariably lead to increased reactivity.

Another catalytic interaction was proposed for the same enzyme involving an C8−H ···O5′ hydrogen bond.[176] C−H bonds are weak hydrogen bond donors,[220,221] capable of forming hydrogen bonds with O. In this case, the hydrogen bond is proposed to help increase the pK_a of N7 in purine substrates. Along with the effect of aromatic face-to-face stacking, this was proposed to raise the pK_a enough to allow N7 to abstract a proton directly from bulk water. One piece of evidence advanced in support of this mechanism was the effect of 5′-deoxy substrates. The value of k_{cat}/K_M decreased by 6000-fold with 5′-deoxyguanosine compared with guanosine, while it decreased only 50-fold with 5′-deoxy-7-methylguanosine compared to 7-methylguanosine. 7-Methylguanosine has a permanent positive charge on the purine ring and does not require protonation to depart. These results were interpreted as supporting the role of the 5′-hydroxyl in raising the pK_a of N7. One caveat is that the values of k_{cat}/K_M were almost identical for guanosine (1.0×10^6 M^{-1} s^{-1}) and 7-methylguanosine (1.7×10^6 M^{-1} s^{-1}) despite the (2×10^4)-fold higher reactivity of the methylated nucleobase.[130] This implies either that a step other than C1′−N9 cleavage was reflected in k_{cat}/K_M or that TvNH IAG interacts 10^4-fold more strongly with guanosine. If that were the case, the cooperativity of interactions[222,223] would ensure that the detrimental effect would be greater for the better substrate than for the worse substrate, *i.e.*, guanosine versus 7-methylguanosine.

3.6.2. Oxacarbenium Ion Stabilization versus Leaving Group and Nucleophile Activation

Although most glycosylases stabilize an oxacarbenium ion-like TS, it appears that they do not all interact equally

strongly with that portion of the TS molecule. While TS analysis can elucidate the TS structure, it cannot directly demonstrate which interactions are energetically important in forming the TS.

Oxacarbenium Ion Stabilization versus Leaving Group Activation. One approach for probing oxacarbenium ion binding is using *p*-nitrophenyl riboside (**12**) as a nucleoside hydrolase substrate.[224] *p*-Nitrophenolate is an excellent leaving group which does not require general acid catalysis. Nucleoside hydrolase IU (NH IU) is nonspecific, hydrolyzing both purine and pyrimidine nucleosides with good efficiency. Given its lack of leaving group specificity and the differing catalytic requirements of purine and pyrimidine leaving groups, NH IU might be expected to operate primarily through oxacarbenium ion stabilization and/or nucleophile activation. This is borne out by (i) its excellent catalytic efficiency with **12**, $k_{cat}/K_M = 4 \times 10^6$ M^{-1} s^{-1},[224] (ii) the

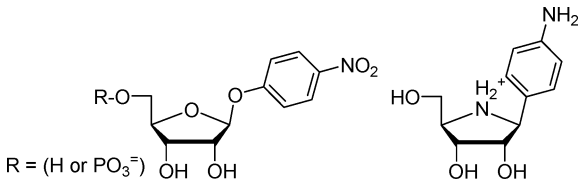

12 **13**

fact that it was inhibited by a wide variety of oxacarbenium ion mimic inhibitors with little specificity for the atoms corresponding to the leaving group,[225] and (iii) the crystal structure of NH IU·**13**, a 4-aza-sugar inhibitor.[65] There were extensive hydrogen bonding and ionic interactions between the enzyme and the ribosyl ring mimic, including to the catalytic Ca^{2+} ion, but few direct contacts with the "leaving group" atoms. It would appear that the catalytic activity of NH IU arises predominantly through interactions in the ribosyl ring, a view that is supported by the fact that 2′-, 3′-, and 5′-deoxynucleosides are poor substrates and deoxy-4-aza-sugars are similarly poor inhibitors.

In contrast, some enzymes appear to function more by leaving group and/or nucleophile activation. Nucleoside hydrolase GI hydrolyzed **12** poorly, with $k_{cat}/K_M = 10^2$ M^{-1} s^{-1}, and was weakly inhibited by compounds that were effective against NH IU.[224] This indicated weaker interactions with the ribosyl ring, even though it also proceeds through an oxacarbenium ion-like TS.[17] bPNP had $k_{cat}/K_M = 1$ M^{-1} s^{-1} for phosphorolysis of **12**[224] while tuberculosis PNP was poorly inhibited by a 4-aza-sugar inhibitor (**14**), with K_d = 2.9 mM.[226] Related inhibitors with purine ring analogues bound with K_d's as low as 28 pM. The structures of bPNP with TSs,[25,30] substrate analogues, a TS mimic inhibitor, and products (see ref 86) showed that it formed multiple, tight interactions with the leaving group (hypoxanthine) and the nucleophile (phosphate) but made few contacts with the ribosyl ring. These enzymes would be classified as leaving group/nucleophile activating.

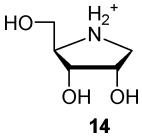

14

It is somewhat artificial to divide enzymes into "oxacarbenium ion stabilizing" and "leaving group/nucleophile activating", as there is undoubtedly a continuum of catalytic strategies and all enzymes likely use some combination of both strategies. An additional caveat is that this analysis assumes that 4-aza-sugar inhibitors are good oxacarbenium ion mimics. This appears to be a reasonable assumption in many cases, but it should be remembered that the positive charge in oxacarbenium ions is centered around C1′, while it is centered on the nitrogen in 4-aza-sugars. Nevertheless, this is a useful distinction from the point of view that even when an enzyme forms an unstable intermediate, that does not necessarily mean that it interacts strongly with that intermediate. This method of classifying enzyme activities is an empirical relation that has so far proven useful in describing enzyme catalytic strategies.

Application to BER Enzymes. There is some evidence that AlkA interacts strongly with the oxacarbenium ion while MutY does not. AlkA is nonspecific for nucleobases, showing the same catalytic enhancement for the natural nucleobases and alkylated nucleobases.[151] Given that fact that there are few or no common features present in the base portion of all its substrates, AlkA might be expected to catalyze hydrolysis through strong interactions with the oxacarbenium ion. This is reflected in the very tight binding with a 4-aza-dR inhibitor, K_d = 16 pM, compared to that with a THF inhibitor, K_d = 45 nM.[227]

4-aza-dR **THF**

The same types of inhibitors interacted differently with MutY, an enzyme that is specific to A residues in OG:A or G:A base pair mismatches. It had the K_d values for DNA containing OG:4-aza-dR (65 pM) and OG:THF (45 pM) base pairs. MutY forms highly oxacarbenium ion-like species during catalysis;[23] the indifferent 4-aza-dR binding implies that it does not form strong, direct interactions with the deoxyribosyl ring. Presumably, TS stabilization in MutY comes from interactions with the adenine nucleobase and/or the water nucleophile.

UDG illustrates some limitations in classifying enzymes as oxacarbenium ion binding or not. It did not detectably bind 4-aza-dR- or THF-containing inhibitors,[227] and it bound 1-aza-dR-containing DNA with the same K_d's as those for THF-containing DNA.[144] On the basis of this evidence, it would be classified as leaving group/nucleophile activating. However, 1-aza-dR binding became (2×10^5)-fold tighter in the presence of uracil, forming a ternary UDG·1-aza-dR·uracil anion complex, clearly indicating strong interactions between UDG, the oxacarbenium ion mimic, and uracil anion. In this circumstance, UDG appears to interact very strongly with the oxacarbenium ion mimic. Thus, enzymes such as MutY that are described as not binding oxacarbenium ions may in fact do so very tightly in the presence of their cognate nucleobase.

3.6.3. Electrophile Migration

The "electrophile migration" model of catalysis was developed from studies of bPNP. Nucleophilic substitutions are commonly described in terms of nucleophile attack and leaving group departure, but the view that emerges with bPNP is that it tightly binds the leaving group and nucleophile and then the electrophile carbon migrates from one site to the other.

bPNP makes extensive contacts with the purine ring to promote catalysis, as seen in the crystal structures with a Michaelis complex analogue, PNP·inosine·sulfate, a product complex, PNP·α-D-ribose-1-phosphate·hypoxanthine,[88] and a 4-aza-sugar inhibitor,[86] immucillin H. There were numerous contacts with the purine ring and the phosphate/sulfate but relatively few with the oxacarbenium ion (Figure 16). Phosphate made a 100-fold contribution to k_{cat},[89] and there was Raman spectroscopy evidence that it is activated by the enzyme for nucleophilic attack.[228] The phosphate anion was located directly beneath the ribosyl ring. In combination with the lone pair electrons of O5′, it could create an electron-rich "sandwich" to stabilize an oxacarbenium ion. *p*-Nitrophenyl β-D-ribofuranoside was a very poor substrate for phosphorolysis.[224] A major driving force for catalysis, then, appears to be stabilization of the purine ring leaving group. The bPNP·immucillin H structure showed hydrogen bonds with N7, O6, and N1H of the purine ring analogue, as well as water-mediated contacts that appear to be the source of the proton at N7 that promotes hypoxanthine departure. Catalysis through leaving group stabilization is further supported by the tight binding of product hypoxanthine, with $K_d = 1$ pM.[89]

Thus, the mechanism involves the leaving group purine and the nucleophile phosphate being tightly bound. The ribosyl ring, which makes few contacts with the enzyme, moves from the immobile leaving group to the immobile nucleophile—an electrophile migration. Since the original proposal, several other enzymes have been described as using electrophile migration, including UDG,[174] APRTase,[229] hen egg white lysozyme,[230] and α-l-arabinofuranosidase.[231] The two defining characteristics of electrophile migration are as follows: (i) The sugar ring undergoes a larger movement in the active site than the leaving group or nucleophile. (ii) The enzyme makes few contacts with the sugar ring throughout the catalytic cycle from substrate, to TS(s) and intermediates, to product.

3.6.4. Nucleophile Activation or Electrostatic Stabilization?

The crystal structures of some monofunctional BER enzymes, as well as the bacterial ADP-ribosylating toxins, have a carboxylic residue, either Asp or Glu, poised near C1′ of the substrate.[192,213,215] As these residues have been shown to be catalytically important, the question arises what their role is. On the basis of their positioning, they could be acting (i) as general base catalysts to activate the approaching nucleophile (usually water), (ii) through electrostatic stabilization of the oxacarbenium ion-like TS, or (iii) by taking both roles. If this residue is acting as a general base, its protonation would reduce its ability to electrostatically stabilize the oxacarbenium ion, though a charge−dipole interaction through the carbonyl oxygen of the (now neutral) carboxylic acid could still be favorable.

No existing experimental technique seems likely to resolve this question directly; however, several lines of evidence are suggestive. Inverting *O*-glycosidases, which have similar catalytic imperatives to *N*-glycosidases, use general base catalysis to activate the incoming nucleophile water,[9,10] but in at least two high-resolution crystal structures with oligosaccharide ligands bound in the active site, this general base residue was not positioned to provide electrostatic stabilization to an oxacarbenium ion-like TS.[232,233]

The crystal structures of several nucleoside hydrolases, including MTA nucleosidase (Scheme 3),[234] and nucleoside

Scheme 3

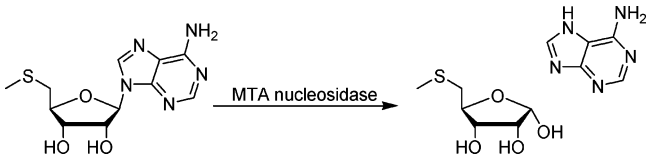

hydrolases IU[65,235] and IAG[236] are informative. MTA nucleosidase is a member of the same superfamily as bPNP. There was a carboxylate residue, Glu12, in MTA nucleosidase located to act as a general base catalyst, well below the ribosyl ring but in contact with the presumed nucleophile, water. It was located 4.8 Å from C1′ of the substrate analogue, almost in line with the C1′−N9 bond, and therefore unlikely to stabilize an oxacarbenium ion electrostatically. The NH IU and IAG structures similarly possessed Asp residues positioned to act as general base catalysts but below the plane of the ribosyl ring and unable to provide electrostatic stabilization. The crystal structures of a mutant NH IAG with a substrate, inosine, or an inhibitor bound in the active site had a residue, Asp40, positioned within 3.1−3.4 Å of C1′ and in the plane of the ribosyl ring. This position could lend itself to electrostatic stabilization of an oxacarbenium ion. However, the Asp40Ala mutation caused only a modest 5- to 10-fold decrease in k_{cat}/K_M.[236] The nucleoside hydrolase structures therefore appear to support the importance of a general base catalyst role more than electrostatic catalysis.

In three crystal structures of human AAG, Glu125 coordinated with a potential water nucleophile positioned directly below the deoxyribosyl ring, in line for nucleophilic attack at C1′ (section 5.5).[191,217,237] Mutations to Glu125 to Gln or Ala caused large rate decreases,[217] though Asp caused only a 15-fold effect. Glu125 was not positioned to electrostatically stabilize an oxacarbenium ion. This BER enzyme also provides support for a role for general base catalysis.

In contrast, Asp238 in AlkA appeared in a cocrystal structure with a 1-aza-dR inhibitor to be positioned by surrounded side chains specifically to interact with the positive charge on N1′.[238] This would provide some support for a role in electrostatic stabilization. On the basis of the above evidence, it would appear that there is good support for a role as general base catalyst in BER enzymes which possess an acidic residue near C1′, with some support for a role in electrostatic stabilization.

4. TS Analysis and Mechanisms of Individual Enzymes

Only one BER enzyme, *E. coli* UDG (eUDG), has so far been subjected to TS analysis with multiple KIEs.[21] Fortunately, TS analyses of other enzymes and nonenzymatic reactions help shed light on BER enzyme chemistry. There have also been numerous TS analysis studies on *O*-glycoside hydrolyses, as reviewed recently.[12]

4.1. Uracil DNA Glycosylase

eUDG removes uridine residues from DNA which arise from spontaneous deamination of cytidine residues or misincorporation of dUTP. Cytosine deamination in DNA to uracil occurs 100−500 times per human cell per day, generating G:U mismatches, which become transition mutations to A:T if the damaged DNA is replicated.[239] Misincorporation of dUTP can also occur, generating A:U

mismatches during DNA replication.[240,241] Apart from TS analysis of eUDG,[21] the catalytic mechanisms of eUDG, hUDG, and hsvUDG have been elucidated in detail by NMR,[140,141,242−246] X-ray crystallography,[141,173,174,213,247−251] Raman spectroscopy,[142] mutational analysis,[140,141,144,175,214,252−254] inhibitor studies,[121,122,144,255] and computation.[256,257] These studies have addressed how UDG searches DNA for uracil residues, the conformational changes involved in flipping the target residue into the active site, plus studies of the chemical steps. Many of the mechanistic findings have been reviewed in detail[1,258] and are outlined briefly below. Detailed knowledge of the UDG mechanism provides the basis to infer mechanistic details of the other members of the UDG superfamily.

4.1.1. TS Analysis

KIEs were measured on a single stranded trinucleotide substrate (pUAddG, ddG = 2′,3′-dideoxyG). A novel dual-label technique was used whereby a nonradioactive isotopic label of interest, *e.g.*, 1′-^{13}C, was placed in the deoxyribosyl ring and a radiolabel, 2-^{14}C, was placed in the uracil ring to act as a reporter on the label of interest. A tritium label in the uracil ring, 5-^{3}H, was used as a reporter on the light isotope at the position of interest, 1′-^{12}C in this case.

The experimental 1′-^{13}C KIE was 1.010 ± 0.009, and the 1′-^{2}H KIE was 1.20 ± 0.02. A highly dissociative A_ND_N mechanism was possible, as the 1′-^{13}C was not unambiguously smaller than the calculated lower limit of 1.013−1.015 for A_ND_N TSs;[22] however, on the basis of the large 1′-^{2}H KIE, the authors concluded that these the KIEs were more consistent with a D_N*A_N mechanism. Further experiments[259] and a computational study[256] have supported the assignment of a D_N*A_N mechanism, including the fact that the best UDG inhibitors found to date are "bipartite" inhibitors where the uracil ring and 1-aza-dR are not covalently joined and are separated by >3.2 Å in the hUDG·uracil·1-aza-dR crystal structure.[174] The β-secondary ^{2}H KIEs were large and nearly equal (2′S-^{2}H KIE = 1.10 ± 0.01 and 2′R-^{2}H KIE = 1.11 ± 0.01), indicating strong hyperconjugation and a 3′-*exo* conformation. The KIEs indicated a 3′-*exo* conformation, representing the maximal possible extent of hyperconjugation.

Thus, TS analysis of eUDG demonstrated (i) a stepwise, D_N*A_N mechanism, (ii) that one of the chemical steps, either uracil departure (D_N) or water attack (A_N), was the first irreversible step, and (iii) that the ring conformation of oxacarbenium ion, a slight 3′-*exo* pucker, maximized hyperconjugative stabilization.

4.1.2. Other Mechanistic Studies

How UDG locates U residues *in vivo* is not yet clear,[1] but *in vitro* it scanned DNA processively.[260−263] The scanning distance depended on salt concentration and switched to a distributive mechanism at physiological salt concentrations. *In vitro*, this search involves trapping nucleotides as they spontaneously flip out of the DNA helix.[242] The extrahelical intermediate is trapped using backbone distortion.[175,242,264] Complete rotation of the nucleotide into the active site is assisted by DNA backbone distortion and a Leu191 "plug" that is inserted into the minor groove behind the flipped out nucleotide (Figure 17).[1,252,265−267] Specificity for uracil is achieved by hydrogen bonding with Asn123 and van der Waals contacts with Tyr66.[268,269] Once uracil is hydrogen bonded with Asn123, the enzyme undergoes a conformational change into the catalytically competent form. This includes additional hydrogen bonding to uracil and increased DNA distortion that brings the phosphates of the flanking nucleotides in closer proximity to the active site.

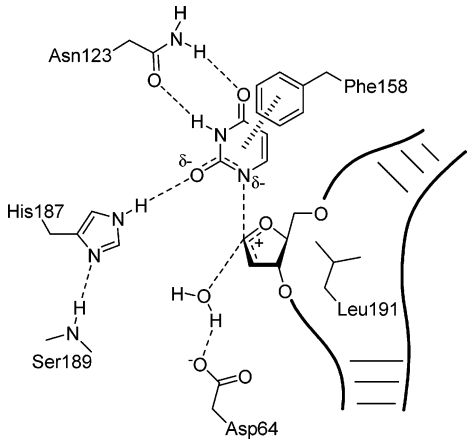

Figure 17. Schematic diagram of UDG active site interactions.

UDG then promotes C−N bond cleavage in the D_N step,[21] forming the oxacarbenium ion intermediate and uracil anion. UDG is proposed to proceed through an electrophile migration, with little interaction between the enzyme and the oxacarbenium ion.[174] Electrostatic stabilization is provided by appropriate location of the DNA phosphodiester backbone oxygens and the uracil anion,[246,256,259] similar to the electrostatic sandwich stabilization of the oxacarbenium ion proposed for the bPNP-catalyzed phosphorolysis of inosine.[224] Hyperconjugation of the C2′−H2′ bonds with C1′ helps to stabilize the oxacarbenium ion character in the deoxyribosyl ring during catalysis.[21] Asp64 promotes catalysis, as evidenced by the 8000-fold, or 5.3 kcal/mol, loss in TS stabilization in the eUDG_Asp64Asn mutation.[143] The 2.9 kcal/mol decrease in binding of an 1-aza-dR inhibitor to the mutant largely reflects electrostatic effects.[144] The negative charge on uracil helps stabilize the oxacarbenium ion, an example of "product assisted" catalysis.[141,144,214] The uracil ring is stabilized in the anion form by strong interactions with His187, which in turn forms hydrogen bonds with the backbone NH of Ser189.

In the A_N step, the water nucleophile approaches the oxacarbenium ion, forming the deoxyribosyl product. At some point during the nucleophilic approach, the water is deprotonated, presumably by Asp64. It is not known whether this occurs before or at the TS to activate the nucleophile, or after the TS to stabilize the product.

Catalysis through the DNA Backbone. A large fraction of the 15 kcal/mol in catalytic power provided by hUDG is mediated through the DNA backbone. There is evidence for both electrostatic[175,256,259] and conformational[174,175] contributions. This has been described in ref 256.

Electrostatic Catalysis through the DNA Backbone. hUDG was able to hydrolyze substrates as small as dUrd, accelerating the reaction (1×10^5)-fold and providing 7 kcal/mol in TS stabilization.[246,259] Adding phosphates and 2′-deoxynucleotides to the minimal substrate improved catalysis by an additional 8 kcal/mol, with the optimal substrate having phosphates in positions +1, −1, and −2.[270] The contribution of the anionic DNA backbone to TS stabilization was determined using methyl phosphonate (MeP)-substituted substrates and inhibitors containing 1-aza-dR.[259] MeP substitution resulted in a linear relationship between log(k_{cat}/

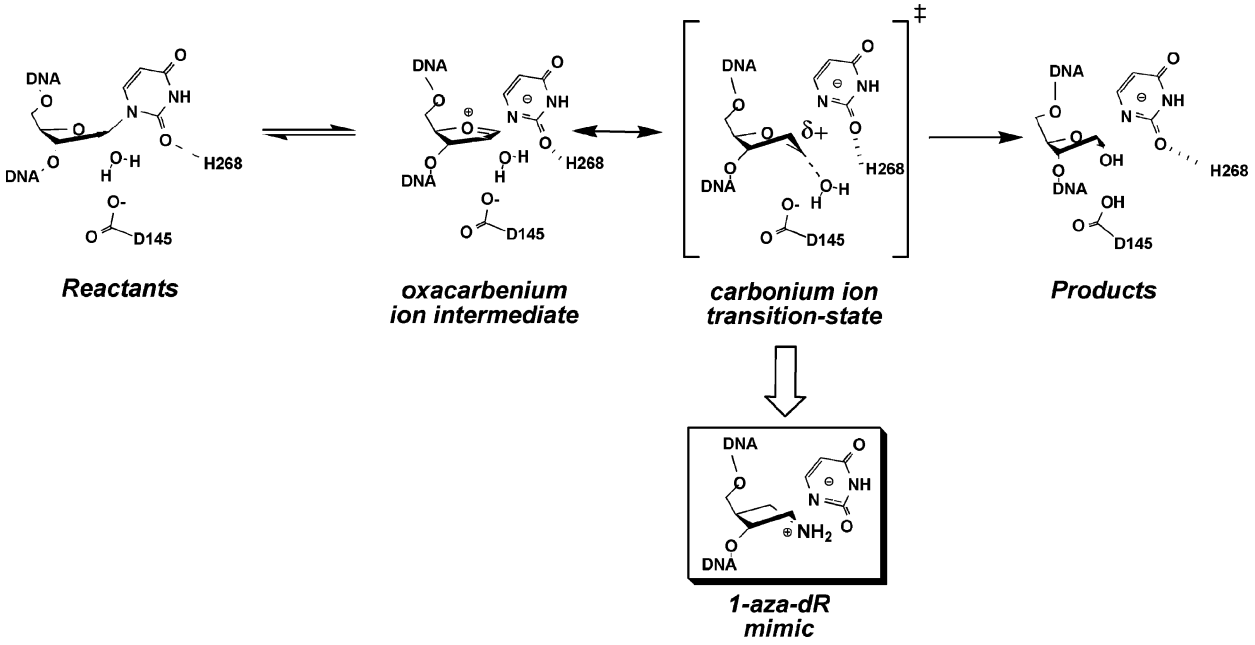

Figure 18. Conformational changes during UDG catalysis. (Reprinted with permission from ref 174. Copyright 2003 American Chemical Society.)

K_M) and log(K_D), with a slope of −1, which provided evidence that 1-aza-dR in the presence of uracil was an excellent mimic of the TS. The deleterious effect of MeP substitutions on k_{cat} corresponded to almost 8 kcal/mol. This is a significant fraction of the total TS stabilization provided by hUDG.[1,259,269] The effects of MeP substitution were proposed to be primarily electrostatic. This is not necessarily to say that the negatively charged phosphodiesters directly stabilized the positive charge on the TS. It is likely that, for example, electrostatic interactions with DNA promote conformational changes in UDG that improve binding to the oxacarbenium ion and/or uracil anion leaving group. This view is supported by the fact that the eUDG_Asp64Asn mutation, which removed a negative charge from a position similar to the location of the positive charge on a 1-aza-dR inhibitor, caused only a modest 1.8 kcal/mol improvement in DNA binding due to decreased electrostatic repulsion between the Asp side chain and the phosphate backbone.[144,265]

Using QM/MM computational methods, the electrostatic interaction of the oxacarbenium ion with the DNA backbone was calculated to contribute 22 kcal/mol to catalysis by hUDG.[256] Even though this energy is unrealistically large, being larger than the total catalytic power of hUDG, 15 kcal/mol,[269] it does nonetheless provide further support for the importance of these electrostatic interactions. It was recently shown through the MeP substitution experiments that the QM/MM study overestimated the contribution from the −2 phosphodiester.[259] The QM/MM study predicted a 5 kcal/mol contribution to catalysis, while the MeP substitution experiments showed that it contributed little to catalysis.

Catalysis through Conformational Changes. Experimental KIEs demonstrated a mild 3′-*exo* pucker at the TS.[21] Recent studies on conformational effects showed that UDG manipulates the deoxyribosyl ring conformation to facilitate catalysis (Figure 18). The crystal structure of hUDG·2′-deoxypseudouridine (ΨdU, a substrate analogue)[173] showed a relatively planar deoxyribosyl ring conformation with a slight 3′-*exo* pucker. This demonstrated that UDG has already induced a conformational change in the Michaelis complex relative to the 2′-*endo* pucker typically found in B-DNA,[271−273] maximizing hyperconjugation as the oxacarbenium ion develops. It also increases the anomeric effect by allowing greater orbital overlap between the lone pair electrons of the ring oxygen, O4′, and the σ^*-orbital of the C1′−N1 bond, weakening the *N*-glycosidic bond and promoting catalysis.[274] The contribution from the anomeric effect would be expected to be modest, 1−2 kcal/mol.[275,276]

The hUDG·1-aza-dR crystal structure provided insight into the second TS, *i.e.*, water attack on the oxacarbenium ion in the A_N step.[174] The 1-aza-dR ring was distorted into an unusual 1′-*exo* conformation, similar to that expected for the second TS in an electrophile migration mechanism. This was clearly different from the *ab initio* optimized 1-aza-dR structure, demonstrating that the enzyme was enforcing the conformation. A computational optimization of 1-aza-dR with O3, C3, C4, and C5 constrained as in the crystal structure gave an 1′-*exo* conformation, illustrating that, by distorting the DNA backbone, hUDG helps enforce deoxyribosyl ring conformations. The 1-aza-dR in the crystal structure was distorted further than in the constrained optimization, with a greater ring pucker at N1 and more distorted bond angles. This was attributed to ion pairing between N1′H_2^+ and the side chain carboxylate of hUDG_Asp145 (equivalent to eUDG_Asp64). This is exactly the distortion expected as the oxacarbenium ion, which is planar about C1′, approaches the water nucleophile in the second TS. A 1′-*exo* pucker would fulfill the dual role of moving C1′ closer to the nucleophile water and breaking the planarity around C1′. This would disrupt the π-bonding between C1′ and O4′, and C1′ and C2′, making C1′ even more reactive. The hUDG·thio-AP·uracil cocrystal structure, *i.e.*, the products of **11** hydrolysis, had the deoxythioribose in the α-anomer, consistent with water attack from below the plane of the ring, and in a more common 2′-*endo* conformation.[173,213]

Substrate Distortion around the *N*-Glycosidic Bond. Two components of the substrate distortion observed in the hUDG·ΨdU crystal structure are proposed to promote catalysis. One component is distortion around the C1′−C1 bond (corresponding to C1′−N1 in uridine), with the sp^2-hybridized C1 atom distorted toward tetrahedral geometry

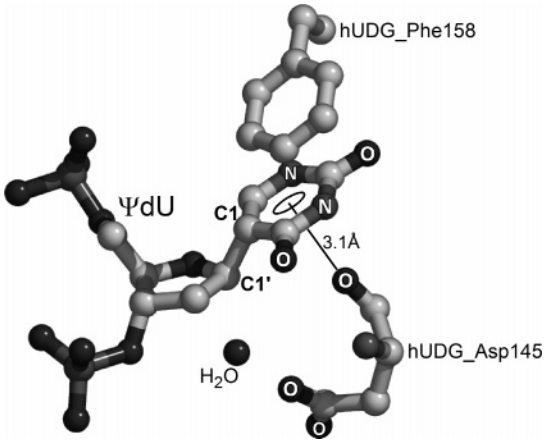

Figure 19. Tetrahedral distortion of pseudouridine (ΨdU) in the cocrystal structure with hUDG.[173] Also shown are a conserved contact between the pseudouracil ring (or uracil in other structures) and the backbone oxygen of hUDG_Asp145, face-to-face stacking with the conserved hUDG_Phe158, the conserved catalytic residue, hUDG_Asp145, and the putative water nucleophile.

(Figure 19). The combined anomeric/$\sigma-\pi$ aromatic effect originally advanced[173] to explain how this distortion could promote C1′−N1 bond cleavage seems unlikely in light of the fact that the structural changes expected to accompany such a stereoelectronic effect have not been observed in Raman spectroscopic studies[142] or computationally.[12] There is little doubt that such a marked distortion would weaken the *N*-glycosidic bond if it occurred in the UDG·substrate complex, but there is not yet experimental evidence for such ground-state destabilization with the true substrate. Nonetheless, it is interesting that the pseudouridine ring in the hUDG·ΨdU structure superimposed very closely with uracil rings in product and inhibitor complexes.[174,213]

The second component of the distortion was rotation of the *N*-glycoside bond conformation from the preferred *syn* or *anti* conformations by about 90°. In all crystal structures solved to date, hUDG_Phe158 formed a parallel stack with the uracil (or pseudouracil) ring.[173,174,213,277−281] There is no evidence that this rotation increases the inherent reactivity of the C1′−N1 bond, but it does bring O2 into hydrogen bonding distance with hUDG_His268, which is essential in stabilizing the uracil anion leaving group. In addition, hUDG_Phe158 will help form a hydrophobic environment around the uracil ring, strengthening the hydrogen bond.[282] The contacts that appear important in substrate distortion were the hUDG_Phe158 side chain and the hUDG_Asp145 backbone carbonyl, in contact with opposite sides of the pseudouracil ring. In eUDG, mutation of the equivalent residue, eUDG_Phe77Ala, caused a 3-fold decrease in k_{cat} with single stranded DNA substrates, implying a modest role in catalysis. The larger, 25-fold effect with double stranded substrates implies additional roles. eUDG_Phe77 is strongly conserved in other UDG superfamily enzymes, with the only exception being hTDG_Tyr152.[279]

DNA Backbone Catalysis with Other UDG Superfamily Members. The catalytic power associated with positioning of the DNA backbone is important in explaining the still considerable catalytic power of members of the UDG superfamily, including eMUG[283] and hTDG,[284,285] which lack the catalytic His and Asp residues (see below) yet lose only 4 kcal/mol in TS stabilization.

Promoting Leaving Group Departure. eUDG promotes uracil departure as the anion.[140−144] The hydrogen bond network of uracil anion, eUDG_His187, and eUDG_Ser189 stabilizes the negative charge on O2 of the imidate tautomer of uracil without transferring a proton, lowering the pK_a of N1 from 9.8 to 6.4 (Figure 17).[141,142,214] The energetic cost of lowering the N1 pK_a, 4.8 kcal/mol, equals the contribution of eUDG_His187 to catalysis.[143] This similarity supports the first TS, leaving group departure, as the first irreversible step in the D_N*A_N mechanism.[214]

The stabilization energy for the oxacarbenium ion appears to depend on direct interaction with uracil anion and/or the effect of uracil anion on the active site. The 1-aza-dR inhibitor in the absence of uracil had a modest K_d, 2 μM, compared with 110−500 pM in its presence.[121,144] Thus, inhibitor binding improved by 4.9−5.8 kcal/mol in the presence of uracil. The fact that UDG did not bind a 4-aza-dR inhibitor without uracil tends to support that conclusion.[227]

eUDG makes uracil-specific hydrogen bonds using eUDG_Asn123, though these appear to contribute little to TS stabilization.[213,252,286] hUDG's specificity was switched to T and C by mutations at hUDG_Tyr147 and hUDG_Asn204 (equivalent to eUDG_Asn123), though the rate with U was reduced drastically.[269]

Oxacarbenium Ion Stabilization. The following interactions provide at least 13 kcal/mol toward eUDG binding of 1-aza-dR and uracil anion: eUDG_His187 (3.4−4.8 kcal/mol), eUDG_Asp64 (2.8 kcal/mol), and the DNA backbone (7 kcal/mol).[144,259] The contribution from eUDG_His187 reflects its role in stabilizing the imidate intermediate, which is positioned above C1′ of the oxacarbenium ion. Therefore, eUDG appears to rely equally on active site functional groups and the DNA backbone to stabilize the oxacarbenium ion.

4.2. Thymidine Phosphorylase

Thymidine phosphorylase (TP) cleaves thymidine to deoxyribose 1-phosphate and thymine, and is involved in pyrimidine salvage, angiogenesis, and chemotaxis in solid tumors.[46]

4.2.1. TS Analysis

TS analysis was performed on hTP-catalyzed arsenolysis of thymidine (Scheme 4).[46,64] Arsenolysis was used because (i) the 2-deoxyribose 1-arsenate rapidly hydrolyzes to 2-deoxyribose and inorganic arsenate, making the arsenolysis reaction irreversible, and (ii) the phosphorolysis reaction is readily reversible, making the KIEs uninterpretable. The experimental KIEs indicated a TS structure that was unprecedented in carbohydrate chemistry: a highly synchronous concerted A_ND_N mechanism, with $n_{LG} = 0.50$ and $n_{Nu} = 0.33$. Until this study, all well-characterized glycoside hydrolysis and transfer reactions had dissociative A_ND_N or D_N*A_N mechanisms.

The 1′-^{14}C KIE was 1.139, the highest measured to date in *N*-glycoside chemistry but comparable to the primary ^{14}C KIEs for other synchronous A_ND_N reactions.[287−291] The primary 1-^{15}N KIE was 1.022. The calculated KIE was smaller, 1.012. The experimental KIE may reflect polarization effects, such as interaction of cationic side chains with O2 and O4 of thymine, changing the resonance stabilization of N1. Thymine was modeled in the anion form, in agreement with the UDG precedent (see above), but there was no direct experimental evidence for or against it leaving as an anion. The secondary hydron KIEs supported a synchronous TS with little oxacarbenium ion character. The 1′-^{3}H KIE was 0.989, as expected for a synchronous TS.[57−59] The stereospe-

Scheme 4

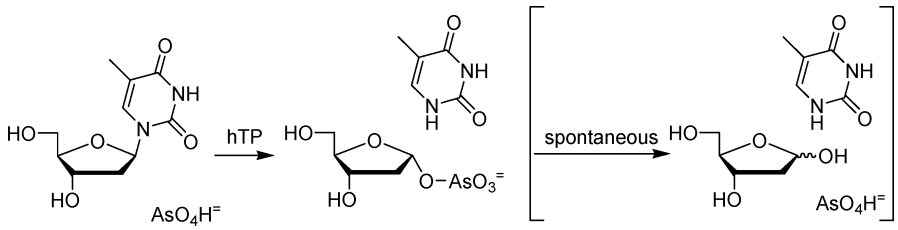

cific 2′-^{3}H KIEs were small, consistent with little oxacarbenium ion character and, therefore, little hyperconjugation. The experimental KIEs were 0.974 for 2′(S)-^{3}H and 1.036 for 2′(R)-^{3}H, and the calculated KIEs matched these values.

As with many other *N*-glycoside enzymes, the 4′-^{3}H and 5′-^{3}H KIEs were large. The EIEs on substrate binding were measured.[64] The 5′-^{3}H EIE was 1.060, compared with the KIE of 1.061, demonstrating that the interactions that caused the large KIE were already present in the Michaelis complex. In contrast, the 4′-^{3}H EIE was near unity, 0.997, compared to the KIE of 1.020. Thus, the 4′-^{3}H KIE was either the result of structural changes inherent to forming the TS or the result of enzyme·substrate contacts that develop only in the TS. The 1′-^{14}C EIE was small, 0.990, demonstrating that the large KIE, 1.139, arose from the reaction coordinate motion in the TS. There is an hTP·inhibitor crystal structure,[292] but the inhibitor was not similar enough to thymidine to allow analysis of interactions in the sugar binding region.

The hTP mechanism was a dramatic departure from all other known phosphorylase or glycosylase mechanisms. Nothing about the enzyme suggested that it would have an unusual mechanism; indeed, two independent computational studies had implicated a D_N*A_N mechanism.[293,294] The charge distribution and electrostatic potential surface of the hTP TS show little accumulation of positive charge in the deoxyribosyl ring (Figure 20).

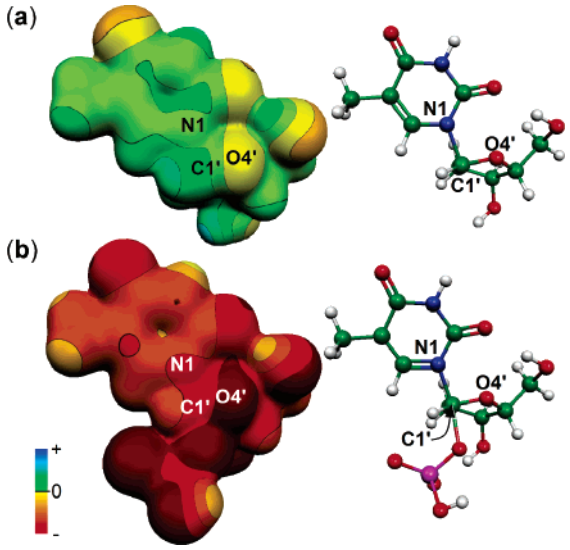

Figure 20. Electrostatic potential surface of the hTP TS,[46] showing thymidine phosphorolysis, using the same color scale as that for Figure 13. (a) TS structure with phosphate removed to illustrate the lack of positive charge around C1′. (b) Complete TS structure, including the phosphate nucleophile. Calculations were the same as those in Figure 13.

Part of the challenge in understanding this TS is that there are no precedents. It is tempting to speculate that only enzymes that are able to strongly bind and activate their nucleophiles will display synchronous A_ND_N mechanisms, namely, phosphorylases, phosphoribosyl transferases, and, in the BER context, bifunctional enzymes that use protein nucleophiles (Lys Nϵ or N-terminal Nα). In this context, it is interesting that the bacterial toxin TSs for ADP-ribosylation were more synchronous than those for hydrolysis reactions catalyzed by the same enzymes. In ADP-ribosylations, the protein-based nucleophile can form multiple contacts with the enzyme.

4.3. Acid-Catalyzed AMP and dAMP Hydrolysis

TS analyses of acid-catalyzed hydrolysis of AMP[27,28] and dAMP[23] have been performed. AMP hydrolysis had an A_ND_N mechanism. The 1′-^{14}C KIE, 1.044, was in the A_ND_N range, and the 9-^{15}N KIE, 1.030, indicated extensive C1′−N9 bond breakage. The reaction was run at pH 1, meaning that N1 was protonated in the reactant. Presumably, N7 was protonated at or before the TS, though the 7-^{15}N KIE was not measured. Protonation at N7 would make the purine ring dicationic and an even better leaving group. The dAMP KIEs indicate a stepwise mechanism with protonation at N7. Thus, the 2′-hydroxyl makes the difference between a concerted reaction with AMP and a stepwise one with dAMP. The 2′-hydroxyl slows acid-catalyzed hydrolysis 650-fold[131] by inductively destabilizing the oxacarbenium ion.

4.4. AMP Nucleosidase

TS analysis of AMP hydrolysis by AMP nucleosidase was conducted in the presence and absence of ATP, an allosteric activator which increased k_{cat} 200-fold with minimal effect on K_M.[27−29,112] The KIEs were similar to those for acid-catalyzed AMP hydrolysis, though the smaller 1′-^{14}C KIEs implied more dissociative A_ND_N TSs: 1′-^{14}C KIE = 1.032 (0.5 mM ATP) and 1.035 (no ATP). The 9-^{15}N KIE was also smaller with ATP (1.025 versus 1.030), implying a lower extent of C1′−N9 bond breakage. Thus, it stabilizes the leaving group more in the presence of ATP, achieving the TS earlier in the C−N bond breakage.

4.5. Ricin—rA and A Hydrolysis

Ricin is a cytotoxic protein from castor beans.[295] The catalytic domain hydrolyzes a single rA residue from 28S ribosomal RNA,[296,297] stopping protein biosynthesis. A single ricin molecule can kill a cell. The minimal substrate is stem-loop RNA or DNA with a stem of at least three base pairs and a rGrArGrA (or GAGA) loop structure.[298−300] It had poor activity against small substrates at physiological pH, but k_{cat} increased with decreasing pH so that, at pH 4, it was within a factor of 10 of k_{cat} with ribosomes.[146]

TS Analysis. TS analysis was conducted with a stem-loop RNA substrate, rA-10,[24] and an analogous DNA substrate, dA-10.[22] In both cases, hydrolysis proceeded through a stepwise D_N*A_N mechanism.

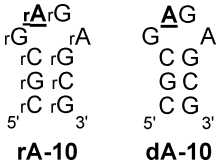

The dA-10 KIEs indicated a $D_N{*}A_N$ mechanism and reflected only the chemical steps. The small primary 1′-^{14}C KIE, 1.015 ± 0.001, was smaller than the calculated minimum for an A_ND_N mechanism, 1.025. The large 9-^{15}N KIE, 1.023, indicated almost complete C−N bond breakage, and the 1′-^{3}H, 2′(S)-^{3}H and 2′(R)-^{3}H KIEs were also large, indicating high oxacarbenium ion character. It is generally not possible to distinguish between $D_N^{\ddagger}{*}A_N$ and $D_N{*}A_N^{\ddagger}$ mechanisms, and that was the case here.

The unusual KIEs for ricin-catalyzed rA-10 hydrolysis were inconsistent with any $D_N{*}A_N$ or A_ND_N mechanism. Instead, the KIEs indicated an oxacarbenium ion intermediate in equilibrium with reactant RNA, with the first irreversible step being isotopically insensitive and occurring after oxacarbenium ion formation. The 1′-^{14}C KIE, 0.993 ± 0.004, was too low for a $D_N{*}A_N$ mechanism. The primary 9-^{15}N KIE, 1.016 ± 0.005, was less than expected for complete C−N bond breakage, 1.024, but still indicated significant bond breakage. The large 1′-^{3}H KIE also indicated high oxacarbenium ion character. These KIEs, especially for 1′-^{14}C, were most consistent with the EIEs of forming an oxacarbenium ion. This will occur if the step after oxacarbenium ion formation, rather than being nucleophilic attack, is irreversible and isotopically insensitive. The nature of this step is not known, but it could be, for example, a protein conformational change or diffusion of water into position to attack the oxacarbenium ion. In either case, an isotopic label in the substrate would have no effect on that step.

The large inverse 7-^{15}N KIE = 0.981 ± 0.008 showed that N7 was protonated in the ricin·oxacarbenium ion·adenine complex, demonstrating general acid catalysis. The k_{cat}/K_M versus pH profile with rA-10 provided evidence for protonation at N1. It was bell-shaped, with a maximum around pH 4,[146] consistent with protonation at N1 of adenine. This was close to the pK_a of an adenine base, suggesting that ricin is contributing little energy to protonate the substrate at N1.[301] It is likely that N1 of the true substrate is protonated by ricin at physiological pH, suggesting that it uses binding energy from interactions with 28 S RNA that are unavailable in rA-10 to protonate N1. The energetic importance of protonation at both N1 and N7 was demonstrated by calculating the C1′−N9 heterolytic bond dissociation energies in the model compound **15**.[24] The bond dissociation energy was 5.5 kcal/mol for N1H,N7H-**15**, compared with 68 and 55 kcal/mol for N1H-**15** and N7H-**15**.

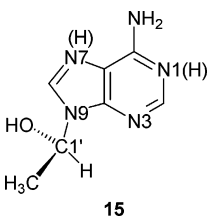

15

Ricin uses interactions with the 2′-hydroxyl of rA to promote catalysis. Acid-catalyzed adenosine hydrolysis was 650-fold slower than that for dAdo,[7,131,302] but the rA-10 k_{cat}/K_M was 6-fold higher than that for dA-10, implying that ricin exerts greater catalytic power on rA by a factor of 3900 (=6 × 650) or 4.8 kcal/mol.

Inhibition Studies. Recent inhibitor design studies provide support for the $D_N{*}A_N$ mechanism for ricin.[119] A 4-aza-sugar inhibitor with an adenine ring analogue, IA-10, gave only

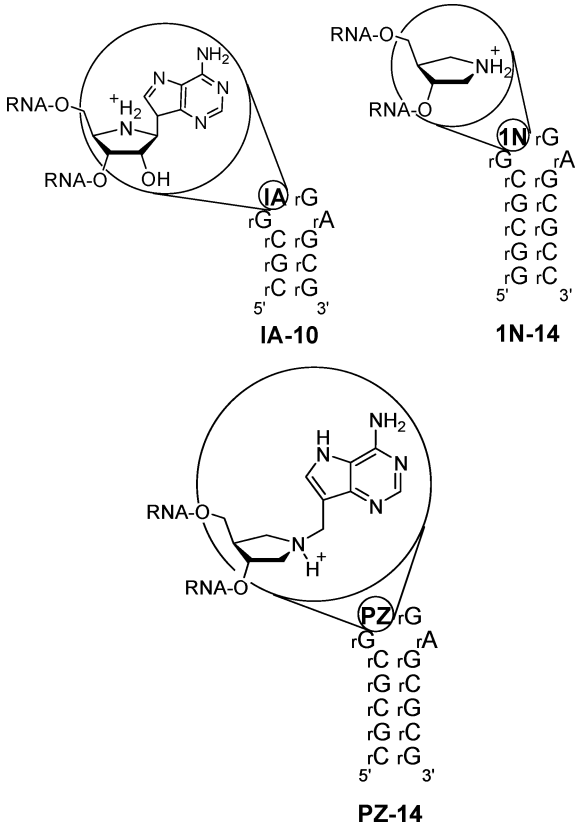

modest inhibition, K_i = 0.6 μM, as did a 1-aza-sugar inhibitor without the purine ring analogue, 1N-14 (K_i = 0.5 μM). Increasing the distance between ribosyl and purine portions of the inhibitor with a methylene bridge in inhibitor PZ-14 improved K_i to 0.094 μM.[120] Better binding with a greater distance between the two portions of the inhibitor molecules was consistent with a mechanism where the adenine leaving group may move a large distance from the oxacarbenium ion intermediate. However, PZ-14 was still not as good an inhibitor as 1N-14 in the presence of adenine, which allowed formation of a ricin·1N-14·adenine complex with K_i = 0.012 μM. Tight binding was expected for the combination of 1N-14 and adenine by analogy to the ricin·oxacarbenium ion·adenine complex, where the distance and/or orientation of the oxacarbenium ion and adenine may not be well mimicked by IA-10.

Several crystal structures of ricin have been reported,[303−307] but none with an oligonucleotide ligand that would demonstrate the extended contact surface.

4.6. Nucleoside Hydrolases

Nucleoside hydrolase IU (CfNH IU) is a purine salvage enzyme from *Crithidia fasciculata*, a free-living trypanosome related to the parasites that cause African sleeping sickness and Chagas' disease.[308] It hydrolyzes all the natural nucleosides efficiently and has the highest specificity for inosine and uridine, hence the "IU" designation.[308] In addition to TS analysis,[31,111] its mechanism has been studied through

kinetic characterization, inhibition, and computational and structural studies.[65,187,224,225,309−320]

TS Analysis. The experimental KIEs were qualitatively similar to those for other *N*-glycoside hydrolysis reactions.[31] The large, primary 1′-^{14}C KIE, 1.044, demonstrated an A_ND_N TS. The primary leaving group 9-^{15}N KIE, 1.026, indicated extensive C1′−N9 bond breakage at the TS. The 1′-^{3}H KIE, 1.15, indicated an oxacarbenium ion-like TS, while the 2′-^{3}H KIE, 1.16, was large, indicating both an oxacarbenium ion-like TS and the extensive hyperconjugation characteristic of a 3′-*exo* conformation. TS analysis initially gave a dissociative A_ND_N TS with relatively high residual bond order to the leaving group adenine, $n_{LG} = 0.19$, and very weak bond order to the water nucleophile, $n_{Nu} = 0.005$. However, later reassessment using the structure interpolation approach[13] indicated a more "balanced" TS, with $n_{LG} = 0.05$ and $n_{Nu} = 0.06$.[12]

CfNH IU was able to hydrolyze *p*-nitrophenyl riboside (**12**) very effectively, with $k_{cat}/K_M = 4 \times 10^6$ M^{-1} s^{-1},[224] indicating that it interacts with the TS largely by stabilizing the oxacarbenium ion-like ribosyl ring, consistent with its wide specificity for leaving groups with very different characters. CfNH IU forms strong interactions with the 2′-, 3′-, and 5′-hydroxyl groups, as evidenced by the fact that deoxynucleosides at these positions were poor substrates and deoxy-4-aza-sugars were similarly poor inhibitors.[308]

Kinetic, Inhibition, and Structural Studies. The TS structure was used to design TS analogue inhibitors, one of which was cocrystallized with the enzyme.[65] CfNH IU was inhibited by a wide variety of 4-aza-sugar inhibitors, with little specificity for portions of the inhibitor corresponding to the leaving group.[225] The crystal structure of CfNH IU with the 4-aza-sugar inhibitor **13** revealed numerous contacts with the ribose ring and few with the leaving group.[315] The inhibitor was bound in a 3′-*exo* conformation, which is the conformation predicted by TS analysis[31] but is uncommon in ribosides.[321] A Ca^{2+} ion bound in the active site was observed in the crystal structure and was subsequently shown to be required for activity.[315] The Ca^{2+} had an octahedral coordination sphere with acidic side chains, and the 2′- and 3′-hydroxyl groups of the inhibitor as ligands. Strong interaction of Ca^{2+} with the 2′-hydroxyl could lead to strong polarization of the C2′−O2′ bond or even deprotonation of O2′H through a catalytic base. The polarized bond or oxyanion would help inductively stabilize the oxacarbenium ion. A water molecule was the last calcium ligand and was ideally located to act as the nucleophile. It is believed that Ca^{2+} helps to activate the nucleophilic water and facilitate its deprotonation, with Asp10 acting as a general base. Thus, Ca^{2+} is proposed to have a role in substrate binding and orientation as well as nucleophile activation and/or possibly interaction with the 2′-hydroxyl. Taken together, these observations are consistent with a mechanism that favors oxacarbenium ion stabilization over leaving group activation.

Relevance to BER Enzymes. There is some evidence that some broad specificity BER enzymes such as AlkA, AAG, endonuclease III, and FPG may operate primarily through oxacarbenium ion stabilization like CfNH IU. However, with a significant fraction of CfNH IU's catalytic power coming from the Ca^{2+} interaction with the 2′-hydroxyl, it is not clear how applicable this specific catalytic strategy is to BER enzymes. Nonetheless, the large number of strong, specific contacts with the ribosyl ring stands in contrast to the case for enzymes that function primarily through leaving group/nucleophile activation, and illustrates some of the strategies used to stabilize an oxacarbenium ion.

4.7. Purine Nucleoside Phosphorylase

Purine nucleoside phosphorylase (PNP) is involved in purine salvage, phosphorolyzing (deoxy)inosine and (deoxy)-guanosine (Scheme 5). TS analysis, inhibition, and crystallographic studies on the nucleoside phosphorylases have recently been reviewed in detail.[18]

Scheme 5

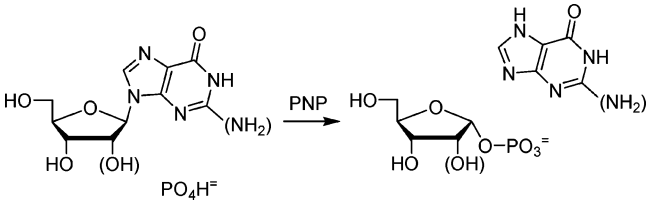

TS Analysis. The bPNP phosphorolysis reaction demonstrated commitment to catalysis, which masked the KIEs on the chemical steps,[25] so TS analyses were performed on inosine arsenolysis catalyzed by the bovine (bPNP),[25] human (hPNP),[26] and malarial (mPNP)[26] enzymes, as well as on bPNP-catalyzed inosine hydrolysis under pre-steady-state conditions.[30] One of the remarkable features of these reactions is that the TSs of the arsenolysis reaction are all quite distinct from each other even though the reactions are the same and the enzymes are similar, with bPNP and hPNP sharing 86% sequence identity.

For bPNP arsenolysis,[25] the 1′-^{14}C KIE, 1.026 ± 0.006, was near the lower limit for an A_ND_N mechanism.[22] The large 1′-^{3}H and 2′-^{3}H KIEs indicated an oxacarbenium ion-like TS. A series of crystal structures of bPNP demonstrate that there is not enough room in the enzyme active site between the leaving group purine and the phosphate nucleophile to form a stable oxacarbenium ion,[86] consistent with a dissociative A_ND_N mechanism. The primary, 9-^{15}N KIE, 1.010, was lower than expected, as discussed below.

KIEs for bPNP-catalyzed inosine hydrolysis were measured under pre-steady-state conditions because of the exceptionally slow dissociation of hypoxanthine (estimated $K_d = 1$ pM).[89] KIEs in the ribosyl ring were typical of an A_ND_N mechanism, with 1′-^{14}C KIE = 1.045, 1′-^{3}H KIE = 1.151, and 2′-^{3}H KIE = 1.145. The larger 1′-^{14}C KIE suggests a more synchronous A_ND_N TS than that for the arsenolysis reaction. Performing the reaction in 20% methanol gave predominantly 1-methylribose as product, in agreement with the higher nucleophilicity of methanol[30] and demonstrating significant nucleophile participation in the reaction coordinate. As with arsenolysis, the primary 9-^{15}N KIE, 1.000 ± 0.005, was lower than expected.

The 1′-^{14}C KIEs for both hPNP and mPNP reactions were too low for a simple D_N*A_N mechanism, being 1.002 ± 0.006 and 0.996 ± 0.006, respectively.[26] As with ricin-catalyzed rA hydrolysis, these KIEs matched well with the calculated EIEs for oxacarbenium ion formation in a 3′-*endo* conformation. This indicated that the oxacarbenium ion intermediate was in equilibrium with the reactant and the first irreversible step was isotopically insensitive, *e.g.*, a conformational change that occurs before nucleophilic attack by arsenate. Another interesting feature of the hPNP and mPNP TSs was the small 2′-^{3}H KIEs, 1.031 and 1.036, respectively. In light of the evidence for an oxacarbenium ion intermediate, such

small KIEs indicate a 3′-*endo* oxacarbenium ion conformation. Unlike ricin-catalyzed rA hydrolysis, where the 3′-*endo* conformation is enforced by the substrate's RNA backbone, there is no reason *a priori* that these enzymes could not select a 3′-*exo* conformation to take advantage of hyperconjugation. Why these reactions pass through a 3′-*endo* conformation is not clear.

The bPNP 9-^{15}N KIEs were anomalously low compared with calculations and other experimental 9-^{15}N KIEs. Complete C1′−N9 bond cleavage should give KIEs of at least 1.026−1.029, the values for inosine hydrolysis by CfNH IU[31] and arsenolysis by hPNP.[26] The cause of the anomalously low bPNP 9-^{15}N KIEs is unknown, but it may arise from strong enzyme·leaving group interactions affecting N9, making it more vibrationally constrained. The size of the anomaly, with 9-^{15}N KIE = 1.010 for arsenolysis and 1.000 for hydrolysis, correlated with the tightness of hypoxanthine binding. Its K_d in the absence of ribose-1-phosphate was 1 pM,[89] and it was ∼5 nM in the presence of ribose-1-arsenate.[12] The primary 9-^{15}N KIE for hPNP was large, 1.029, in reasonable agreement with the calculated EIE, 1.025, and the corresponding KIE for CfNH IU-catalyzed inosine hydrolysis, 1.026.[31] It indicated complete C1′−N9 bond cleavage, consistent with the D_N*A_N mechanism. In contrast, the mPNP 9-^{15}N KIE was 1.019, which is not consistent with equilibrium formation of [oxacarbenium ion + hypoxanthine] in a D_N*A_N mechanism but is reminiscent of the anomalous 9-^{15}N KIEs with bPNP.

The electrophile migration model was proposed based on the bPNP reaction. It is consistent with both A_ND_N and D_N*A_N mechanisms, so the hPNP and mPNP reactions are still consistent with this model. Formation of a discrete intermediate implies that the distance between the purine ring and phosphate is >6 Å. The interactions responsible for changing an A_ND_N mechanism into a D_N*A_N one may be subtle.

Relevance to BER Enzymes. The TS analysis and structural studies with PNPs illustrated several principles of potential importance for BER enzymes. bPNP was the enzyme for which the electrophilic migration model of catalysis was developed. The BER enzyme UDG has been proposed to proceed through an electrophilic migration mechanism,[174] and more examples are likely to emerge. The large differences in TSs between bPNP (A_ND_N, strong hyperconjugation) and hPNP (D_N*A_N, weak hyperconjugation), despite 86% sequence identity, illustrates that there may be important differences in mechanism even between closely related enzymes. The lack of strong hyperconjugative stabilization in hPNP and mPNP was not expected and may be observed in other enzymes.

4.8. Purine Phosphoribosyl Transferases (PRTases)

Phosphoribosyl transferases synthesize *N*-glycosidic bonds.[38] KIEs were measured on the reverse orotate phosphoribosyltransferase (OPRTase)-catalyzed reaction, cleavage of orotidine monophosphate (OMP) to phosphoribosyl pyrophosphate (PRPP) (Scheme 6).[38] Phosphonoacetic acid, an alternate substrate, was used because pyrophosphate gave small KIEs, suggesting commitment to catalysis. The 1′-^{14}C KIE, 1.040, indicated a dissociative A_ND_N TS. The secondary ^{3}H KIEs suggested high oxacarbenium ion character, with 1′-^{3}H KIE = 1.200 and 2′-^{3}H KIE = 1.140. The primary 1-^{15}N KIE was measured with substrate doubly ^{15}N-labeled,

Scheme 6

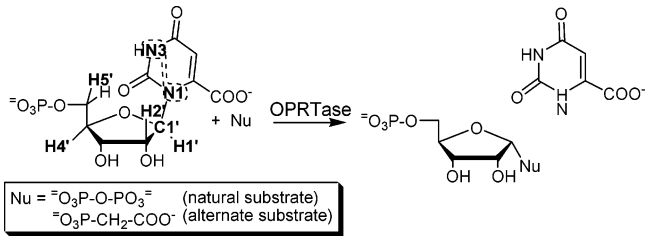

at N1 and N3, making it difficult to interpret. As with PNP, a model of the TS structure docked with the crystal structure of OPRTase showed many interactions with the orotate ring and with the pyrophosphate nucleophile but few direct contacts with the ribosyl ring, suggesting an electrophile migration mechanism.[322,323]

4.9. ADP-Ribosylating Toxins and Nonenzymatic NAD$^+$ Hydrolysis

Some bacteria exert their pathogenic effects by covalent modification of host proteins by ADP-ribosylation with NAD$^+$ (Scheme 7).[324] Like alkylated nucleobases, nicotina-

Scheme 7

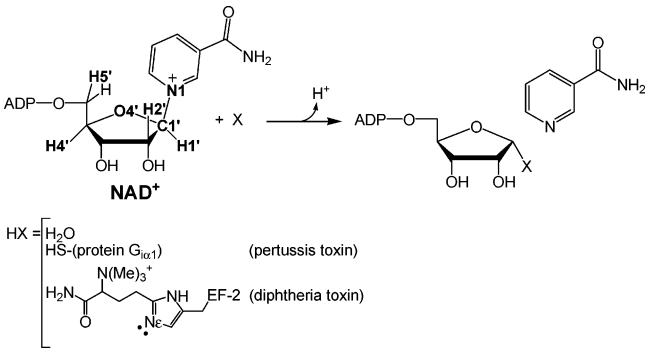

mide is positively charged in the reactant and is able to depart without protonation. Diphtheria,[325] cholera,[326] and pertussis[327] toxins ADP-ribosylate cellular G-proteins and will slowly hydrolyze NAD$^+$ *in vitro*. TS analysis has been performed on NAD$^+$ hydrolysis catalyzed by diphtheria,[35] cholera,[36] and pertussis[37] toxins, spontaneous NAD$^+$ hydrolysis,[41] and ADP-ribosylation by diphtheria[34] and pertussis toxins.[32,33]

NAD$^+$ Hydrolysis. The NAD$^+$ hydrolyses all proceeded through highly dissociative A_ND_N TSs. The TS for spontaneous hydrolysis had n_{LG} = 0.02 and n_{Nu} = 0.005. The 1′-^{14}C KIE was 1.016, very close to the lower limit for an A_ND_N reaction with NAD$^+$. (This KIE was smaller than those of normal bases because the NAD$^+$ C1′−N1 bond is weak due to the cationic, quaternary N1.) The primary, 1-^{15}N KIE, 1.020, demonstrated extensive C1′−N1 bond breakage while the 1′-^{3}H KIE, 1.194, and 2′-^{3}H KIE, 1.11, demonstrated an oxacarbenium ion-like TS in a 3′-*exo* conformation.

TS structures initially reported for cholera[36] and pertussis[37] toxin-catalyzed NAD$^+$ hydrolysis differed somewhat from that for diphtheria toxin,[35] but when they were reanalyzed using the structure interpolation approach, the TS structures were essentially the same as each other, with n_{LG} = 0.02 and n_{Nu} = 0.03.[12] For diphtheria toxin, the 1′-^{14} C KIE, 1.034, indicated a more synchronous A_ND_N TS, while the 1-^{15}N KIE, 1.030, demonstrated extensive C1′−N1 bond cleavage. The 1′-^{3}H KIE, 1.200, and 2′-^{3}H KIE, 1.142, indicated an oxacarbenium ion-like TS in a 3′-*exo* conformation. Thus,

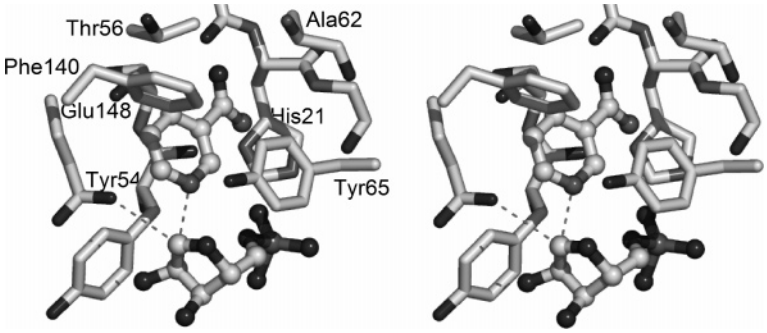

Figure 21. TS for diphtheria toxin-catalyzed NAD^+ hydrolysis. The TS is shown without the water nucleophile in this A_ND_N mechanism. The protein structure is shown as the stick model with N and P atoms as gray and O atoms as black. The NAD^+ TS, truncated at the α-phosphate, is the ball-and-stick model. The residual C1′−N1 bond and the potential electrostatic stabilization of C1′ by Glu148 are shown with dashed lines.

the enzymatic TSs were very similar to those for the spontaneous reaction, with the increased nucleophile bond order, n_{Nu}, possibly due to the invariant Glu residue helping to orient and/or activate the water nucleophile.

ADP-Ribosylation. TS analyses have been performed on three ADP-ribosylation reactions: pertussis toxin with a model peptide[32] and the true target, protein $G_{i\alpha1}$,[33] and diphtheria toxin with its target, EF-2.[34] The diphtheria toxin KIEs were very similar, except at the remote positions. The 1′-^{14}C KIE, 1.055 ± 0.003 versus 1.049 ± 0.003 for pertussis toxin, indicated a slightly more synchronous A_ND_N TS. The reported TS structure had lower nucleophile bond order, $n_{Nu} = 0.03$, cf. 0.09 for pertussis toxin, a modest difference that revolved around a different choice of reactant models. The discussion below refers to the pertussis toxin TS.[33]

ADP-ribosylation was more synchronous than hydrolysis, but it was still a dissociative A_ND_N mechanism, with $n_{LG} = 0.11$ and $n_{Nu} = 0.09$. The sum of n_{LG} and n_{Nu} was 0.2, compared with 0.05 for the hydrolysis reactions, indicating that the enzymes use binding energy to increase nucleophile participation at the TS. The pertussis toxin TSs were the same for the 20-mer peptide and protein $G_{i\alpha1}$, showing that all the structural determinants needed to define the structure of the TS are present in the 20-mer peptide. Remote interactions with protein $G_{i\alpha1}$ increased k_{cat}/K_M 800-fold without changing the TS. It is remarkable that the diphtheria toxin-catalyzed reaction was so similar considering that the protein substrates, especially the nucleophile atoms, are different. The target in protein $G_{i\alpha1}$ is Cys, an anionic and extremely potent nucleophile, compared with Nϵ of a diphthamide residue (Scheme 7), a much weaker, secondary nitrogen nucleophile.

Structural Studies. The experimental TS structure was docked with the diphtheria toxin·NAD^+ crystal structure.[192] One feature of the diphtheria toxin·TS interactions was a deep, form-fitting hydrophobic pocket for the nicotinamide ring. The low dielectric environment of this pocket would lower the energy difference between the reactant and the TS by increasing the energy of the positively charged nicotinamide ring relative to the neutral form at the TS, a case of ground state destabilization. The Glu148 side chain was positioned to act as a general base and/or electrostatic catalyst. It was directly adjacent to C1′, positioned to orient and/or deprotonate the water or diphthamide nucleophile, and could stabilize positive charge accumulating at C1′ in the TS (Figure 21). It had been shown previously by photoaffinity labeling[328] and mutagenesis[329] to be important for catalysis, and it is conserved in all bacterial ADP-ribosylating toxins. The pertussis toxin·TS model structure shared most of the important features of the diphtheria toxin complex, including Glu129 directly adjacent to C1′.[33,330,331]

Two features of the bacterial toxin reactions stand out. First, the TS structures for hydrolysis were effectively identical to each other, as were the ADP-ribosylation TS structures, even though the nucleophiles were different in the diphtheria toxin and pertussis toxin reactions. This is in sharp contrast to the case of the PNP reactions, where the three arsenolysis TS structures were different from each other. The second notable feature was that the ADP-ribosylation reactions were more synchronous than the hydrolysis reactions, indicating that the enzymes use binding energy from interactions with the protein substrate to increase nucleophile participation at the TS.

Relevance to BER Enzymes. The nicotinamide ring of NAD^+ departs in the neutral form, making it a prototype for BER enzymes that act on alkylated nucleobases. Such BER enzymes may be able to use hydrophobic binding pockets, like diphtheria toxin, to promote catalysis through ground-state destabilization. The more synchronous A_ND_N TSs for ADP-ribosylation reactions may be relevant to bifunctional BER enzymes, where the enzymes may activate the amine nucleophile as well as the leaving groups.

5. BER Enzymes

5.1. Superfamilies

There are several BER enzyme superfamilies. A superfamily is any group of proteins that can be shown to have descended from a common ancestor, no matter how low their sequence identity. The UDG superfamily is specific to U, T, and several types of derivatized pyrimidines. The HhH superfamily contains both monofunctional and bifunctional BER enzymes, demonstrating that the two distinct sets of activities had a common origin. The phylogenetic relationships among BER enzymes have been investigated.[5,332−336]

5.2. UDG Superfamily—Monofunctional Enzymes

Uracil DNA glycosylases (UDGs) are a superfamily of monofunctional BER enzymes that occur in viruses, prokaryotes, and eukaryotes (see ref 337). The superfamily is divided into families based on conserved active site residues and specificity (Figure 17, Table 3).[337,338] They use nucleotide flipping to position the damaged nucleotide into the active site, and they have a high affinity for the AP product, making product release rate limiting. One surprising feature is the poor conservation of eUDG_Asp64 and eUDG_His187,

Table 3. Conservation of Catalytically Important Residues in the UDG Superfamily[a]

enzyme									
hUDG[173]	eUDG[253]	hsvUDG[280]	MUG[278,279]	TDG[339]	xSMUG1[280]	*hSMUG1*[280]	TthUDGa[281]	*PaUDGb*[340]	proposed role
D145	D64	D88	N18	N140	N96	*N85*	G42(E41)	*A68*	general base/oxacarbenium ion electrostatic stabilization
H268	H187	H210	N140	S271	H250	*H239*	H155	*H196*	uracil O2 anion stabilization
N204	N123	N147			N174	*N163*	N80		specificity through Watson−Crick face
Y147	Y66	Y90			G98/M102	*G87/M91*	E47		steric interactions with Hoogstein face
L272	L191	L214	L144	R275	R254	*R243*	R161		damaged strand wedge
			R146		P256	*P245*			opposite strand wedge
			G143/R146	A274					recognition of orphaned G
F158	F77	F101	F30	Y152	F109	*F98*	F54		π-stacking with uracil ring

[a] A blank indicates either that the enzyme does not perform a given role or that the residues performing that role are unknown. Normal text indicates residues identified by comparison of X-ray crystal structures. *Italics* indicates residues identified by sequence analysis only.

active site residues that contribute up to (3×10^7)-fold (10 kcal/mol) to catalysis. Surprisingly, in the absence of these catalytic residues, the other UDG superfamily members lose only 10^3-fold in catalytic enhancement. The lack of conservation outside UDG (UDG family 1, section 5.2.1) may reflect the large number of different catalytic strategies available to these enzymes.

5.2.1. UDG Family 1—UDG

UDG family 1 enzymes, also called UNGs, are ubiquitous.[239] The human (hUDG), *E. coli* (eUDG), and herpes simplex virus type 1 (hsvUDG)[251,255] enzymes are the most thoroughly characterized examples.[1,337] UDG is specific to U, removing it from single and double stranded DNA with little regard for the opposite base. Mammalian UDGs appear to play a role in somatic hypermutation (see ref 341). The wealth of mechanistic and structural studies on eUDG and hUDG provides the most complete picture of catalysis for any BER enzyme (section 4.1).

5.2.2. UDG Family 2—MUG

UDG family 2 includes prokaryotic mismatch-specific uracil DNA-glycosylases (MUGs), also called G:T/U eMUG,[278] and eukaryotic thymine DNA glycosylases (TDG),[339,342] also called G:T mismatch-specific TDG.[337] *E. coli* MUG (eMUG) and human TDG (hTDG) have little specificity for the opposite base, using contacts around the lesion and the strength of base pairing to the target residue to define substrate preference.[283−285,343,344] hTDG prefers lesions in a CpG:N context in single turnover experiments, with 5-hydroxymethyluracil and uracil removed >20-fold faster than other nucleotides.[280] eMUG prefers pyrimidine:G mismatches, with ϵC removed 5-fold faster than U in single turnover experiments.[283,345,346] Thymine excision was (7×10^4)-fold slower than that of ϵC, likely due to a clash between the 5-methyl and eMUG_Ser23, an interaction not present in hTDG.[279]

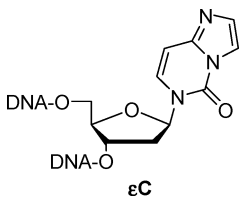

εC

Active Site Differences. The family 2 enzymes lack equivalents to eUDG_Asp64 and eUDG_His187 (Figure 17). The structurally equivalent residues are eMUG_Asn18 and eMUG_Asn140, and hTDG_Asn140 and hTDG_Ser271.[337,339] Although they dispense with these "essential" Asp and His residues, it is important to note that eMUG and hTDG have rates 10^3-fold lower than that for eUDG. Nonetheless, they still provide almost 12 kcal/mol in TS stabilization relative to nonenzymatic hydrolysis.[280,283]

eMUG Structure. The eMUG crystal structure with 1-(2′-deoxy-2′-fluoro-β-D-arabinofuranosyl)-uracil (βFU),[279] a stable U analogue, revealed similarities to UDG, including the fact that the βFU is flipped into the active site and the DNA backbone is compressed, bringing the phosphodiester groups to within 10 Å of C1′.[278] This feature has been shown to contribute to oxacarbenium ion stabilization,[256,259] similar to hUDG; however, unlike the case for hUDG, this geometry is maintained in the product structure. The "serine pinch" mechanism employed by eMUG is different from that for UDG, using a variety of residues and main chain contacts with the +1, −1, −2, and −3 phosphodiester groups to position the strand.

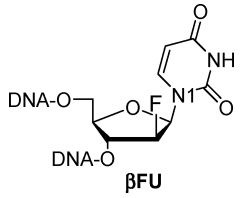

βFU

Leaving Group Activation. N1 was not tetrahedrally distorted in the eMUG·βFUstructure[279] like C1 was in hUDG·ΨdU; however, the conserved Phe, Phe30, was positioned to orient the uracil ring. It could also π-stack with the etheno ring of ϵC,[279] consistent with its higher activity G:ϵC than G:U.[346] There was no equivalent to eUDG_His187 in eMUG·βFU[279] and no obvious replacements to stabilize the uracil anion (Figure 17). There were no obviously catalytically relevant contacts with the leaving group. The observed contacts were water hydrogen bonding with N3 and O4, the backbone amides of the Ile17 and Phe30 hydrogen bonding to O2 and O4, respectively, and Ser23 hydrogen bonding with O4, though this residue is an Ala in TDG.

Nucleophile Activation. Unliganded eMUG had a water positioned by hydrogen bonds to Asn18 that would be positioned 1.7 Å away from C1′ in the eMUG·βFU structure, oriented for nucleophilic attack.[278,279] Mutation of the equivalent residue, hTDG_Asn140Ala, eliminated activity, though it was partially restored with a substrate containing an activated leaving group, 2′-deoxy-5-fluorouridine (**16**).[285] This could indicate a role positioning the water nucleophile, even if it cannot act as a general base catalyst. Both residues superimpose closely with eUDG_Asp64.[173,278] The observed rotation of the uracil ring out of the *anti* conformation in

eMUG·βFU would position O2 within 2.3 Å of the water, where the enolate form of the base could potentially deprotonate water in an A_ND_N mechanism or in the second step of a $D_N{*}A_N$ mechanism.

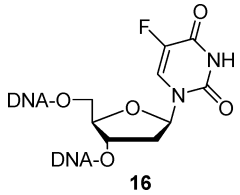

16

Oxacarbenium Ion Stabilization. hTDG bound its AP product tightly, with dissociation half-times of 5−10 h.[347] It bound CpG:4-aza-dR with K_d = 16 pM, only 1.4-times tighter than CpG:THF.[227] The similarity of the K_d's would place TDG in the group of enzymes that do not strongly stabilize the oxacarbenium ion.

5.2.3. UDG Family 3—SMUG1

UDG family 3 members are single strand selective monofunctional uracil−DNA glycosylases (SMUG1), also called 5-formyluracil−DNA glycosylases,[348] and are found in vertebrates and insects.[349,350] The best characterized members are hSMUG1 from humans,[351,352] xSMUG1 from *Xenopus laevis*,[280,337,349] and rSMUG1 from rats.[348,351,353]

Substrate Specificity and Kinetics. xSMUG1 cleaved U from G:U substrates at 9 s^{-1}, only 13-fold slower than eUDG, thus providing a (6×10^9)-fold rate enhancement.[280] xSMUG1 acted on U, 5-hyroxymethyluracil, 5-hydroxyuracil, and 5-formyluracil and, contradictory to the name, had a 700-fold preference for uracil in double stranded DNA,[280] with a 25-fold preference for U:G over U:A. It had very low activity with T and ϵC.[337,351] The surprising specificity of xSMUG1, which rejects T but accepts residues both smaller than T, such as U, and larger than T, such as 5-hyroxymethyl-, 5-hydroxy-, and 5-formyluracil, was explained by the presence of a tightly bound water molecule in the active site. Uracil could bind without disrupting the water molecule, and so, it was a substrate. Uracil derivatives were proposed to displace the water but form new hydrogen bonds to compensate for the loss of the water. In contrast, the 5-methyl of thymine would displace the water without forming new hydrogen bonds.

Structures and Catalysis. The xSMUG1·dUrd crystal structure[280] had an almost identical active site to that of hUDG/eUDG, including the catalytic His, xSMUG1_His250, but substituting xSMUG_Asn96 for the catalytic Asp. This Asn was positioned similarly to hUDG_Asp145, implying that it could stabilize the C1′ positive charge and/or orient the water nucleophile. There was a water close to the proposed water nucleophile of hUDG·ΨdU. The hSMUG1_Asn85Ala mutation (equivalent to xSMUG1_Asn96) gave a 90-fold decrease in k_{cat}/K_M, demonstrating a role in catalysis, though much smaller than that of eUDG_Asp64/hUDG_Asp145.[351] Mutation of the catalytic His, hSMUG1_His239Leu, decreased k_{cat}/K_M (1×10^4)-fold. The hSMUG_Phe98Leu mutant (equivalent to hUDG_Phe158) reduced k_{cat}/K_M (2×10^3)-fold, while the hSMUG_Phe98His mutant had almost-wild-type activity, indicating a ring interaction was required for catalysis and/or substrate recognition.

5.2.4. UDG Family 4—UDGa

UDG family 4 includes UDGa from *Thermus thermophilus* (TthUDGa),[281] *Pyrobaculum aerophilum* (PaUDGa),[354,355] and *Thermotoga maritim*e (TmUDGa).[356,357] The important characteristics of family 4 enzymes include substitution of TthUDGa_Ala40 or PaUDGa_Gly40 for the catalytic Asp and the presence of an iron−sulfur cluster, Fe_4S_4. There is no homology with Fe_4S_4-containing members of the HhH superfamily.[281,354] Fe_4S_4 is not known to have a direct role in catalysis, but there is some evidence for a role in regulating DNA binding in eMutY.[358−360] TthUDGa and PaUDGa steady-state kinetics were complicated by their high affinity for the AP product, with K_d = 9 nM.[281] It was possible to demonstrate activity on U in double and single stranded DNAs, and a preference for mismatches with G.[340]

Structures, Mutations, and Catalysis. Comparing the TthUDGa·uracil[281] structure with hUDG·ΨdU[173] showed that they make similar contacts with the uracil ring, including the catalytic His and the backbone carbonyl (Figure 19). Presumably these interactions indicate the use of similar strategies to activate the leaving group. TthUDGa_Phe54 occupied the same position as hUDG_Phe158, implying a similar role in orienting uracil. The catalytic Asp is replaced by TthUDGa_Gly42, and there is no obvious candidate general base catalyst to replace it.[281]

5.2.5. UDG Family 5—UDGb

The family 5 UDGs, UDGb's, were only recently recognized.[340] They were found in the bacteria *T. thermophilus*, *Streptomyces coelicolor*, and *Mycobacterium tuberculosis* and in the archaea *P. aerophilium*. These enzymes bound AP sites tightly, making rate-limiting product release likely. They had broad substrate specificity, removing 5-hydroxymethyluracil, ϵC, and uracil with similar steady-state rates, and they showed a preference for U:G mismatches over U:A. They also showed weak activity with hypoxanthine, but they could not remove thymine. Sequence alignments show a His residue that may be equivalent to hUDG_His268, and the *P. aerophilium* UDGb_His196Asn mutant had a 50-fold decrease in steady-state rate.[340] On the basis of sequence alignments, family 5 enzymes have Ala68 in place of the catalytic Asp. The *P. aerophilium* UDGb_Ala68Asp mutation caused a 10-fold decrease in steady-state rate, indicating that families that do not possess an active site Asp have evolved alternate catalytic strategies.

5.3. HhH Superfamily—Monofunctional and Bifunctional Enzymes

The HhH superfamily has both monofunctional and bifunctional members. It is named for a helix−hairpin−helix (HhH) structural motif that appears to be involved in nonspecific DNA binding.[361] Following the HhH motif is a Gly/Pro-rich loop and an invariant Asp residue (except in TAG). This superfamily is also referred to as the endo III, Nth, or HhH-GPD superfamily.[4] The endonuclease III-like family sequences contain an iron−sulfur, Fe_4S_4, cluster, including MutY, MIG, MBD4, and endonuclease III. The Fe_4S_4 cluster is not located near the DNA binding sites and was previously thought only to be involved in maintaining protein stability. Recent studies have implicated eMutY Fe_4S_4 in recognizing DNA lesions through redox chemistry.[358−360] Fe_4S_4-containing BER enzymes that are not part of the HhH superfamily also exist (section 5.2.4).

5.3.1. Conserved Asp

The role of the conserved Asp residue in HhH enzymes is not clear. Mutation to Asn caused significant decreases in

Scheme 8

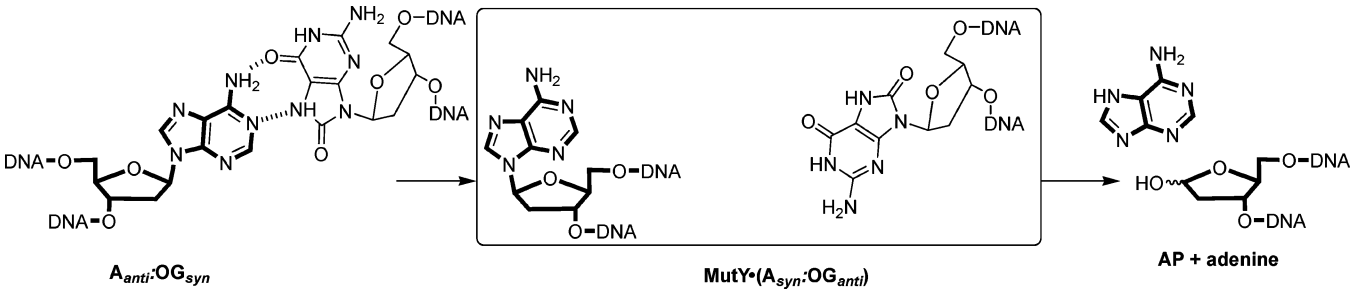

activity for MutY,[203] MIG,[362] AlkA,[238] and hOGG1.[105] It has been proposed to act as a general base catalyst to deprotonate the water nucleophile in monofunctional enzymes or Lys Nϵ in bifunctional enzymes or to electrostatically stabilize oxacarbenium ion intermediates. It approaches C1′ and O4′ (or their equivalents) about equally closely in several structures. Support for an important role is undermined by the observations that (i) the Ala mutant in MIG had only a 16-fold reduction in activity, compared with Asn abolishing activity, and (ii) in hOGG1 the Asn mutant decreased activity 65-fold but the Glu and Gln mutants had near-wild-type activity. This Asp residue was not conserved in TAG, though its feeble catalytic power makes the significance of this change unclear. The protein backbone adopts a different fold in this region, and there is no equivalent residue. In all other HhH enzymes, Asp forms helix-capping hydrogen bonds at the N-terminus of an α-helix, which implies a structural role (see Figure 30). These hydrogen bonds constrain its flexibility, limiting its ability to interact with the substrate. The small effects of mutations other than Asn imply that the conserved Asp does not have a large catalytic role and that the detrimental effects of Asn mutations derive, at least in part, from new, catalytically unfavorable interactions not present with Asp or the other mutants.

5.3.2. MutY/MYH

Bacterial MutY and eukaryotic MYH, also called adenine DNA glycosylase, are monofunctional glycosylases that catalyze the hydrolysis of adenine, an undamaged base, from 8-oxo-guanine:A (OG:A) mismatches (Scheme 8).[363,364] OG is a mutagenic lesion generated by reactive oxygen species.[365] Estimates of the steady-state levels of OG in human cells vary from $\sim 2 \times 10^3$ to 10^5 per cell.[366−368] OG adopts a *syn* orientation in DNA,[369,370] and OG$_{syn}$ encodes like T during replication, causing A to be incorporated with a 200-fold preference over C.[371] Biallelic mutations in human MYH (hMYH) have been correlated with increases in G to T transversions in the adenomatous polyposis coli gene that are linked to colorectal adenomas and cancer.[364,372−375] The catalytic mechanism of MutY has been studied largely with the *E. coli* enzyme (eMutY).[2,5] Recently, the *B. stearothermophilus* (bMutY),[203] *S. pombe*,[376] mouse (mMYH),[377] rat,[378] and human (hMYH)[379,380] enzymes have been characterized.

Preliminary TS Analysis. TS analysis of eMutY was performed using a stem-loop DNA strand containing an isotopically labeled A residue in a G:A mismatch.[23] The experimental KIEs were consistent with a TS structure with significant oxacarbenium ion character, in agreement with most other TS analyses of *N*-glycoside hydrolyses, including the DNA glycosylase reactions, namely UDG-catalyzed uracil hydrolysis,[21] and ricin-catalyzed DNA hydrolysis.[22] An inverse 7-^{15}N KIE indicated N7 protonation to promote leaving group departure, as with ricin-catalyzed hydrolysis of a RNA substrate.[24]

Structures. The following MutY structures have been solved: the N-terminal domains of eMutY_Lys20Ala•adenine,[381] and eMutY_Asp138Asn•adenine,[215] and full length bMutY_Asp144Asn complexed with OG:A, OG:RAP, and [OG:RAP plus adenine].[203] The N-terminal domain of MutY belongs to the HhH superfamily, while the C-terminal domain provides specificity for OG[382−385] and is homologous with *E. coli* MutT, a dOGTP pyrophosphatase.[203,382] Removing the C-terminal domain decreased activity and caused a mutator phenotype in *E. coli*.[215,383−386] The bMutY_Asp144Asn•(OG:A) crystal structure[203] showed that OG bound completely differently to MutY than to MutT. The structure also showed that MutY does not use a double flipping mechanism. It was previously proposed that MutY flips both OG and A out of the helix base stack, and conformational changes in pre-steady-state experiments were ascribed to nucleotide flipping.[382,387] The bMutY_Asp144Asn•(OG:A) structure showed A flipped into an extrahelical, *syn* conformation, while OG remained in the base stack but adopted an *anti* conformation. Ethylation interference experiments[388] and the bMutY_Asp144Asn•(OG:A) structure[203] indicated that the enzyme makes specific contacts with nonbridging phosphate oxygens in the +2, +1, −2, and −3 phosphodiester groups.

The conserved HhH superfamily Asp residue has been proposed to participate in nucleophile orientation/activation and/or oxacarbenium ion stabilization in MutY.[203,215] In crystal structures, bMutY_Asp144 and eMutY_Asp138 were almost superimposable. In mutant bMutY, Asn144 was located $\sim$5 Å from the proposed nucleophile but only 3.4 Å from C1′ (Figure 15). In this orientation, Asp could stabilize the oxacarbenium ion intermediate, consistent with the activity loss in the Asn mutation.

The crystal structures had a water positioned 3.2 Å from C1′ and within 2.8 Å of the side chain and backbone oxygens of the conserved bMutY_Glu43/eMutY_Glu37 residues (Figures 15 and 22). If Glu acts as a hydrogen bond donor and/or general base catalyst, the lone pair electrons of the water will be ideally oriented for nucleophilic attack on C1′. The mechanism proposed by Fromme et al.,[203] where bMutY_Glu43 first acts as an acid, to transfer a proton to N7, and then acts as a base to deprotonate the bound water, fits well with the positioning of the water molecule in all of these structures.

The target A residue was in a 2′-*endo* conformation in the bMutY_Asp144Asn•(OG:A) structure, while TS analysis demonstrated a 3′-*exo* oxacarbenium ion intermediate. This suggests either that the enzyme does not enforce this conformation in the Michaelis complex, as UDG does,[173,174] or that the catalytically important contacts were not fully

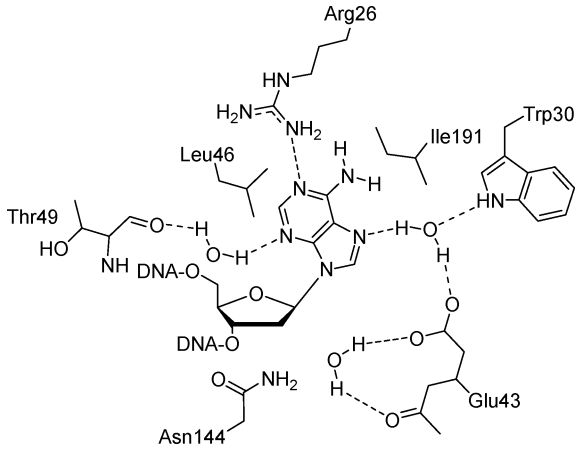

Figure 22. Active site contacts with the substrate A formed by the bMutY_Asp144Asn mutant.[203]

developed in this stalled recognition complex. Other members of the HhH superfamily bound nucleosides as the 3′-*exo* conformer.[191,389,390]

Specificity and Kinetics. Picomolar affinity for the OG:AP product makes product dissociation rate limiting.[377,391−393] Under steady-state conditions, G:A mismatches appear to be better substrates than OG:A because MutY's lower affinity for G:AP makes product dissociation faster. Human AP endonuclease (APE1) increased the rate of OG:AP dissociation from mMYH, thus increasing the steady-state rate. eMutY showed similar behavior with *E. coli* AP endonucleases, but only with G:A substrates.[394]

Single turnover rates of A hydrolysis from OG:A substrates with mMYH and eMutY were 1.5 and 15 min^{-1}, respectively, corresponding to rate accelerations of (10^7 to 10^8)-fold or 9.5 to 11 kcal/mol in TS stabilization.[377,393,395] The rate was 10-fold slower with G:A mismatches and (50−350)-fold slower with C:A mismatches.[396−398] The rate also depended on sequence context.[344,393,399] For example, G:A hydrolysis was 3-fold faster in A*A*G and T*A*G than it was in G*A*A and T*A*T contexts.[393,399] The differences with OG:A substrates were smaller, but the trends were the same. There was no clear correlation with thermal stability of the DNA or preferred orientation of the G:A base pair, *e.g.*, G_{syn}:A_{syn} versus G_{anti}:A_{syn}.[399]

Target Recognition and Base Flipping. eMutY's mechanism for locating OG:A mismatches *in vivo* is not clear. *In vitro*, it scanned DNA processively at salt concentrations below 50 mM to find G:A mismatches.[400] Long-range DNA charge transport[401] and fluorescence experiments[387] demonstrated that nonspecific eMutY binding did not disrupt the DNA strand. Upon recognizing OG:A, fluorescence changes showed that eMutY caused a number of structural changes[203,387] which were thought to involve OG flipping, A flipping, and an enzyme isomerization.[1,387] The bMutY_Asp144Asn·(OG:A) crystal structure revealed that it flipped only the A residue extrahelically. The similarity between the rate attributed to OG flipping in eMutY, 108 s^{-1}, and the rate of spontaneous A:T pair opening, 15−240 s^{-1},[402−404] is reminiscent of the UDG mechanism, where the stalled complex relies on spontaneous opening of the double stranded DNA substrate as the initial step to position the target residue into the active site.

Leaving Group Activation. eMutY_Glu37/bMutY_Glu43 has been proposed as a general acid catalyst to protonate N7. It was in direct contact with N7 in the bMutY·adenine[203] and eMutY·adenine[215] structures, or through a water, or waters, in the bMutY_Asp144Asn·(OG:A) structure (Figures 15 and 22).[203] Evidence for general acid catalysis by Glu includes the facts that eMutY_Glu37Ser was inactive[215] and that eMutY was unable to hydrolyze 7-deaza-2′-deoxyadenosine (**17**) in OG:**17** or G:**17** mismatches.[405]

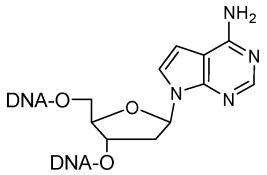

17

Enzyme interactions with adenine N1 and N3 are important for leaving group departure.[406,407] Removing N3 from OG:**18** to give OG:**19** reduced the single turnover rate 170-fold and decreased K_d ∼4-fold.[407] Similarly, a 36-fold decrease in the single turnover rate was found with the 3-deazaadenine (OG:**20**) substrate analogue compared to OG:A. [406] Together, these results indicate that N3 accounts for between 2.2 and 3.2 kcal/mol in TS stabilization. Single turnover rates with 1-deazaadenine (OG:**21**) were 270-fold worse than those with OG:A and consistent with N1 contributing 3.5 kcal/mol to TS stabilization. Therefore, N3 and N1 accounted for almost half of the 12 kcal/mol in TS stabilization provided by eMutY.

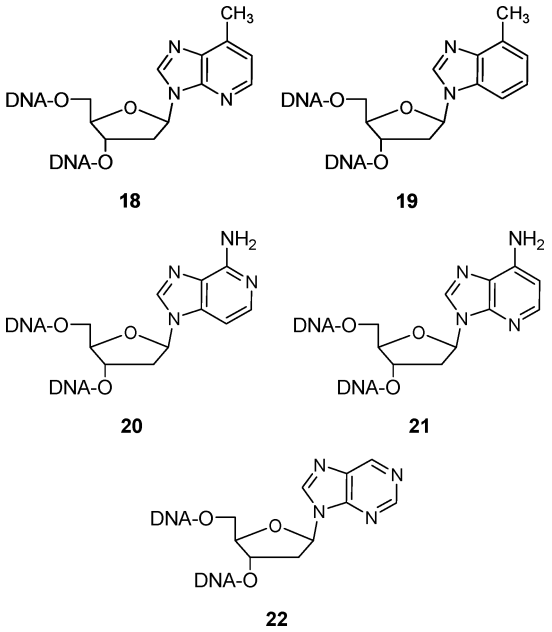

In bMutY_Asp144Asn·(OG:A), the only contact with N3 was a poor hydrogen bond to a water molecule 3.2 Å away and 40° out of the plane of the adenine ring. This water hydrogen bonded in turn with the main chain oxygen of bMutY_Thr49. bMutY_Arg26 was the only group in contact with N1 and was positioned 3.3 Å away and 22° out of the plane of the adenine ring. N1 or N3 protonation appears unlikely given the facts neither nitrogen was in contact with a suspected active site acid and that eMutY hydrolysis of purine deoxynucleoside (**22**) was only 3-fold slower than that of A.[384] The N1 and N3 pK_a's of **22** are ∼2 units lower than those for adenosine, implying that the eMutY-catalyzed rate would have been expected to decrease ∼100-fold if either one was being protonated.[129,408]

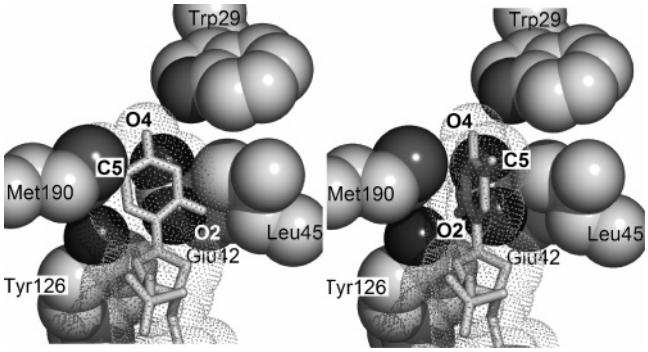

Figure 23. Thymine contacts in the active site of mtfMIG as a function of ring orientation. (left) 90° clockwise twist in base; (right) *anti* orientation. Model structures were built by aligning the active site residues of mtfMIG with bMutY_Asp144Asn·(OG:A)[203] and substituting T for A in the aligned structure.

Oxacarbenium Ion Stabilization. The K_d's of eMutY with an oxacarbenium ion mimic, OG:4-aza-dR, and a product mimic, OG:THF, were very similar, 65 pM and 45 pM, respectively.[227] This would place eMutY in the group of enzymes that do not use oxacarbenium ion stabilization to promote catalysis (section 3.6.2).

5.3.3. Thymine–DNA Mismatch Glycosylases (MIG and MBD4)

The thymine−DNA mismatch glycosylases are monofunctional BER enzymes found in thermophilic eubacteria,[409−412] hyperthermophilic archaebacteria (MIG),[413] and mammals (MBD4).[414,415] The mammalian enzyme is also called MED1.[415] They are functional analogues of MUG and TDG from the UDG superfamily, being specific for thymine in G:T mismatches.[409,413,415,416] MIG enzymes have the characteristic conserved Asp residue equivalent to bMutY_Asp43, an HhH motif, and an Fe_4S_4 cluster.[362,413] The C-terminal domain of MBD4 is from the HhH superfamily, while the N-terminal domain contains a 5MeCpG binding domain.[417]

Specificity, Kinetics, and Structure. Single turnover analysis of the enzymes from *Methanobacterium* thermoautotrophicum (mthMIG) and *M. thermoformicicum* (mtfMIG) with G:T mismatches gave $k_{cat} = 0.01\ s^{-1}$ at 65 °C, corresponding to a rate acceleration of only 10^5-fold over the nonenzymatic rate or 7 kcal/mol in TS stabilization.[362,409] Human MBD4 (hMBD4) also had $k_{cat} = 0.01\ s^{-1}$, but at 37 °C this corresponded to a (2×10^7)-fold acceleration or 10 kcal/mol in TS stabilization.[415] On the basis of the similarity between the MtfMIG and bMutY active sites, an mthMIG_(Ala50Val,Leu187Gln) double mutant was made, expanding its substrate specificity to include A, which was removed from G:A mismatches with a 2-fold preference over T from G:T mismatches.[412]

It was proposed that mtfMIG twists the thymine base 90° upon flipping it into the active site,[362] reminiscent of the twisted conformation in UDG·ΨdU, arguing that twisting would assist C−N cleavage.[173] To our knowledge, there are no reports of ring torsions destabilizing *N*-glycosidic bonds. Re-examining substrate interactions in light of the newer bMutY_Asp144Asn·(OG:A) structure[203] indicates that the *anti* conformation forms potential catalytic contacts between O2 and mtfMIG_Tyr126 and possibly mtfMIG_Glu142, as well as fitting well in the binding pocket (Figure 23). In the twisted conformation, O2 moves toward the mtfMIG_Leu45 side chain and C5 clashes sterically with mtfMIG_Met190.

Role of mtfMIG_Asp144. While the mtfMIG_Asp144Asn mutation abolished detectable activity, the Ala mutant reduced activity only 16-fold, with a 2-fold increase in K_d,[362] indicating that the Asp is not absolutely required for catalysis. Asp to Asn mutants have been used in the other HhH superfamily enzymes as evidence that the conserved Asp is required for catalysis, though mutations to Ala have not generally been made. Therefore, the apparent dependence on the conserved Asp could be the result of new, unfavorable interactions introduced by Asn in the active site rather than a real dependence on Asp for catalysis. This discrepancy may have made the conserved Asp appear more important to catalysis than it really is.

Other Mutations. mMBD4[417] and mtfMIG[362] had similar potential contacts with substrates. The major difference was mtfMIG_Glu42 (equivalent to bMutY_Glu43) being replaced by mMBD4_Thr437, with no nearby acidic residue to compensate. The mtfMIG_Glu42Ser mutant lost 26-fold in activity, in contrast to the eMutY_Asp37Ser mutation, which abolished activity.[215] Even though the acidic residue is conserved in mtfMIG, its catalytic role may not be. mtfMIG_Tyr126Phe caused a 60-fold loss in the single turnover rate and a 1.5-fold decrease in K_d,[362] indicating a catalytic role rather than a mere binding role. There were potential contacts with the DNA phosphodiester backbone at positions +2, +1, −2, and −3 in both mtfMIG and mMBD4.

5.3.4. Alkylation Repair

Alkylation from endogenous electrophiles such as *S*-adenosyl methionine and environmental alkylating agents is a common form of DNA damage.[3,127,149,150] Cells have several pathways to repair small alkyl adducts, including BER, while larger adducts are repaired through nucleotide excision repair. At least five DNA glycosylases remove alkylation damage.[418,419] Some are specific for 3MeA residues, including 3MeA DNA glycosylase I (TAG),[420,421] *Thermotoga maritime* 3MeA DNA glycosylase (MpgII),[411] and *Helicobacter* pylori 3MeA DNA glycosylase IV (MagIII).[419] 3MeA DNA glycosylase II (AlkA, or Mag1[422] in yeast) hydrolyzes a broad range of alkylation, deamination, and oxidation products.[151] These enzymes are all members of the HhH superfamily and are found in prokaryotes. Plants and mammals do not appear to possess HhH superfamily homologues of the 3MeA DNA glycosylase family, but rather they use AAG (section 5.5).[418]

5.3.5. 3-Methyladenine DNA Glycosylases I (TAG)

E. coli TAG (eTAG) is the best studied member of this 3-alkylpurine-specific monofunctional BER family,[423] removing 3MeA in preference to 3MeG and showing no activity with 1MeA, 7MeA, or 7MeG (Scheme 9).[421,424,425] The instability of 3MeA, with $t_{1/2} = 35$ min,[1] has limited kinetic studies of eTAG. It appears to follow biphasic kinetics,[426,427] indicating a rate-limiting step after catalysis, presumably product release. TS stabilization is estimated at as little as 2 kcal/mol.[421,426]

TAG is the only HhH enzyme lacking the conserved Asp residue. It has a different fold in this part of the protein structure.[428] eTAG_Glu38 was equivalent to eMutY_Glu37, and titration experiments demonstrated that the protonated form was important in 3MeA binding. The proton resides on eTAG_Glu38 in the product complex, with 3-methyladenine being in the N9H tautomer.[420] On the basis of this observation, eTAG_Glu38 is predicted to have a pK_a between

Scheme 9

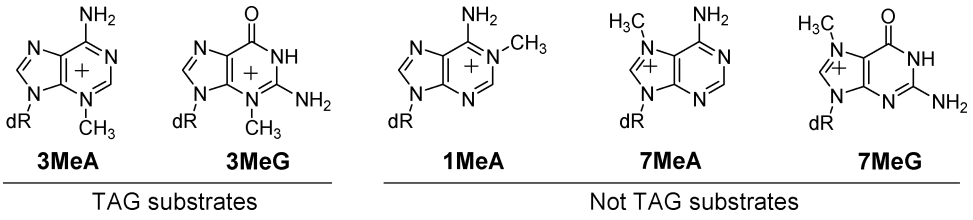

Scheme 10

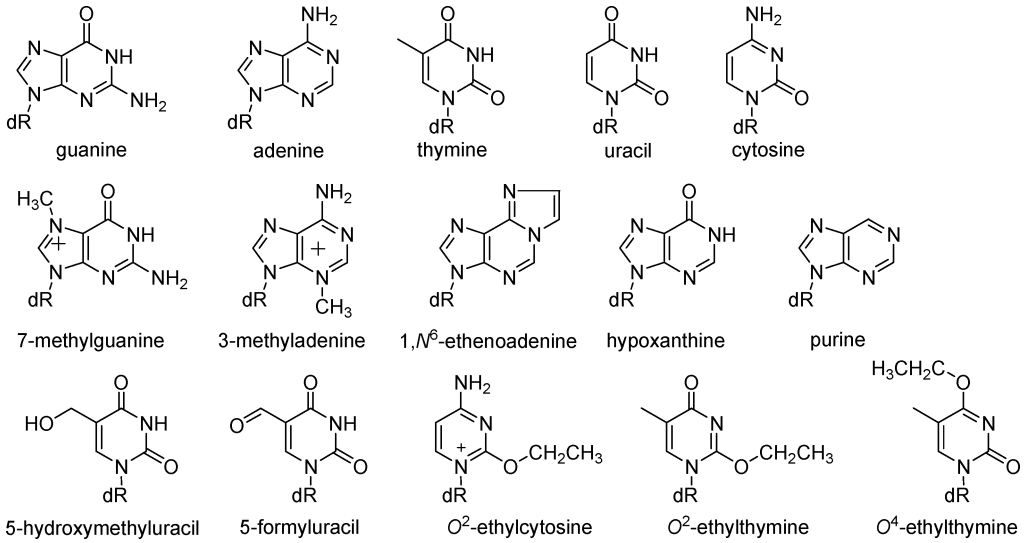

7.5 and 9. Protonated Glu could play a role in TS stabilization by forming a stronger hydrogen bond with N7 as it becomes more basic during *N*-glycoside bond cleavage.

eTAG was inhibited by 3-alkyladenine bases, with IC_{50} ranging from 1.5 mM for the 3-methyladenine base to 0.4 μM for 3-benzyladenine.[424,426,429] The NMR structures of eTAG and eTAG·3-methyladenine showed that Trp46 moved to make contact with the 3-methyl group in an induced fit mechanism (Figure 24).[420] Lower affinity for positively

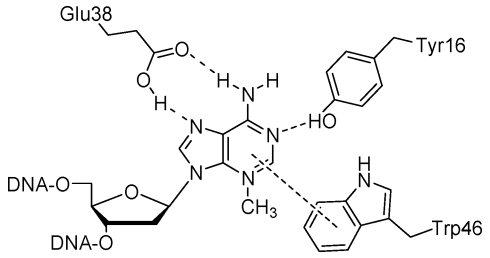

Figure 24. Proposed enzyme·substrate contacts for eTAG. (Adapted from ref 420.)

charged 3,9-dimethyladenine, $K_d = 300$ μM, than 3-methyladenine, $K_d = 42$ μM, showed that the hydrophobic binding pocket preferred neutral rather than cationic bases. This was consistent with the affinity of the eTAG_Trp46Ala mutant decreasing 12-fold for 3-methyladenine but only 3-fold for 3,9-dimethyladenine. A ground state destabilization mechanism for leaving group activation was proposed based on these results. The energetically unfavorable binding of the cationic substrate and a stronger $\pi-\pi$ interaction between eTAG_Trp46 and neutral 3-methyladenine serve to induce *N*-glycosidic bond rupture. A similar mechanism for diphtheria toxin has been proposed (section 3.6.1).

5.3.6. 3-Methyladenine DNA Glycosylases II (AlkA)

The best characterized member of the inducible 3-methyladenine DNA glycosylases II family is *E. coli* AlkA (eAlkA), a monofunctional BER enzyme which hydrolyzes alkylpurines and alkylpyrimidines,[151,430] deamination products,[431,432] oxidative lesions,[151,433−435] and undamaged purines and pyrimidines (Scheme 10).[436] eAlkA's broad specificity appears to be the result of a non-base-specific active site that is able to provide 7−8 kcal/mol in TS stabilization for purines, 6 kcal/mol for T and U, and 9 kcal/mol for C.[151] It is also active on single stranded DNA, albeit at a reduced rate.[425]

Single turnover rates with eAlkA showed an effect from base pair strength that was not reflected in substrate dissociation constants. 7MeG:C was removed 250-fold more slowly than 7MeG:T even though the K_d's were similar, 230 nM and 250 nM, respectively.[151] Specific glycosylases such as MutY and UDG appear to flip their target bases extrahelically in order to form specific interactions in the highly selective active sites.[173,203] That is, they change the equilibrium constant for flipping the damaged base extrahelically, K_{flip} (Scheme 11). In contrast, eAlkA appears not to alter

Scheme 11

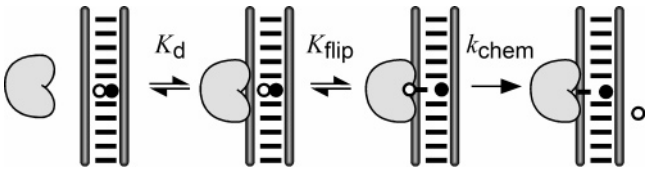

K_{flip} but rather uses the higher K_{flip} of unstable base pairs to achieve specificity for damaged bases. Its catalytic specificity is defined by (i) the effect of damage on K_{flip}, a measure of

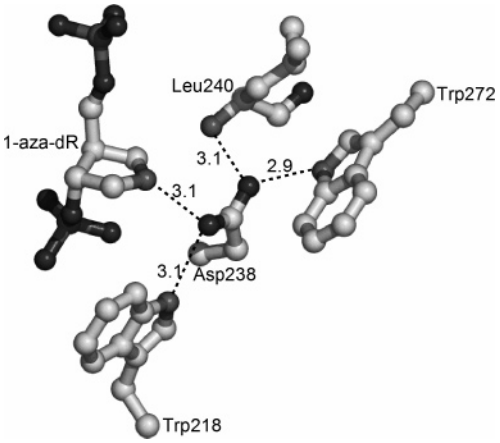

Figure 25. Contacts formed by eAlk_Asp238[389] in the active site. C atoms are white, N and P are gray, and O atoms are black.

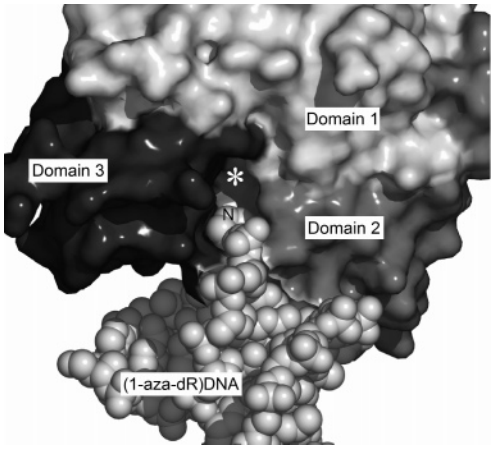

Figure 26. eAlkA·(A:1-aza-dR) structure,[238,389] showing domains 2 and 3 in contact with an oxacarbenium ion mimic inhibitor. Domains 2 and 3 are proposed to move when an alkylated nucleobase is bound. The N1 atom of 1-aza-dR is labeled, and the empty alkyl base binding pocket is indicated (*).

base pair strength, and (ii) the intrinsic stability of the *N*-glycoside bond.[151] This combination of effects helps ensure that unstable alkylated nucleobases in unstable base pairs are excised faster than normal nucleobases. Nonetheless, AlkA overexpression leads to increased mutation rates *in vivo*, indicating some cleavage of normal bases.[436] Product release appears to be rate limiting with eAlkA,[151] consistent with the cases of other BER enzymes and consistent with eAlkA's >3-fold greater affinity for THF apurinic analogues over intact DNA substrates.[151,227]

Oxacarbenium Ion Stabilization. eAlkA binding with oxacarbenium ion mimics has been studied by electrophoretic mobility shift assays (EMSA)[389,437] and fluorescence anisotropy.[151] The EMSA studies showed that AlkA bound A:1-aza-dR and T:4-aza-dR oxacarbenium ion mimics with K_d's of 100 pM and 16 pM, respectively, as compared to 45 nM for the T:THF product mimic.[238] Fluorescence anisotropy-based assays showed weaker binding than EMSAs, with K_d's of 18 nM and 15 nM, respectively, for C:1-aza-dR and C:4-aza-dR.[151] The cause of this 200- to 1000-fold discrepancy is not known, though it may arise in part from the different bases in the opposite strand. On the basis of the EMSA K_d's, eAlkA had the highest preference for oxacarbenium ion over product mimics of all HhH enzymes tested.[227] This 450-fold preference suggests that eAlkA uses strong oxacarbenium ion stabilization to promote catalysis (section 3.6.2), consistent with its wide specificity.

The eAlkA·(A:1-aza-dR) crystal structure[389] had enzyme contacts with the DNA backbone of the damaged strand at the +2, +1, −1, −2, and −3 positions. It also coordinated a sodium ion with the −3 phosphate using the main chain carbonyl oxygens of Gln210, Phe212, and Ile215. Such remote DNA backbone contacts are important in UDG-catalyzed reactions; however, unlike UDG, AlkA does not compress the backbone.

Mutation of the conserved Asp, eAlkA_Asp238, to Asn decreased 1-aza-dR binding 50-fold.[238] The orientation and protonation state of Asp238 appears to be controlled by NH hydrogen bonds from the Trp272 and Trp218 side chains, and the main chain amide of Leu240 (Figure 25). These interactions place Oδ within 3.1 Å of the inhibitor atom equivalent to C1′. This arrangement is not found in other HhH enzymes and may be evidence for direct participation of Asp238 in catalysis by aiding in the development and stabilization of an oxacarbenium ion in a $D_N{*}A_N$ mechanism.

Leaving Group Activation. Modeling studies indicated that 3-methyladenine could stack against Trp272 in eAlkA, forming $\pi-$cation or $\pi-\pi$ interactions.[389] On the basis of the eAlkA·(A:1-aza-dR) structure, Trp272 would have to rotate ~90° to position the aromatic ring within stacking distance of the leaving group (Figure 25). The aromatic residues proposed to interact with the leaving group, Tyr222, Tyr273, Phe18, and Trp218, line the bottom of the active site pocket. An induced fit mechanism, with these groups moving into contact with the leaving group, is supported by the fact that native eAlkA crystals cracked or had changes in the unit cell when soaked with methylated purine bases or nucleosides.[238] These changes were ascribed to motions in domains 2 and 3, which define the walls of the active site cleft (Figure 26).[438] The single turnover rate for 7MeG hydrolysis was pH independent above 7, with one pK_a near 6.6.[151] As the pK_a for 7-methylguanosine is 7.0,[129] this observation, plus the observed similar rate enhancements for damaged and undamaged purines, demonstrated that eAlkA was not selective for cationic leaving groups.

General Acid/Base Catalysis. The pH profile for G substrates was bell-shaped, with pK_a's of 6.0 and 6.9,[151] indicating general acid and base catalysis. Possible acid catalysts include Tyr273 and Tyr222. Tyr273 is positioned at the top of the active site cleft and would require a conformational change to protonate the leaving group. Tyr222 is positioned at the end of the pocket and could be positioned close to N3 of purine or O2 of pyrimidine leaving groups. The most likely candidate for the general base catalyst was eAlkA_Asp238, the conserved Asp residue, with a potential role in deprotonating the water nucleophile, as described above.

Nucleophile Activation. The absence of a potential nucleophile in the eAlkA·(A:1-aza-dR) structure and the close approach of the eAlkA_Asp238 side chain to N1 of the 1-aza-dR, at 3.2 Å, lead to the suggestions (i) that the enzyme uses a $D_N{*}A_N$ mechanism with nucleophilic attack on the same face of the oxacarbenium ion as the leaving group or (ii) that eAlkA_Asp238 forms a covalent intermediate, as retaining *O*-glycosidases do.[8,389] The eAlkA_Asp238Asn mutant, equivalent to bMutY_Asp144, was inactive, demonstrating its importance to catalysis.[151,238] However, a covalent mechanism seems exceedingly unlikely given the fact that there is no known example of a retaining mechanism in the *N*-glycoside literature and the fact that, among the *O*-glycosidases, families are either retaining or inverting, not

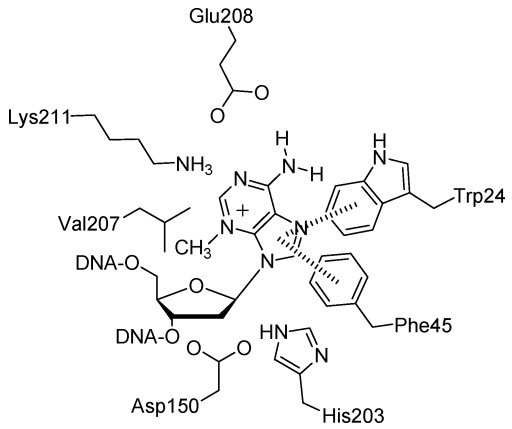

Figure 27. Proposed active site contacts between MagIII and a 3MeA substrate.

both. It is likely that the conformational change required for nucleobase binding, as demonstrated by crystal cracking, would also allow water binding, especially if the eAlkA_Asp238 carboxylate did not approach the neutral C1′ as closely as it does the positively charged N1 of 1-aza-dR.

5.3.7. 3-Methyladenine DNA Glycosylase (MagIII)

MagIII was recently identified in *H. pylori*.[418] It preferred 3MeA substrates over 7MeG and ϵA, similar to the case for eTAG.[418,419,421,423−425] Crystal structures of MagIII with 3,9-dimethyladenine and 1,N^6-ethenoadenine showed the nucleobases sandwiched between Phe45 and Trp24 (Figure 27).[419] 3,9-Dimethyladenine, 3-methyladenine, and 1,N^6-ethenoadenine bound with similar K_i's, showing that selectivity was not based on charge.[419] It preferred modified over unmodified adenine, though the mechanism for discriminating against unmodified adenine was not evident.

The MagIII·3,9-dimethyladenine structure indicated that the damaged base binds in the *syn* conformation, similar to the case for bMutY. The only potential active site contact with the leaving group was Glu208, which could interact with N1 and/or N6, forming hydrogen bonds and potentially protonating N1. The other clear potential contacts with the nucleobase were Phe45 and Trp24.

Oxacarbenium Ion Stabilization. MagIII bound its AP product weakly compared with the cases of other HhH enzymes, with $K_d > 16$ μM.[419] Dissociation constants with a 1-aza-dR inhibitor, $K_d = 0.5$ μM, a THF product analogue, $K_d > 4$ μM, and a 4-aza-dR inhibitor, $K_d > 3$ μM, demonstrated a >8-fold preference for the oxacarbenium ion mimic and a >6-fold preference for the positive charge to be at the anomeric position. This suggested that MagIII employs oxacarbenium ion stabilization to promote catalysis, though the 8-fold preference for 1-aza-dR over THF was less than that for AlkA, with its 450-fold preference for 1-aza-dR.

The MagIII_Asp150Asn mutation (equivalent to bMutY_Asp43) did not affect 1-aza-dR binding, but it decreased activity 22-fold, indicating a modest role in catalysis. MagIII_His203 appears capable of interacting with C1′ through a bound water. Mutation to Ala and Asn decreased 1-aza-dR binding 14-fold in both mutants, and it decreased activity 13- and 15-fold, respectively.[419]

5.3.8. Ogg Family—Bifunctional Enzymes

The OG DNA glycosylases (Ogg), also called MMH,[439] are bifunctional members of the HhH superfamily. They prefer OG but differ in specificity for the complementary base. Human Ogg 1 (hOGG1)[440−443] and yeast Ogg 1 (yOGG1)[443−445] prefer OG:C mismatches, which arise directly from oxidation of G residues. OG:A mismatches arise from misincorporation of A opposite OG or OG opposite A in DNA replication. In the former case, OG:A is the target of MutY/MYH. Yeast Ogg 2 (yOGG2, also called Ntg1) was reported to preferentially remove OG from mismatches with purines, including OG:A,[446−448] though this finding was not universal,[449,450] and it has also been shown to act on Fapy sites. Recently, yOGG2 was shown to act on more highly oxidized forms of G.[443] A human Ogg 2 has also been reported.[451] An Ogg from the archaea *Pyrobaculum aerophilum*, Pa-AGOG, removed OG base paired with any normal nucleobase and from single stranded DNA.[452] In the lyase step, Ogg catalyzes β-elimination, forming an AP site with a strand break on the 3′-side.

Structure and Catalytic Mechanism. Crystal structures of hOGG1 and its mutants have been solved, including those of the native protein,[453] a recognition complex,[454] a substrate complex,[105,455] borohydride-trapped complexes with 8-oxoguanine, 8-aminoguanine, and 8-bromoguanine,[96] THF-containing complexes,[105,456] and product complexes.[457] OG had a 3′-*exo* conformation in the substrate complexes, unusual for nucleosides but common with BER enzymes.[103,173,191,315] hOGG1 bound OG in an *anti* conformation, rather than the preferred *syn* conformation. This was in contrast to the cases of bFPG,[103] which bound OG_{syn}, and bMutY, which bound A_{syn}, despite the base's normal preference for *anti*.[203] Pa-AGOG was crystallized in the unliganded form and complexed with 8-oxo-2′-deoxyguanosine.[390]

Deducing the hOGG1 mechanism has been a challenge. The catalytic residues are expected to include Asp268, Lys249, and Cys253. Lys249 is the nucleophile that attacks C1′, forming the Schiff base intermediate. Mutation to Gln abolished glycosylase activity,[442,455] and alkylating the inactive Lys249Cys mutant with 1-bromoethylamine restored activity.

hOGG1_Asp268 is the conserved HhH superfamily Asp. It was initially proposed to deprotonate Lys249, but in DNA-bound hOGG1 structures, Lys249 and Asp268 were not in hydrogen bonding distance, and Asp268 was involved in helix-capping hydrogen bonds that constrained its flexibility. Its orientation was remarkably constant in all the structures, including when mutated to Asn268, which was 65-fold less active in the glycosylase reaction. Two mutants retained near-wild-type activity, Asp268Glu and Asp268Gln. Asp268Glu had a distorted side chain conformation that allowed it to form the same helix-capping interactions as Asp and perform the same putative catalytic functions. However, Asp268Gln did not form helix-capping interactions, was less thermally stable, caused changes in the active site structure, and did not possess a carboxylate functional group, yet it was still fully active. Thus, the significance of the conserved Asp268 residue is not clear.

Cys253 has been proposed to form an ion pair with Lys249 to increase specificity for OG over G,[454] based on the hOGG1_Lys249Ala·(OG:C) and hOGG1:(G:C) structures. G "stalled" outside the active site, while OG fully inserted into the active site pocket. Key sources of discrimination were proposed to be (i) a hOGG1_Gly42 C=O ··· H−N7 hydrogen bond and (ii) favorable antiparallel interaction of the dipoles around N7 and O8 in OG and the putative $Lys249^+-Cys253^-$ ion pair (Figure 28). The ion pair could

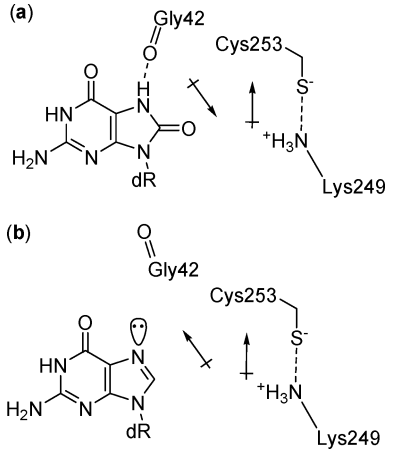

Figure 28. Proposed substrate recognition in hOGG1. (a) Favorable, antiparallel dipole−dipole interaction of OG with the proposed $Lys249^{+}-Cys253^{-}$ ion pair, compared with (b) an unfavorable, parallel interaction with G.[454]

aid substrate recognition, but deprotonating Lys249 to make it a nucleophile would destroy that effect.

hOGG1 lacked multiple, strong interactions with either the deoxyribosyl ring or the 8-oxoguanine leaving group, unlike, for example, FPG (section 5.4.1). A recently proposed mechanism uses 8-oxoguanine in a product-assisted $D_N{*}A_N$ mechanism (Figures 29 and 30).[105] According to this model, Lys249 would attack the oxacarbenium ion from the β-face, leading to an overall retention of configuration. Elucidating the hOGG1 mechanism remains a work in progress.

The Pa-AGOG fold revealed it as a member of the HhH superfamily, though there were significant changes in the supersecondary structure.[390] The 8-oxoguanine ring bound in a similar location as that in hOGG1, but the deoxyribosyl ring was positioned such that it was sterically impossible to extend it into a DNA chain, indicating that the observed sugar binding was not catalytically relevant. The overall DNA binding groove was expected to be similar to that for hOGG1.

5.3.9. Endonuclease III/Nth—Bifunctional Enzymes

Endonuclease III (Endo III), also called Nth, is a bifunctional HhH enzyme with glycosylase and β-elimination activities. It occurs in archaea, eubacteria, and eukaryotes and contains an Fe_4S_4 cluster.[452] It was first investigated in *E. coli* (eEndo III).[458,459] Enzymes from *B. stearothermophilus* (bEndo III)[460] and the eukaryotic equivalents from humans (hNth1),[461−463] mice (mNth1),[464] *Saccharomyces*

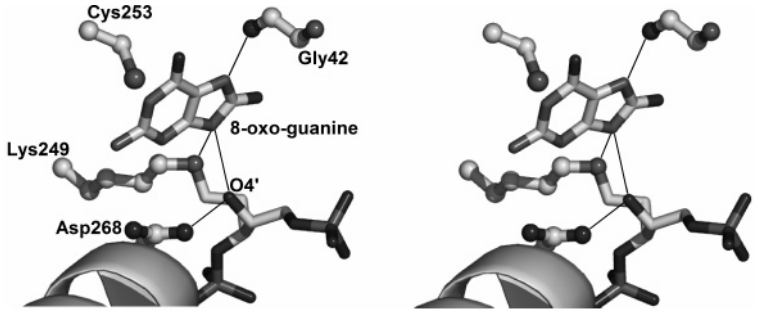

Figure 29. Active site structure of hOGG1 with a borohydride trapped covalent intermediate and 8-oxoguanine.[96] Except for the C−N bond being reduced, this corresponds to the Schiff base intermediate in Figure 30. The 8-oxoguanine was proposed to be in the anion form, hydrogen bonding to Nϵ Lys249 and O4′, though its similar pK_a to that of Lys and the close approach of Asp268 to O4′ (2.9 Å) suggest another possible hydrogen bonding arrangement. The N-terminal end of helix αM, with which Asp268 forms helix-capping hydrogen bonds, is shown.

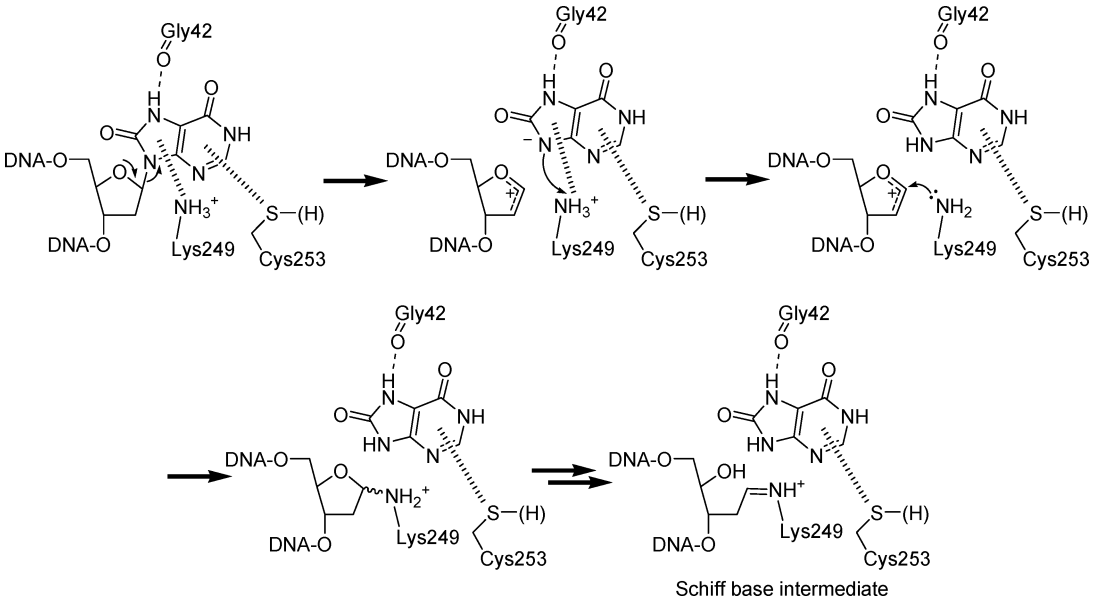

Figure 30. Product-assisted glycosylase step in the hOGG1 reaction, adapted from refs 96, 105, and 454. The protonation states of protein side chains differ between proposals. In this mechanism, the 8-oxoguanine anion deprotonates Nϵ of Lys249, making it nucleophilic. In the second last step shown, a base catalyst is required for Schiff base formation. Alternatively, the first step could have Lys249 in the neutral form, allowing the leaving group anion to catalyze Schiff base formation. 8-Oxoguanine is also proposed to catalyze β-elimination.

Scheme 12

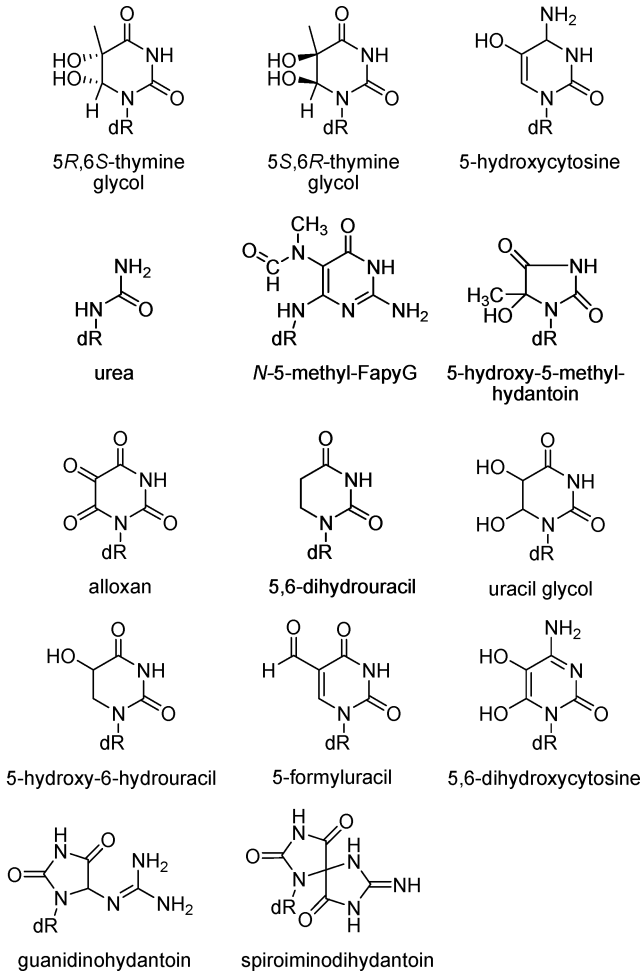

cerevisiae (yNth1, yNth2),[464] and *S. pombe*[465] have also been characterized. Endo III/Nth enzymes recognize many oxidized pyrimidines (Scheme 12).[97,461,464,466−470] AP DNA was also a substrate, undergoing β-elimination. In organisms with two copies, they had distinct but overlapping activities. Product release was rate limiting in hNth1 but relieved by truncating the N-terminal domain.[467]

Structure. The essential nucleophilic Lys residue was identified as eEndo III_Lys120. Mutation to Gln decreased activity 10^5-fold,[334,471] as did the equivalent mutant in hNth1, Lys212Gln. The Lys212Arg mutant's activity only dropped 85-fold even though it would be unusual for Arg to be a nucleophile.[469] The conserved Asp residue in HhH enzymes, Asp138, was also catalytically important, with activity decreasing 100-fold upon mutation to Asn.

Crystal structures have been reported for eEndo III in unliganded form,[334,471] and for bEndo III[460] with a THF inhibitor, and as the covalent borohydride-trapped intermediate, with G or A in the estranged strand. bEndo III made contact with the opposite strand, both through the DNA backbone and through the estranged residue, forming strong contacts with G, weaker ones with A, and not complexing C or T, consistent with its role in repairing damaged pyrimidines.[460] Fe_4S_4 was suggested to play only a structural role, though results with eMutY suggest the possibility of a role in lesion recognition.[358−360] bEndo III_Lys121 was positioned for nucleophilic attack in the THF complex. In the trapped complexes, bEndo III_Asp139, the conserved HhH Asp residue, was within hydrogen bonding distance of

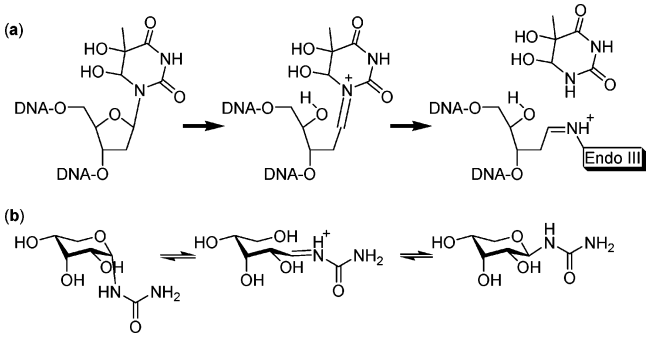

Figure 31. (a) Proposed endocyclic mechanism for Endo III.[206] (b) Observed anomeric equilibrium for urea riboside in aqueous solution.[473] It forms a ribopyranosyl ring rather than ribofuranosyl.

O4′, but in the THF complex, it moved such that the carboxylate oxygen was slightly closer to C1′. Curiously, the reported stereochemistries of deprotonation of the Schiff base intermediate for bEndo III[460] and eEndo III[472] were opposite, being *pro-R* and *pro-S*, respectively. bEndo II-I_Asp45 was advanced as a possible general base catalyst, acting through a bridging water molecule. The nucleobase binding site was lined with polar and aliphatic residues, consistent with its ability to accept a variety of oxidized pyrimidines.

Mechanism. eEndo III was proposed to use an endocyclic mechanism (Figure 31).[206] The proposal was based on the facts that (i) eEndo III cleaved urea residues faster than thymine glycol and (ii) urea residues anomerize in solution, indicating an equilibrium with the ring-opened Schiff base form.[473] Thus, it was proposed that the enzymatic mechanism also involved ring opening. We have argued above against endocyclic mechanisms (section 3.5). Given the fact that Endo III evolved in a superfamily containing monofunctional enzymes that catalyze normal *N*-glycoside cleavage, we would expect Endo III to behave similarly. It is conceivable that urea residues would proceed through an endocyclic mechanism, but it is more likely that pyrimidine substrates will proceed through the more common direct displacement mechanism.

5.4. FPG/Nei (Endonuclease VIII) Superfamily—Bifunctional Enzymes

The FPG/Nei superfamily consists of two groups of bifunctional BER enzymes with similar specificities for oxidative lesions.[332,335] They have AP lyase activity, catalyzing both β- and δ-eliminations. The protein structures include an H2TH (helix−two turns−helix) motif which was proposed to have a role in nonspecific DNA binding, much like the HhH motif.[474] They also possess a zinc finger motif, which was proposed to be involved in base-flipping, or a "zinc-less finger", which lacks Zn^{2+} but has the same structure and DNA-binding function.[211]

5.4.1. FPG/MutM

The FPG enzymes are also called MutM in prokaryotes, or 8-oxoguanine glycosylase.[101] The Schiff base intermediate can be trapped by reduction with $NaBH_4$.[475] It was first isolated from *E. coli* (eFPG) on the basis of its ability to act on ring-opened 7MeG substrates (*i.e.*, 2,6-diamino-4-hydroxy-5-*N*-methylformamidopyrimidine), as well as FapyA and FapyG.[476,477] Its biological target was later shown to be OG.[478,479] FPG's activity overlaps with that of the nonhomologous Ogg enzymes.

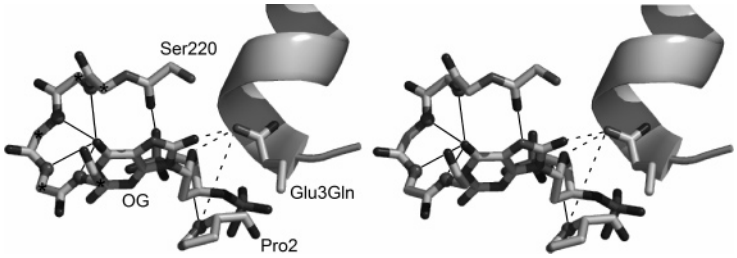

Figure 32. Active site contacts in the bFPG_Glu3Gln·(OG:C) structure.[103] There are four potential hydrogen bonds between the backbone amides of residues 222−225 (Cα's marked with *) and O6 of the OG residue. A hydrogen bond from the bFPG_Ser220 backbone O to N7H has been proposed to differentiate G from OG. C1′ undergoes nucleophilic attack from bFPG_Pro2 Nα. Possible catalytic interactions of bFPG_Glu3 are shown with dotted lines (see text). The Gln3 side chain occurs in a very similar position to that of Glu3 and acts as a helix cap.

Substrate Specificity. FPG acts on Fapy derivatives of purines, on OG, on other 8-oxo-purines, and on other oxidized bases and will act directly on AP sites, but it was inactive against single stranded DNA.[97,443,478−485] Its specificity has also been examined computationally.[485,486] For OG substrates, k_{cat}/K_M was sensitive to the complementary base in the order OG:T > OG:G > OG:C ≫ OG:A.[481] Presumably, OG:C was slightly worse than OG:T and OG:G because base pairing with C made extrahelical OG flipping more difficult. OG:A mismatches are the correct substrates of MutY/MYH, explaining the 17-fold lower specificity with FPG. With an OG:C substrate, eFPG catalyzed the glycosylase reaction with an intrinsic rate of 0.16 min^{-1}, and the β-elimination step at 0.1 min^{-1}.[487] eFPG·DNA binding became stronger as the length was increased up to 11 base pairs.[488]

Structure and Catalytic Mechanism. Structures have been reported for the unliganded enzyme from *Thermus thermophilus* (tFPG),[474] for *Lactococcus lactis* FPG with a 1,3-propanediol-containing DNA,[489] for a borohydride-trapped covalent intermediate of eFPG,[98] for the *B. stearothermophilus* enzyme (bFPG) with a reduced AP site (RAP:C), for the borohydride-trapped covalent intermediate, for the product complex, for the (AP:T) and (AP:G) recognition complexes,[102] and for the bFPG_Glu3Gln·(OG:C) complex.[103]

In the bFPG_Glu3Gln·(OG:C) complex, bFPG formed hydrogen bonds to the DNA backbone in the damaged strand at positions −2 to +2, including the target base at positions −1 and +1, but no backbone contacts with the complementary strand. The backbone phosphodiester groups at −1 and +1 were "pinched" by the Arg264 side chain, which formed ionic interactions to both groups. This interaction would help force the target residue out of the base stack and into the active site. The AP-containing structures had favorable contacts between the Arg112 side chain and the "estranged" T or C. Arg112 would clash with A, conferring specificity against OG:A mismatches.

bFPG residues 221−234, which form the OG binding loop, were unstructured in all except the bFPG_Glu3Gln·(OG:C) structure (Figure 32). bFPG bound the OG_{syn} conformer, in contrast to hOGG1, which bound OG_{anti}.[105,454,455] The enzyme formed a remarkable four hydrogen bonds between O6 and the backbone amides of residues 222−225. A hydrogen bond between the backbone oxygen of Ser220 and N7H of OG was the only contact capable of distinguishing OG from G. There were no water-mediated interactions and no π-face interactions evident. O8 hydrogen bonded Gln3 Nε, but this was regarded as an artifact because Glu3 in the wild-type enzyme would likely be deprotonated. It was a helix-capping residue, tending to make it unusually acidic.[490]

Proposed Mechanisms. The FPG glycosylase step involves nucleophilic attack by the N-terminal residue, bFPG_Pro2, on C1′.[95] One proposed mechanism appeared to involve endocyclic cleavage, but the timing of leaving group departure was ambiguous.[98] The other proposed mechanisms involved normal C−N bond cleavage, with nucleophilic attack by bFPG_Pro2 causing the leaving group to depart in an A_ND_N mechanism. bFPG_Glu3 was essential for the glycosylase reaction,[100] but its role remains ambiguous. It could hydrogen bond or even protonate O8, assisting leaving group departure, though its function as a helix cap residue makes it less likely to have an unusually high pK_a. If it has a high pK_a, an alternative mechanism would be to hydrogen bond to O4′, polarizing the C−N bond, as proposed for PDG.[491] In the carboxylate form, it could deprotonate Nα of bFPG_Pro2, though this would require a structural change, as it was not close to bFPG_Pro2 in any of the structures. It could also electrostatically stabilize an oxacarbenium ion in $D_N{*}A_N$ or dissociative A_ND_N mechanisms. OG bound in a 3′-*exo* conformation, helping hyperconjugation in an oxacarbenium ion-like TS. eFPG showed a 7-fold preference for 4-aza-dR inhibitors, K_d = 350 nM, over THF, 2600 nM, indicating an ability to stabilize oxacarbenium ions somewhere between the extremes of MutY (no preference) and AlkA (450-fold preference).

Leaving Group Activation and Recognition. The most striking feature of the bFPG_Glu3Gln·(OG:C) structure was the four hydrogen bonds to O6 of the nucleobase (Figure 32). These interactions suggest leaving group activation through stabilization of an O6 oxyanion and 8-oxo-guanine departure as an anion (Figure 33). Alternatively, if general acid catalysis were operative, it would have to be through O8 or N3, given the hydrogen bonds to O6. No potential general acid was identified near N3. eFPG_Lys217 was proposed to be important in recognizing OG, based on molecular dynamics calculations, but the effect of a eFPG_Lys217Thr mutation was modest, decreasing k_{cat}/K_M only 5-fold,[485] and Lys217 was disordered in all structures, arguing against an important role.

5.4.2. Nei/Endonuclease VIII

The Nei/endonuclease VIII enzymes are found in prokaryotes,[335] including *E. coli* Nei (eNei),[492] and eukaryotes, including the mammalian *Nei*-like family (hNEIL1, hNEIL2, and hNEIL3 in humans), also called Nei or NEH.[211,493,494] Although the Nei family occurs in both prokaryotes and eukaryotes, its occurrence is uneven and many organisms

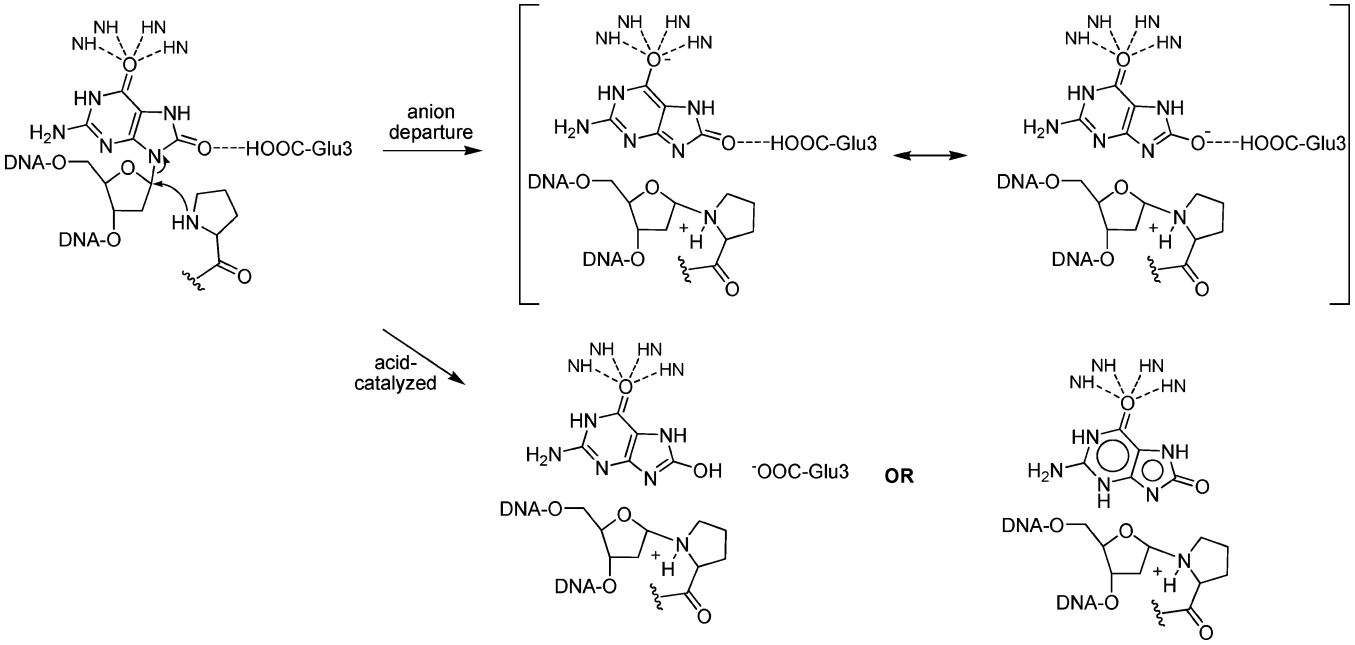

Figure 33. Potential leaving group activation mechanisms for FPG. (top) Leaving group departure as an anion could be stabilized by strong hydrogen bonding to O6 through backbone amides, as observed in the crystal structure, and a hypothetical hydrogen bonding interaction through O8. (bottom) Acid-catalyzed activation could occur through protonation at O8 or N3, though no candidate proton donor to N3 has been identified.

do not possess Nei.[335] Nei enzymes have the H2TH motif and a zinc (or zinc-less) finger motif.[495] hNEIL3 has Val2 as the nucleophile, rather than Pro2 in other Nei and FPG family enzymes.[495]

Substrate Specificity and Kinetics. Nei catalyzes glycosylase and β/δ-elimination reactions.[94] Nei[461,492,496] and hNEIL1[461,462] have broad lesion specificity, with a preference for oxidized pyrimidines, similar to the case of eEndo III, which is unrelated.[492] They are active on oxidized pyrimidines and, to a lesser extent, oxidized purines, including OG paired with G, A, or C (Scheme 13).[97,431,461,492,496] Nei had the highest rates with thymine glycol and did not distinguish between the diastereomeric 5*S*,6*R*- and 5*R*,6*S*-forms, with $k_{cat} = 5.7$ and 4.6 min^{-1}, respectively,[464] though hNEIL1 had a 380-fold preference for the 5*S*,6*R*-form, with $k_{cat} = 0.6$ min^{-1}.[464] hNEIL2 only acted on AP sites, which may reflect its true activity or the inability to find its true *N*-glycoside substrate.[461]

Structure and Catalytic Mechanism. The crystal structures of unliganded hNEIL1[211] and eNei,[497] plus eNei in a borohydride-trapped complex have been reported.[208] eNei formed DNA backbone interactions with positions +2 to −3 of the damaged strand and formed backbone contacts with the opposite strand at positions −1 and −2. Like FPG, it did appear to use a "pinch" mechanism, as the interphosphate distance between residues +1 and −1 was reduced. The structures of the catalytic Pro1 and Glu2 residues were similar to those of the equivalent residues in bFPG. A model of a thymine glycol substrate was created in the active site, implicating Phe227, Phe230, and Tyr169 in substrate recognition. On the basis of this modeled structure, the authors concluded that Nα of Pro1 was poorly oriented to displace the thymine glycol base by direct nucleophilic displacement, and instead they proposed an endocyclic mechanism, with nucleophilic attack displacing O4′ from C1′ (Figure 34). Endocyclic mechanisms raise some concerns, and this mechanism, in particular, seems problematic. The first step involves protonating two substrate oxygens, both of which

Scheme 13

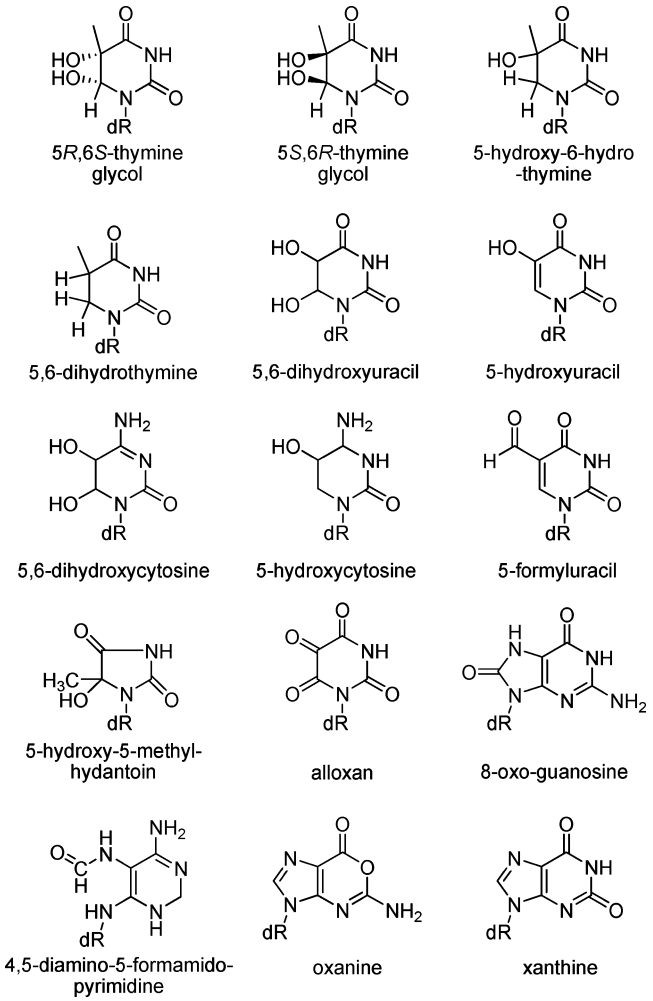

are very acidic. O2, in particular, would have $pK_a < -3$, compared with $pK_a > 10$ for Pro2 Nα. O2 would have to

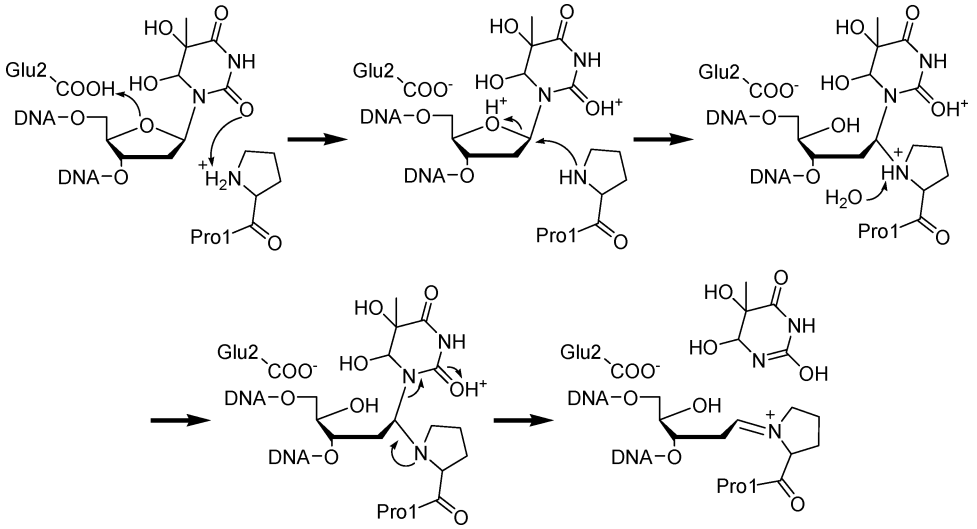

Figure 34. Endocyclic mechanism for the glycosylase step of eNei proposed in ref 208.

deprotonate Nα, with $K_{eq} < 10^{-13}$, and remain protonated through several reaction steps. Direct C−N cleavage could be accommodated by a small conformational change in eNei_Pro2, and is more probable. As with FPG, the role of eNei_Glu2 is not obvious. Mutating it to Asp, Ala, or Gln[208,210] resulted in little or no glycosylase activity but almost-wild-type lyase activity.

5.5. Alkyladenine DNA Glycosylase (AAG)—Monofunctional Enzymes

Alkyladenine DNA glycosylase (AAG), also known as alkylpurine−DNA glycosylase (ANPG) and *N*-methylpurine DNA glycosylase (MPG), is a monofunctional BER enzyme found in mammals, plants, and some bacteria.[152,498] It is not related to other BER enzymes. The best characterized member of the AAG family is human AAG (hAAG).

5.5.1. Substrate Specificity

hAAG hydrolyzes undamaged purines, alkylpurines, and purine deamination products such as Hx and oxanine (Scheme 14).[499−501] Unlike eAlkA, its activity appears to be limited to purines.[502] The best substrate was hypoxanthine (Hx), providing (9×10^7)-fold rate enhancement, or 11 kcal/mol in TS stabilization.[499] The rate enhancement for Hx was more than 100-fold greater than that for other purine substrates and 1000-fold greater than that for 3MeA or 7MeG. Alignment of the hAAG·(T:4-aza-dR),[237] hAAG_Glu125Gln·(T:ϵA), and hAAG·(T:ϵA) crystal structures[191] showed that the active site was rigid, with amino acids positioned to select for substrates based on hydrogen bonding, π-stacking, and steric interactions.[503] The Hx preference appears to be based on a hydrogen bond from the His136 backbone amide to O6, providing 800-fold specificity relative to purine deoxynucleoside.[499] The unfavorable interaction with $N6H_2$ of A decreased the rate (7×10^4)-fold relative to that for Hx. Alkylation of A to form ϵA creates a hydrogen bond acceptor at N6 and increased the rate 200-fold. Saturating the ϵA etheno group to form 1,N^6-ethanoadenine reduced the rate 65-fold,[503] which was attributed to loss of π-stacking with His136. Asn169 contributed to specificity by steric crowding at N2 of G, decreasing the rate 6400-fold relative to that for Hx (Figure 35).

The rate appears to be affected by the stability of the base pair; for example, 7MeG:T was removed 28-fold faster than

Scheme 14

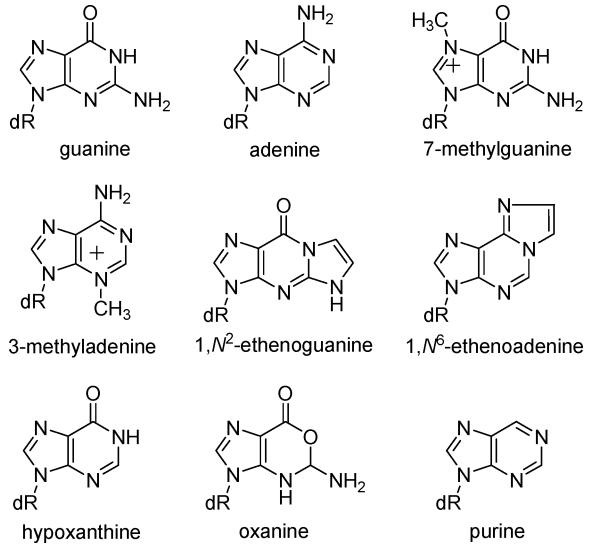

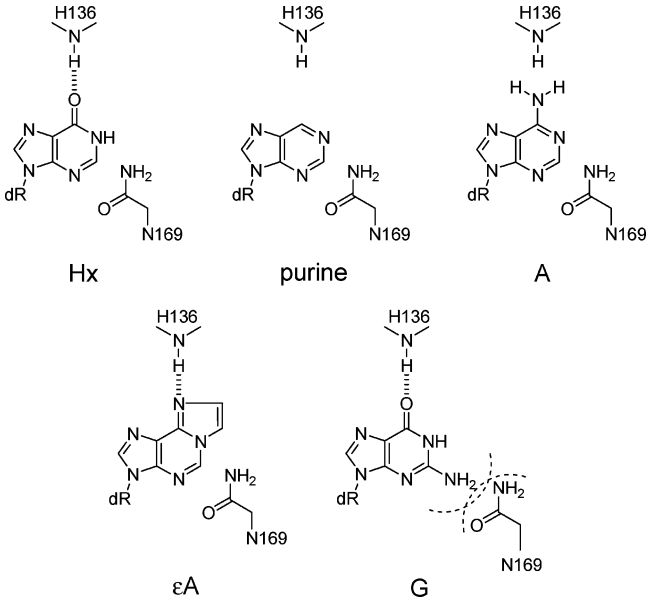

Figure 35. Proposed interactions of the 6-position of purine substrates and the hAAG_His136 backbone amide. (Adapted from ref 499.)

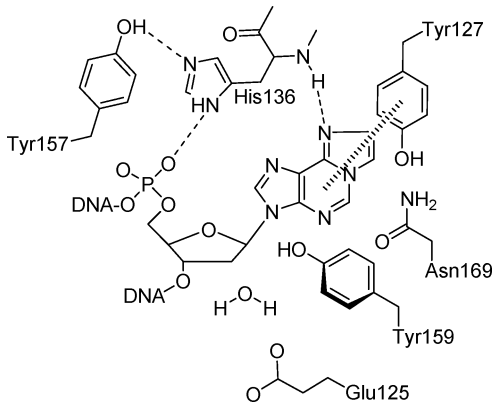

Figure 36. Proposed active site contacts for hAAG with an ϵA substrate.

7MeG:C.[504] hAAG behaved similarly to eAlkA in this regard, with the rate controlled by K_{flip} of the target base pair.[499] Product release was rate limiting.[505] Like MutY, the steady-state rate was increased *in vitro* by human APE1 and the proliferating cell nuclear antigen.[377]

5.5.2. Leaving Group Activation

hAAG made face-to-face and edge-to-face aromatic contacts with ϵA through Tyr127, Tyr159, and His136 (Figure 36). The backbone amide of His136 could hydrogen bond N6. The single turnover rate was 10^7-fold lower with 7-deazainosine than Hx, consistent with N7 protonation.[217] The pH profile for 7MeG hydrolysis was pH independent above pH 7. Given the N1 pK_a of 7MeG, 7.0, this could indicate that hAAG does not select for positively charged residues. However, bearing in mind the strong environmental dependence of the N1 pK_a of 7MeG, it is not necessarily safe to assume that it was deprotonated above pH 7 in the hAAG active site (Figure 12).

Single turnover rates for ϵA and Hx hydrolysis decreased at higher pH's with pK_a's of 7.3 for ϵA and 6.4 for Hx.[217] Mutation experiments failed to identify a general acid catalyst from the candidate residues His136, Tyr159, and Tyr127, with decreases in single turnover rates of <40-fold, except for 7MeG substrates, which cannot be protonated at N7, which had rate decreases of up to 800-fold.[217,499] Alternatively, on the basis of the hAAG_Glu125Gln·(T:ϵA) crystal structure,[191] a water positioned 2.8 Å from N7 could be the general acid catalyst. It was coordinated by the backbone oxygen of Ala134 and was part of a network that could relay a proton to N7 from bulk solvent.

5.5.3. Oxacarbenium Ion Stabilization

hAAG had a moderate 7-fold preference for binding T:4-aza-dR, K_d = 23 pM, over T:THF, 160 pM.[506] In the hAAG·ϵA and hAAG·4-aza-dR cocrystal structures,[191] the flipped nucleoside in the active site had a 3′-*exo* conformation, optimal for hyperconjugation in the oxacarbenium ion. The +1 phosphodiester was positioned above the sugar ring, with a nonbridging oxygen hydrogen bonding with the His136 side chain, and the bridging oxygen was positioned above the deoxyribosyl ring 3.0 Å from C1′ and was potentially able to stabilize the oxacarbenium ion. Positioning of the +1 phosphodiester was assisted by contacts in the extended binding site, including up to eight phosphodiester contacts at the +1, −1, −2, and −3 positions in the damaged strand and −3, −4, and −5 in the undamaged strand.[191,237] Tyr127 Oη was positioned 3.5 Å from C1′ and could help stabilize positive charge at C1′, along with Glu125 (see below).

5.5.4. Nucleophile Activation

The single turnover rates with ϵA, Hx, and 7MeG decreased at acid pH, with pK_a's of 5.0,[217] or 6.5 for 7MeG. The pH profiles implied general base catalysis, with Glu125 being the prime candidate. In crystal structures, it coordinated with a potential water nucleophile directly below the deoxyribosyl ring, in line for attack at C1′ (Figure 36).[191,217,237] The backbone oxygen of Val262 could hydrogen bond the proposed nucleophile. Mutation of Glu125 to Gln or Ala resulted in a ≥16 000-fold rate decrease with ϵA and a ≥8000-fold decrease with 7MeG,[217] though the decrease was only 15-fold with Glu125Asp. This suggests that hAAG derives a large fraction of its catalytic power through general base catalysis by Glu125. hAAG was proposed to use an A_ND_N mechanism where water or hydroxide attack at C1′ facilitates *N*-glycosidic bond cleavage. This proposal is reasonable, but it should be remembered that a candidate water nucleophile is observed in a similar location in the crystal structures of UDG and MutY, enzymes with D_N*A_N mechanisms.

5.6. Pyrimidine Dimer Glycosylase (PDG)—Bifunctional Enzymes

Short wavelength UV light forms cyclobutane pyrimidine dimers, with thymidyl(3′-5′)thymidine dimers (T◊T) as the predominant product (Scheme 15).[2] In eukaryotes, T◊T

Scheme 15

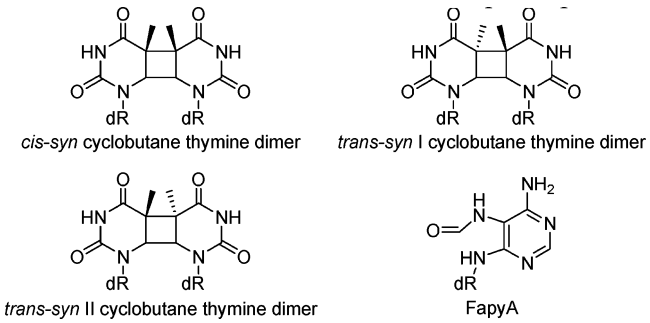

are removed by the NER pathway.[507] In prokaryotes and viruses, they are removed by photolyases, the NER pathway, and pyrimidine dimer glycosylase (PDG), known previously as T4 endonuclease V, CPD glycosylase, or UV endonuclease.[2,507−509] PDG is not homologous with other BER enzymes.[510,511] The bacteriophage T4 (T4PDG) and *Paramecium bursaria Chlorella* virus-1 (cvPDG)[512] enzymes are the best studied. It is a bifunctional enzyme, with glycosylase and β-elimination activities. It is the only BER enzyme characterized to date that gains access to the target residue by flipping a base from the undamaged strand.[511]

5.6.1. Substrate Specificity

T4PDG and cvPDGs prefer *cis-syn* pyrimidine dimers but also have activity on *trans-syn II* dimers and minimal activity on *trans-syn I* dimers.[512−514] T4PDG also has activity against FapyA.[515] Single turnover analysis of the T4PDG and cvPDG glycosylase steps with *cis-syn* T◊T showed rate enhancements of [(1−4) × 10^8]-fold, corresponding to 12 kcal/mol in TS stabilization.[512,516,517] The lyase step was 10-fold slower, and AP DNA was a substrate.[99,512,513,518]

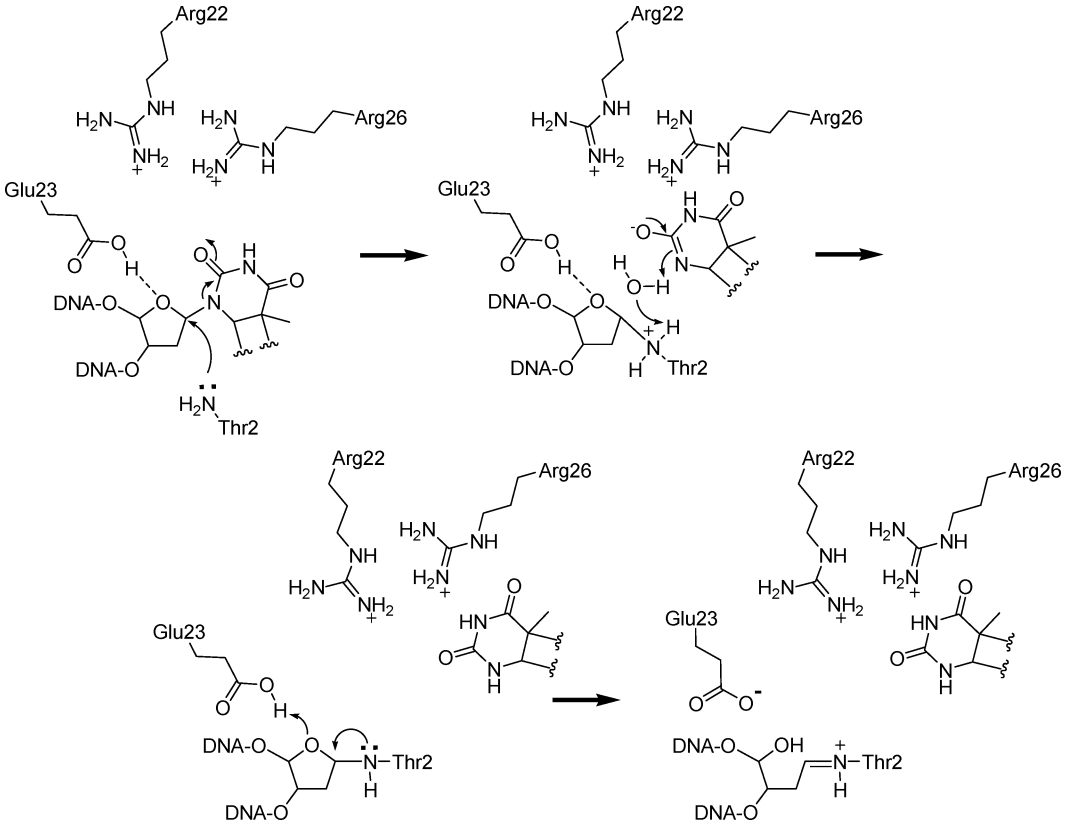

Figure 37. Proposed active site contacts and a possible glycosylase mechanism of T4PDG. (Adapted from refs 491 and 1.)

5.6.2. Catalytic Mechanism

T4PDG acted on 2′α-fluorothymidine-containing dimers.[519] The fluoro modification stabilizes the *N*-glycosidic bond by inductively destabilizing the oxacarbenium ion. Similar structures effectively inhibited eMutY, hTDG, eMUG, and eUDG.[279,344,520,521] A number of catalytic mechanisms for T4PDG have been proposed based on trapping studies,[475,522] mutational analysis,[513,516,518,523,524] oligonucleotide analogues,[519] X-ray crystallography,[510,511,524,525] and computational simulations[491] (Figure 37). The T4PDG_Glu23Gln·(T◊T) crystal structure[525] showed T4PDG_Gln23 < 4 Å from O2 of T◊T, the O′4 ring oxygen, and Nα of T4PDG_Thr2, suggesting several possible mechanistic roles.[2] Mutagenesis studies showed that Glu23 from both T4PDB and cvPDG was an important residue, with the Glu23Gln mutant being devoid of glycosylase activity.[513,516] The results with Glu23Asp were contradictory, with cvPDG retaining activity against *cis-syn* substrates but losing it against *trans-syn II*, while T4PDG had no glycosylase activity. Glu23 is located similarly to acidic residues which are proposed to act as general base/electrostatic catalysts in other BER enzymes. In the PDG case, its role as a general base catalyst would be to deprotonate Nα of Thr2, the nucleophile in the glycosyl transfer step. Alternatively, Glu23 was proposed act as a hydrogen bond donor to O4′, helping to polarize the *N*-glycosidic bond and activate it for nucleophilic attack.[491] This proposal was consistent with the high calculated pK_a of T4PDB_Glu23, 7.8 in the substrate complex. Glu23 could also act as a general acid catalyst, protonating O2 of the thymine ring to make it a better leaving group. This role was not supported by the computational model, which supported thymine leaving in the anion form. It could also act as a general acid catalyst to protonate O4′, facilitating ring opening and formation of the Schiff base intermediate. T4PDG_Glu23 was implicated because the lyase step had a pH optimum of 5.5, decreasing to 5.0 for T4PDG_Glu23Asp.[518] Also, the T4PDG and cvPDG Glu23Gln mutants lacked lyase activity, while the Glu23Asp mutants were active.[513,526]

5.6.3. Leaving Group Activation

An essential difference between T◊T dimers and other damaged bases is that the rings are not aromatic after reduction of the C5−C6 bond. The practical upshot is that if it departs in the anion form, extensive delocalization of the negative charge will not be possible, as it is with T and U. Instead, the charge will be localized on N1 or O2. This implies that either the enzyme will be effective at stabilizing a localized (and therefore high-energy) negative charge or it will protonate the leaving group. T4PDG_Arg26 was located close to O2 in the crystal structure,[525] possibly indicating a role in stabilizing a negative charge at O2. T4PDG_Arg22 was also located within 5 Å of the target base. Mutating these Arg's to Gln reduced catalysis by 110-fold and 17-fold, respectively.[516] Computational studies suggested that the enzyme would destabilize the O2 protonated substrate by 6.6 kcal/mol relative to solution, arguing against O2 protonation.[491] The same study showed that the enzyme stabilized the neutral base, but did not examine departure in the anion form because it was believed to be a poor leaving group.

5.6.4. Oxacarbenium Ion and/or Schiff Base Stabilization

T4PDG made contacts with the damaged strand at the +1 and −1 phosphodiester groups using a conserved cluster of basic amino acids, His16, Arg3, Lys121, and Arg117. Mutational analysis of this cluster indicated a role in substrate binding rather than catalysis.[516] Detailed analysis of

His16 suggested a catalytic role in the lyase step.[523] The T4PDG_Glu23Gln·(T◊T) structure[525] showed that Glu23 and O4′ of the 3′−T residue of the T◊T dimer were positioned within 4 Å of C1′ of the target nucleotide and could be important in stabilizing an oxacarbenium ion or a Schiff base intermediate. T4PDG inhibition studies gave $K_d = 9$ nM for a reduced AP site (RAP) compared with 17 nM for the 4-aza-dR mimic and 140 nM for THF.[527] The 8-fold preference for 4-aza-dR over THF is similar to the cases of several other BER enzymes, between the extremes of MutY (no preference) and AlkA (450-fold preference). Inhibition studies with cvPDG gave similar results, with a 4-fold preference for 4-aza-dR over THF and RAP, 2.5 nM versus 10 nM and 12 nM.[513]

6. Summary

In this review, we have attempted to illustrate the contributions that TS analysis has made to understanding BER enzymes, either directly, as in TS analysis of UDG, or indirectly, through TS analyses of related reactions, such as the ricin-catalyzed reactions. As the number of TS analyses of BER enzymes is not likely to increase dramatically in the future, studies of enzymes with related activities will remain a rich source of knowledge. The detailed understanding of BER enzymes that TS analysis can provide will be enormously important, particularly for enzymes where the basic details of catalysis remain open questions. Even with the best studied enzyme, UDG, significant questions remain, such as the role of Asp64/145 in catalysis and whether it acts as a general base catalyst and/or by electrostatic stabilization of the oxacarbenium ion.

Some major questions regarding BER enzymes include the following: (i) For purine substrates, is N7 always the site of ring protonation, and do enzymes diprotonate purine leaving groups? (ii) Do all pyrimidine reactions have an anionic leaving group like UDG, or do some enzymes use general acid catalysis? (iii) Similarly, does OG cleavage proceed through an anionic leaving group, or is there general acid catalysis? (iv) Do any enzymes use an endocyclic cleavage mechanism? (v) Do any BER enzymes use a synchronous A_ND_N mechanism like thymidine phosphorylase? (vi) For each enzyme, what are the identities and roles of catalytic residues? (vii) What are the relative contributions of oxacarbenium ion stabilization and leaving group/nucleophile activation for a given enzyme? (viii) There have been few detailed mechanistic studies of lyase (β- and β/δ-elimination) activity, and even the basic features of these reactions remain to be elucidated. TS analysis can significantly contribute to the answers of all these questions.

"What mechanistic questions remain for DNA glycosylases? The answer to this question is straightforward—many."[1] Many questions remain, but we have learned a great deal in the last couple of years and we are optimistic about future progress.

7. Acknowledgments

We thank Prof. Sheila David for providing results on base analogues with MutY before publication, and Dr. Matthew Birck for the coordinates of the hTP TS. We thank an anonymous reviewer for helpful suggestions. We also acknowledge funding by NSERC (Natural Sciences and Engineering Research Council of Canada), including a postgraduate scholarship to J.A.B.M.

8. Abbreviations

AAG	alkyl purine DNA glycosylase
AlkA	*E. coli* alkyl purine DNA glycosylase II
AP	abasic (apurinic/apyrimidinic) site in DNA
APE1	human AP endonuclease
1-aza-dR	1-azadeoxyribosyl residue
4-aza-dR	4-aza-deoxyribosyl residue, also called iminoribitol or pyrrollidine derivatives
BER	base excision repair
bMutY	MutY from *Bacillus stearothermophilus*
BOVA	bond order vibrational analysis
bPNP	bovine PNP
CfNH IU	nucleoside hydrolase IU from *Crithidia fasciculata*
dAdo	2′-deoxyadenosine
dAMP	2′-deoxyadenosine monophosphate
dCyd	2′-deoxycytidine
dGuo	2′-deoxyguanosine
EIE	equilibrium isotope effect
EMSA	electrophoretic mobility shift assay
eUDG, eMUG, *etc.*	enzyme names starting with "e" are from *Escherichia coli*
EXC	contribution to an isotope effect from vibrationally excited states
FapyA	4,6-diamino-5-formamidopyrimidine
FapyG	2,6-diamino-4-hydroxy-5-formamidopyrimidine
Hx	hypoxanthine
KIE	kinetic isotope effect
3MeA, 7MeG, *etc.*	normal nucleobases, methylated at the indicated positions, *e.g.*, N^3-methyl-2′-deoxyadenosine and N^7-methyl-2′-deoxylguanosine
5MedCyd	5-methyl 2′-deoxycytidine
7MedGuo	7-methyl 2′-deoxyguanosine
MeP	methyl phosphonate
MMI	contribution to an isotope effect from mass and moments of inertia
mPNP	malarial (*Plasmodium falciparum*) PNP
mtfMIG	mismatch glycosylase from *Methanobacterium thermoformicicum*
mthMIG	mismatch glycosylase from *M. thermoautotrophicum*
MUG	mismatch-specific uracil DNA glycosylase
NAD^+	nicotinamide adenine dinucleotide
NH	nucleoside hydrolase
n_{ij}, n_{LG}, n_{Nu}	Pauling bond order between atoms *i* and *j*, between C1′ and the leaving group, and between C1′ and the incoming nucleophile
OG	8-oxo-2′-deoxyguanosine residue
Ogg	OG DNA glycosylase
OMP	orotidine monophosphate
OPRTase	orotate phosphoribosyltransferase
PDG	pyrimidine dimer glycosylase
PNP	purine nucleoside phosphorylase
PRPP	phosphoribosyl pyrophosphate
QM/MM	quantum mechanical/molecular mechanical (computational methods)
rA	adenosine residue in RNA
TAG	*E. coli* 3-methyladenine DNA glycosylase I
TDG	thymine−DNA glycosylases
Thd	thymidine
THF	tetrahydrofuran
TS	transition state
TvNH IU	nucleoside hydrolase IU from *Trypanosoma vivax*
UDG	uracil DNA glycosylase
ZPE	contribution to an isotope effect from vibrational zero point energies
βFU	1-(2′-deoxy-2′-fluoro-β-D-arabinofuranosyl)-uracil
ϵA	1,N^6-ethenoadenosine
ϵC	3,N^4-ethenocytosine
ΨdU	2′-deoxypseudouracil

9. References

(1) Stivers, J. T.; Jiang, Y. L. *Chem. Rev.* **2003**, *103*, 2729.
(2) David, S. S.; Williams, S. D. *Chem. Rev.* **1998**, *98*, 1221.
(3) Lindahl, T. *Nature* **1993**, *362*, 709.
(4) Fromme, J. C.; Verdine, G. L. *Adv. Protein Chem.* **2004**, *69*, 1.
(5) McCullough, A. K.; Dodson, M. L.; Lloyd, R. S. *Annu. Rev. Biochem.* **1999**, *68*, 255.
(6) Krokan, H. E.; Standal, R.; Slupphaug, G. *Biochem. J.* **1997**, *325*, 1.
(7) Capon, B. *Chem. Rev.* **1969**, *69*, 407.
(8) Sinnott, M. L. *Chem. Rev.* **1990**, *90*, 1171.
(9) Zechel, D. L.; Withers, S. G. *Acc. Chem. Res.* **2000**, *33*, 11.
(10) Ly, H. D.; Withers, S. G. *Annu. Rev. Biochem.* **1999**, *68*, 487.
(11) Davies, G.; Sinnott, M. L.; Withers, S. G. In *Comprehensive Biological Cataysis*; Sinnott, M., Ed.; Academic Press: London, 1997; p 120.
(12) Berti, P. J.; Tanaka, K. S. E. *Adv. Phys. Org. Chem.* **2002**, *37*, 239.
(13) Berti, P. J. *Methods Enzymol.* **1999**, *308*, 355.
(14) Schramm, V. L. *Methods Enzymol.* **1999**, *308*, 301.
(15) Schramm, V. L. *Curr. Opin. Chem. Biol.* **2001**, *5*, 556.
(16) Schramm, V. L. *Biochim. Biophys. Acta* **2002**, *1587*, 107.
(17) Schramm, V. L. *Acc. Chem. Res.* **2003**, *36*, 588.
(18) Schramm, V. L. *Arch. Biochem. Biophys.* **2005**, *433*, 13.
(19) Schramm, V. L.; Horenstein, B. A.; Kline, P. C. *J. Biol. Chem.* **1994**, *269*, 18259.
(20) Schramm, V. L.; Shi, W. *Curr. Opin. Struct. Biol.* **2001**, *11*, 657.
(21) Werner, R. M.; Stivers, J. T. *Biochemistry* **2000**, *39*, 14054.
(22) Chen, X.-Y.; Berti, P. J.; Schramm, V. L. *J. Am. Chem. Soc.* **2000**, *122*, 6527.
(23) McCann and Berti, unpublished results.
(24) Chen, X.-Y.; Berti, P. J.; Schramm, V. L. *J. Am. Chem. Soc.* **2000**, *122*, 1609.
(25) Kline, P. C.; Schramm, V. L. *Biochemistry* **1993**, *32*, 13212.
(26) Lewandowicz, A.; Schramm, V. L. *Biochemistry* **2004**, *43*, 1458.
(27) Mentch, F.; Parkin, D. W.; Schramm, V. L. *Biochemistry* **1987**, *26*, 921.
(28) Parkin, D. W.; Schramm, V. L. *Biochemistry* **1987**, *26*, 913.
(29) Parkin, D. W.; Mentch, F.; Banks, G. A.; Horenstein, B. A.; Schramm, V. L. *Biochemistry* **1991**, *30*, 4586.
(30) Kline, P. C.; Schramm, V. L. *Biochemistry* **1995**, *34*, 1153.
(31) Horenstein, B. A.; Parkin, D. W.; Estupinan, B.; Schramm, V. L. *Biochemistry* **1991**, *30*, 10788.
(32) Scheuring, J.; Schramm, V. L. *Biochemistry* **1997**, *36*, 8215.
(33) Scheuring, J.; Berti, P. J.; Schramm, V. L. *Biochemistry* **1998**, *37*, 2748.
(34) Parikh, S. L.; Schramm, V. L. *Biochemistry* **2004**, *43*, 1204.
(35) Berti, P. J.; Blanke, S. R.; Schramm, V. L. *J. Am. Chem. Soc.* **1997**, *119*, 12079.
(36) Rising, K. A.; Schramm, V. L. *J. Am. Chem. Soc.* **1997**, *119*, 27.
(37) Scheuring, J.; Schramm, V. L. *Biochemistry* **1997**, *36*, 4526.
(38) Tao, W.; Grubmeyer, C.; Blanchard, J. S. *Biochemistry* **1996**, *35*, 14.
(39) Unrau, P. J.; Bartel, D. P. *Proc. Natl. Acad. Sci. U.S.A.* **2003**, *100*, 15393.
(40) Parkin, D. W.; Leung, H. B.; Schramm, V. L. *J. Biol. Chem.* **1984**, *259*, 9411.
(41) Berti, P. J.; Schramm, V. L. *J. Am. Chem. Soc.* **1997**, *119*, 12069.
(42) Several names have been used for the cationic form of sugars after leaving group departure. From newest to oldest, these include oxacarbenium ion, oxocarbenium ion, oxycarbonium ion, oxonium ion, plus several rare variants. The first two terms are now the most common.
(43) Jencks, W. P. *Chem. Rev.* **1985**, *85*, 511.
(44) The Pauling bond order between atoms *i* and *j*, n_{ij}, is $n_{ij} = e^{(r_{ij}-r_1)/0.3}$; where r_{ij} is the bond length between atoms *i* and *j* and r_1 is the bond length for a single bond between atoms of elements *i* and *j*. (a) Sims, L. B.; Lewis, D. E. In *Isotope Effects: Recent Developments in Theory and Experiment*; Buncel, E., Lee, C. C., Eds.; Elsevier: New York, 1984; Vol. 6. (b) Johnston, H. S. *Gas-Phase Reaction Rate Theory*; Ronald Press: New York, 1966.
(45) We use the more descriptive IUPAC convention for reaction mechanisms. In IUPAC nomenclature, a reaction mechanism is divided into elementary steps, with A_N representing nucleophilic addition and D_N representing nucleophilic dissociation. A concerted, bimolecular (S_N2) reaction is represented as A_ND_N. $D_N{*}A_N$ and $D_N{+}A_N$ mechanisms are stepwise (S_N1), with a discrete intermediate formed between leaving group departure and nucleophile approach. The signs "*" or "+" denote, respectively, an intermediate too short-lived for the leaving group to diffuse into solution, or one that is diffusionally equilibrated with solvent. (a) Commission on Physical Organic Chemistry. *Pure Appl. Chem.* **1989**, *61*, 57. (b) Commission on Physical Organic Chemistry. *Pure Appl. Chem.* **1989**, *61*, 23.
(46) Birck, M. R.; Schramm, V. L. *J. Am. Chem. Soc.* **2004**, *126*, 2447.
(47) Bigeleisen, J.; Goeppert Mayer, M. *J. Chem. Phys.* **1947**, *15*, 261.
(48) Bigeleisen, J.; Wolfsberg, M. *Adv. Chem. Phys.* **1958**, *1*, 15.
(49) Huskey, W. P. In *Enzyme mechanism from isotope effects*; Cook, P. F., Ed.; CRC Press: Boca Raton, FL, 1991; p 37.
(50) Suhnel, J.; Schowen, R. L. In *Enzyme mechanism from isotope effects*; Cook, P. F., Ed.; CRC Press: Boca Raton, FL, 1991; p 3.
(51) Buddenbaum, W. E.; Shiner, V. J., Jr In *Isotope effects on enzyme-catalyzed reactions*; Cleland, W. W., O'Leary, M. H., Northrop, D. B., Eds.; University Park Press: Baltimore, MD, 1977; p 1.
(52) Swain, C. G.; Stivers, E. C.; Reuwer, J. F., Jr.; Schaad, L. J. *J. Am. Chem. Soc.* **1958**, *80*, 5885.
(53) Stern, M. J.; Vogel, P. C. *J. Am. Chem. Soc.* **1971**, *93*, 4664.
(54) Hirschi, J.; Singleton, D. A. *J. Am. Chem. Soc.* **2005**, *127*, 3294.
(55) Melander, L.; Saunders: W. H., Jr. *Reaction rates of isotopic molecules*; John Wiley & Sons: New York, 1980.
(56) We previously estimated that the maximum ^{14}C KIE for an A_ND_N mechanism would be 1.075.[12] The experimental value for thymidine phosphorylase shows this was too low, likely because the reaction coordinate contribution was too small. Those previous estimates, based on existing experimental KIEs, have proven useful for dissociative A_ND_N and $D_N{*}A_N$ mechanisms.
(57) Matsson, O.; Westaway, K. C. *Adv. Phys. Org. Chem.* **1998**, *31*, 143.
(58) Westaway, K. C.; VanPham, T.; Fang, Y. R. *J. Am. Chem. Soc.* **1997**, *119*, 3670.
(59) Glad, S. S.; Jensen, F. *J. Am. Chem. Soc.* **1997**, *119*, 227.
(60) Poirier, R. A.; Wang, Y.; Westaway, K. C. *J. Am. Chem. Soc.* **1994**, *116*, 2526.
(61) Sunko, D. E.; Szele, I.; Hehre, W. J. *J. Am. Chem. Soc.* **1977**, *99*, 5000.
(62) Ashwell, M.; Guo, X.; Sinnott, M. L. *J. Am. Chem. Soc.* **1992**, *114*, 10158.
(63) Singh, V.; Lee, J. E.; Nunez, S.; Howell, P. L.; Schramm, V. L. *Biochemistry* **2005**, *44*, 11647.
(64) Birck, M. R.; Schramm, V. L. *J. Am. Chem. Soc.* **2004**, *126*, 6882.
(65) Degano, M.; Almo, S. C.; Sacchettini, J. C.; Schramm, V. L. *Biochemistry* **1998**, *37*, 6277.
(66) Gawlita, E.; Lantz, M.; Paneth, P.; Bell, A. F.; Tonge, P. J.; Anderson, V. E. *J. Am. Chem. Soc.* **2000**, *122*, 11660.
(67) Saunders, M.; Laidig, K. E.; Wolfsberg, M. *J. Am. Chem. Soc.* **1989**, *111*, 8989.
(68) Anisimov, V.; Paneth, P. *J. Math Chem.* **1999**, *26*, 75.
(69) Glad, S. S.; Jensen, F. *J. Phys. Chem.* **1996**, *100*, 16892.
(70) Scott, A. P.; Radom, L. *J. Phys. Chem.* **1996**, *100*, 16502.
(71) Wong, M. W. *Chem. Phys. Lett.* **1996**, *256*, 391.
(72) Johnston, H. S. *Gas-Phase Reaction Rate Theory*; Ronald Press: New York, 1966.
(73) Sims, L. B.; Lewis, D. E. In *Isotope Effects: Recent Developments in Theory and Experiment*; Buncel, E., Lee, C. C., Eds.; Elsevier: New York, 1984; p 161, Vol. 6.
(74) Burton, G. W.; Sims, L. B.; Wilson, J. C.; Fry, A. *J. Am. Chem. Soc.* **1977**, *99*, 3371.
(75) Berti, P. J.; Schramm, V. L. In *Transition state modeling for catalysis*; Trulhar, D. G., Morokuma, K., Eds.; American Chemical Society: Washington, DC, 1999; p 473.
(76) Sims, L. B.; Burton, G. W.; Lewis, D. E. *BEBOVIB-IV, QCPE No. 337*; Quantum Chemistry Program Exchange, Department of Chemistry, University of Indiana: Bloomington, IN, 1977.
(77) Huskey, W. P. *J. Am. Chem. Soc.* **1996**, *118*, 1663.
(78) Casamassina, T. E.; Huskey, W. P. *J. Am. Chem. Soc.* **1993**, *115*, 14.
(79) k_{cat}/K_M is the specificity constant. When two substrates, A and B, are present simultaneously, the ratio of products P and Q, respectively, is a function only of k_{cat}/K_M, with $[P]/[Q] = ((k_{cat}/K_M)_A/(k_{cat}/K_M)_B) \times [A]/[B]$. Similarly, in the presence of two isotopologues, the ratio of products is a function only of k_{cat}/K_M for each isotopic label. (Fersht, A. R. *Enzyme structure and mechanism*, 2nd ed.; W. H. Freeman and Co.: New York, 1985.)
(80) This statement applies to multiple turnover experiments only. In single turnover experiments, the first irreversible step is still the relevant step, but the beginning and ending points may be different.
(81) Cleland, W. W. *Methods Enzymol.* **1982**, *87*, 625.
(82) Rose, I. W. *Methods Enzymol.* **1980**, *64*, 47.
(83) Northrop, D. B. *Annu. Rev. Biochem.* **1981**, *50*, 103.
(84) Xue, H.; Wu, X.; Huskey, W. P. *J. Am. Chem. Soc.* **1996**, *118*, 5804.
(85) Zhou, X. Z.; Toney, M. D. *J. Am. Chem. Soc.* **1998**, *120*, 13282.
(86) Fedorov, A.; Shi, W.; Kicska, G.; Fedorov, E.; Tyler, P. C.; Furneaux, R. H.; Hanson, J. C.; Gainsford, G. J.; Larese, J. Z.; Schramm, V. L.; Almo, S. C. *Biochemistry* **2001**, *40*, 853.
(87) Wang, F.; Miles, R. W.; Kicska, G.; Nieves, E.; Schramm, V. L.; Angeletti, R. H. *Protein Sci.* **2000**, *9*, 1660.
(88) Mao, C.; Cook, W. J.; Zhou, M.; Federov, A. A.; Almo, S. C.; Ealick, S. E. *Biochemistry* **1998**, *37*, 7135.
(89) Kline, P. C.; Schramm, V. L. *Biochemistry* **1992**, *31*, 5964.

(90) Miles, R. W.; Tyler, P. C.; Furneaux, R. H.; Bagdassarian, C. K.; Schramm, V. L. *Biochemistry* **1998**, *37*, 8615.
(91) Kicska, G. A.; Long, L.; Horig, H.; Fairchild, C.; Tyler, P. C.; Furneaux, R. H.; Schramm, V. L.; Kaufman, H. L. *Proc. Natl. Acad. Sci. U.S.A.* **2001**, *98*, 4593.
(92) Shi, W.; Ting, L. M.; Kicska, G. A.; Lewandowicz, A.; Tyler, P. C.; Evans, G. B.; Furneaux, R. H.; Kim, K.; Almo, S. C.; Schramm, V. L. *J. Biol. Chem.* **2004**, *279*, 18103.
(93) Fujii, T.; Saito, T.; Nakasaka, T. *Chem. Pharm. Bull.* **1989**, *37*, 2601.
(94) Jiang, D.; Hatahet, Z.; Melamede, R. J.; Kow, Y. W.; Wallace, S. S. *J. Biol. Chem.* **1997**, *272*, 32230.
(95) Zharkov, D. O.; Rieger, R. A.; Iden, C. R.; Grollman, A. P. *J. Biol. Chem.* **1997**, *272*, 5335.
(96) Fromme, J. C.; Bruner, S. D.; Yang, W.; Karplus, M.; Verdine, G. L. *Nat. Struct. Biol.* **2003**, *10*, 204.
(97) Zhang, Q. M.; Miyabe, I.; Matsumoto, Y.; Kino, K.; Sugiyama, H.; Yonei, S. *J. Biol. Chem.* **2000**, *275*, 35471.
(98) Gilboa, R.; Zharkov, D. O.; Golan, G.; Fernandes, A. S.; Gerchman, S. E.; Matz, E.; Kycia, J. H.; Grollman, A. P.; Shoham, G. *J. Biol. Chem.* **2002**, *277*, 19811.
(99) McCullough, A. K.; Sanchez, A.; Dodson, M. L.; Marapaka, P.; Taylor, J. S.; Lloyd, R. S. *Biochemistry* **2001**, *40*, 561.
(100) Lavrukhin, O. V.; Lloyd, R. S. *Biochemistry* **2000**, *39*, 15266.
(101) Bhagwat, M.; Gerlt, J. A. *Biochemistry* **1996**, *35*, 659.
(102) Fromme, J. C.; Verdine, G. L. *Nat. Struct. Biol.* **2002**, *9*, 544.
(103) Fromme, J. C.; Verdine, G. L. *J. Biol. Chem.* **2003**, *278*, 51543.
(104) Zharkov, D. O.; Rosenquist, T. A.; Gerchman, S. E.; Grollman, A. P. *J. Biol. Chem.* **2000**, *275*, 28607.
(105) Norman, D. P.; Chung, S. J.; Verdine, G. L. *Biochemistry* **2003**, *42*, 1564.
(106) Hill, J. W.; Hazra, T. K.; Izumi, T.; Mitra, S. *Nucleic Acids Res.* **2001**, *29*, 430.
(107) BeMiller, J. N. *Adv. Carbohydr. Chem. Biochem.* **1967**, *22*, 25.
(108) Jencks, W. P. *Chem. Soc. Rev.* **1981**, *10*, 345.
(109) Highly dissociative A_ND_N reactions are occasionally referred to as being "S_N1-like", which is incorrect. If both the nucleophile and the leaving group are in the reaction coordinate at the TS, then the mechanism is A_ND_N (S_N2) no matter how dissociative the TS. In this review, highly dissociative A_ND_N TSs are referred to as "oxacarbenium ion-like" rather than "S_N1-like".
(110) Yang, J.; Schenkman, S.; Horenstein, B. A. *Biochemistry* **2000**, *39*, 5902.
(111) Kline, P. C.; Rezaee, M.; Lee, T. A. *Anal. Biochem.* **1999**, *275*, 6.
(112) Parkin, D. W.; Schramm, V. L. *J. Biol. Chem.* **1984**, *259*, 9418.
(113) Lee, J. K.; Bain, A. D.; Berti, P. J. *J. Am. Chem. Soc.* **2004**, *126*, 3769.
(114) Huang, X. C.; Tanaka, K. S. E.; Bennet, A. J. *J. Am. Chem. Soc.* **1997**, *119*, 11147.
(115) Bruner, M.; Horenstein, B. A. *Biochemistry* **2000**, *39*, 2261.
(116) Bennet, A. J.; Sinnott, M. L. *J. Am. Chem. Soc.* **1986**, *108*, 7287.
(117) Zhang, Y.; Bommuswamy, J.; Sinnott, M. L. *J. Am. Chem. Soc.* **1994**, *116*, 7557.
(118) Bunton, C. A.; Humeres, E. *J. Org. Chem.* **1969**, *34*, 572.
(119) Tanaka, K. S. E.; Chen, X.-Y.; Ichikawa, Y.; Tyler, P. C.; Furneaux, R. H.; Schramm, V. L. *Biochemistry* **2001**, *40*, 6845.
(120) Roday, S.; Amukele, T.; Evans, G. B.; Tyler, P. C.; Furneaux, R. H.; Schramm, V. L. *Biochemistry* **2004**, *43*, 4923.
(121) Jiang, Y. L.; Ichikawa, Y.; Stivers, J. T. *Biochemistry* **2002**, *41*, 7116.
(122) Jiang, Y. L.; Cao, C. Y.; Stivers, J. T.; Song, F. H.; Ichikawa, Y. *Bioorg. Chem.* **2004**, *32*, 244.
(123) Page, M. I.; Jencks, W. P. *Proc. Natl. Acad. Sci. U.S.A.* **1971**, *68*, 1678.
(124) Kati, W. M.; Wolfenden, R. *Science* **1989**, *243*, 1591.
(125) Wolfenden, R. *Bioorg. Med. Chem.* **1999**, *7*, 647.
(126) Lindahl, T.; Nyberg, B. *Biochemistry* **1972**, *11*, 3610.
(127) Gates, K. S.; Nooner, T.; Dutta, S. *Chem. Res. Toxicol.* **2004**, *17*, 839.
(128) Lindahl, T.; Karlstrom, O. *Biochemistry* **1973**, *12*, 5151.
(129) Kampf, G.; Kapinos, L. E.; Griesser, R.; Lippert, B.; Sigel, H. *J. Chem. Soc., Perkin Trans. 2* **2002**, 1320.
(130) Zoltewicz, J. A.; Clark, D. F.; Sharpless, T. W.; Grahe, G. *J. Am. Chem. Soc.* **1970**, *92*, 1741.
(131) Venner, H. *Z. Physiol. Chem.* **1964**, *339*, 14.
(132) Cadet, J.; Teoule, R. *J. Am. Chem. Soc.* **1974**, *96*, 6517.
(133) Venner, H. *Hoppe-Seyler's Z. Physiol. Chem.* **1966**, *344*, 189.
(134) Garrett, E. R.; Seydel, J. K.; Sharpen, A. J. *J. Org. Chem.* **1966**, *31*, 2219.
(135) Shapiro, R.; Kang, S. *Biochemistry* **1969**, *8*, 1806.
(136) Shapiro, R.; Danzig, M. *Biochemistry* **1972**, *11*, 23.
(137) Hevesi, L.; Wolfson-Davidson, E.; Nagy, J. B.; Nagy, O. B.; Bruylants, A. *J. Am. Chem. Soc.* **1972**, *94*, 4715.
(138) Bennet, A. J.; Kitos, T. E. *J. Chem. Soc., Perkin Trans. 2* **2002**, 1207.
(139) Poulter, C. D.; Frederick, G. D. *Tetrahedron Lett.* **1975**, 2171.
(140) Drohat, A. C.; Stivers, J. T. *Biochemistry* **2000**, *39*, 11865.
(141) Drohat, A. C.; Xiao, G.; Tordova, M.; Jagadeesh, J.; Pankiewicz, K. W.; Watanabe, K. A.; Gilliland, G. L.; Stivers, J. T. *Biochemistry* **1999**, *38*, 11876.
(142) Dong, J.; Drohat, A. C.; Stivers, J. T.; Pankiewicz, K. W.; Carey, P. R. *Biochemistry* **2000**, *39*, 13241.
(143) Drohat, A. C.; Jagadeesh, J.; Ferguson, E.; Stivers, J. T. *Biochemistry* **1999**, *38*, 11866.
(144) Jiang, Y. L.; Drohat, A. C.; Ichikawa, Y.; Stivers, J. T. *J. Biol. Chem.* **2002**, *277*, 15385.
(145) Lonnberg, H.; Lehikoinen, P. *Nucleic Acids Res.* **1982**, *10*, 4339.
(146) Chen, X. Y.; Link, T. M.; Schramm, V. L. *Biochemistry* **1998**, *37*, 11605.
(147) The pK_a of N7 is not known for dAdo; its value was estimated based on pK_a's of −1.5 (N7) and 3.6 (N1) of adenosine compared with $pK_a = 3.8$ for N1 of dAdo.[129,130]
(148) Assuming that the observed $pK_a = -2.4$ in guanosine corresponds to N3, and that dGuo is similar.[130]
(149) Sedgwick, B. *Nat. Rev. Mol. Cell Biol.* **2004**, *5*, 148.
(150) Pieper, R. O. In *DNA Damaga and Repair*; Nickoloff, J. A., Hoekstra, M. F., Eds.; Humana Press: Totawa, NJ, 1998; Vol. 2.
(151) O'Brien, P. J.; Ellenberger, T. *J. Biol. Chem.* **2004**, *279*, 26876.
(152) Aamodt, R. M.; Falnes, P. O.; Johansen, R. F.; Seeberg, E.; Bjoras, M. *J. Biol. Chem.* **2004**, *279*, 13601.
(153) Fujii, T.; Saito, T.; Date, T. *Chem. Pharm. Bull.* **1989**, *37*, 1208.
(154) Fujii, T.; Itaya, T. *Heterocycles* **1998**, *48*, 1673.
(155) Jang, Y. H.; Goddard, W. A.; Noyes, K. T.; Sowers, L. C.; Hwang, S.; Chung, D. S. *Chem. Res. Toxicol.* **2002**, *15*, 1023.
(156) Fujii, T.; Sarro, T.; Iguchi, K. *Chem. Pharm. Bull.* **1994**, *42*, 495.
(157) Singer, B.; Kroger, M.; Carrano, M. *Biochemistry* **1978**, *17*, 1246.
(158) Hunt, C.; Gillani, N.; Farone, A.; Rezaei, M.; Kline, P. C. *Biochim. Biophys. Acta* **2005**, *1751*, 140.
(159) Remaud, G.; Zhou, X. X.; Chattopadhyaya, J.; Oivanen, M.; Lonnberg, H. *Tetrahedron* **1987**, *43*, 4453.
(160) Kinjo, Y.; Ji, L. N.; Corfu, N. A.; Sigel, H. *Inorg. Chem.* **1992**, *31*, 5588.
(161) Knobloch, B.; Da Costa, C. P.; Linert, W.; Sigel, H. *Inorg. Chem. Commun.* **2003**, *6*, 90.
(162) Remaud, G.; Zhou, X. X.; Chattopadhyaya, J.; Oivanen, M.; Lonnberg, H. *Nucleic Acids Symp. Ser.* **1987**, 145.
(163) Major, D. T.; Laxer, A.; Fischer, B. *J. Org. Chem.* **2002**, *67*, 790.
(164) Hendler, S.; Furer, E.; Srinivasan, P. R. *Biochemistry* **1970**, *9*, 4141.
(165) Richard, J. P.; Williams, K. B.; Amyes, T. L. *J. Am. Chem. Soc.* **1999**, *121*, 8403.
(166) Richard, J. P. *Tetrahedron* **1995**, *51*, 1535.
(167) Andrews, C. W.; Bowen, J. P.; Fraser-Reid, B. *J. Chem. Soc., Chem. Commun.* **1989**, 1913.
(168) Winkler, D. A.; Holan, G. *J. Med. Chem.* **1989**, *32*, 2084.
(169) Andrews, C. W.; Fraser-Reid, B.; Bowen, J. P. *J. Am. Chem. Soc.* **1991**, *113*, 8293.
(170) Kajimoto, T.; Liu, K. K. C.; Pederson, R. L.; Zhong, Z.; Ichikawa, Y.; Porco, J. A., Jr.; Wong, C. H. *J. Am. Chem. Soc.* **1991**, *113*, 6187.
(171) Smith, B. J. *J. Am. Chem. Soc.* **1997**, *119*, 2699.
(172) Namchuk, M. N.; McCarter, J. D.; Becalski, A.; Andrews, T.; Withers, S. G. *J. Am. Chem. Soc.* **2000**, *122*, 1270.
(173) Parikh, S. S.; Walcher, G.; Jones, G. D.; Slupphaug, G.; Krokan, H. E.; Blackburn, G. M.; Tainer, J. A. *Proc. Natl. Acad. Sci. U.S.A.* **2000**, *97*, 5083.
(174) Bianchet, M. A.; Seiple, L. A.; Jiang, Y. L.; Ichikawa, Y.; Amzel, L. M.; Stivers, J. T. *Biochemistry* **2003**, *42*, 12455.
(175) Werner, R. M.; Jiang, Y. L.; Gordley, R. G.; Jagadeesh, G. J.; Ladner, J. E.; Xiao, G.; Tordova, M.; Gilliland, G. L.; Stivers, J. T. *Biochemistry* **2000**, *39*, 12585.
(176) Loverix, S.; Geerlings, P.; McNaughton, M.; Augustyns, K.; Vandemeulebroucke, A.; Steyaert, J.; Versees, W. *J. Biol. Chem.* **2005**, *280*, 14799.
(177) Becke, A. D. *Phys. Rev. A* **1988**, *38*, 3098.
(178) Perdew, J. P.; Wang, Y. *Phys. Rev. B* **1992**, *45*, 13244.
(179) Frisch, M. J.; Trucks, G. W.; Schlegel, H. B.; Scuseria, G. E.; Robb, M. A.; Cheeseman, J. R.; Zakrzewski, V. G.; Montgomery, J. A.; Stratmann, R. E.; Burant, J. C.; Dapprich, S.; Millam, J. M.; Daniels, A. D.; Kudin, K. N.; Strain, M. C.; Farkas, O.; Tomasi, J.; Barone, V.; Cossi, M.; Cammi, R.; Mennucci, B.; Pomelli, C.; Adamo, C.; Clifford, S.; Ochterski, J.; Petersson, G. A.; Ayala, P. Y.; Cui, Q.; Morokuma, K.; Malick, D. K.; Rabuck, A. D.; Raghavachari, K.; Foresman, J. B.; Cioslowski, J.; Ortiz, J. V.; Stefanov, B. B.; Liu, G.; Liashenko, A.; Piskorz, P.; Komaromi, I.; Gomperts, R.; Martin, R. L.; Fox, D. J.; Keith, T.; Al-Laham, M. A.; Peng, C. Y.; Nanayakkara, A.; Gonzalez, C.; Challacombe, M.; Gill, P. M. W.; Johnson, B. G.; Chen, W.; Wong, M. W.; Andres, J. L.; Head-Gordon, M.; Replogle, E. S.; Pople, J. A. *Gaussian 98 (Revision A.6)*; Gaussian, Inc.: Pittsburgh, PA, 1998.

(180) Portmann, S.; Luthi, H. P. *Chimia* **2000**, *54*, 766.
(181) Jespersen, T. M.; Dong, W.; Sierks, M. R.; Skrydstrup, T.; Lundt, I.; Bols, M. *Angew. Chem., Int. Ed. Engl.* **1994**, *33*, 1778.
(182) Ichikawa, Y.; Igarashi, Y. *Tetrahedron Lett.* **1995**, *36*, 4585.
(183) Igarashi, Y.; Ichikawa, M.; Ichikawa, Y. *Tetrahedron Lett.* **1996**, *37*, 2707.
(184) Bols, M.; Hazell, R. G.; Thomsen, I. B. *Chem.—Eur. J.* **1997**, *3*, 940.
(185) Bols, M. *Acc. Chem. Res.* **1998**, *31*, 1.
(186) Liu, H.; Liang, X.; Shoel, H.; Bülow, A.; Bols, M. *J. Am. Chem. Soc.* **2001**, *123*, 5116.
(187) Parkin, D. W.; Schramm, V. L. *Biochemistry* **1995**, *34*, 13961.
(188) Legler, G. *Adv. Carbohydr. Chem. Biochem.* **1990**, *48*, 319.
(189) Shi, W.; Li, C. M.; Tyler, P. C.; Furneaux, R. H.; Cahill, S. M.; Girvin, M. E.; Grubmeyer, C.; Schramm, V. L.; Almo, S. C. *Biochemistry* **1999**, *38*, 9872.
(190) Sauve, A. A.; Cahill, S. M.; Zech, S. G.; Basso, L. A.; Lewandowicz, A.; Santos, D. S.; Grubmeyer, C.; Evans, G. B.; Furneaux, R. H.; Tyler, P. C.; McDermott, A.; Girvin, M. E.; Schramm, V. L. *Biochemistry* **2003**, *42*, 5694.
(191) Lau, A. Y.; Wyattt, M. D.; Glassner, B. J.; Samson, L. D.; Ellenberger, T. *Proc. Natl. Acad. Sci. U.S.*A. **2000**, *97*, 13573.
(192) Bell, C. E.; Eisenberg, D. *Biochemistry* **1996**, *35*, 1137.
(193) Inouye, S.; Tsuruoka, T.; Ito, T.; Niida, T. *Tetrahedron* **1968**, *23*, 2125.
(194) Jeong, J. H.; Murray, B. W.; Takayama, S.; Wong, C. H. *J. Am. Chem. Soc.* **1996**, *118*, 4227.
(195) Hoos, R.; Huixin, J.; Vasella, A.; Weiss, P. *Helv. Chim. Acta* **1996**, *79*, 1757.
(196) Yagi, M.; Kouno, T.; Aoyagi, Y.; Murai, H. *Nippon Nogei Kagaku Kaishi* **1976**, *50*, 571.
(197) Legler, G.; Julich, E. *Carbohydr. Res.* **1984**, *128*, 61.
(198) Evans, S. V.; Fellows, L. E.; Shing, T. K. M.; Fleet, G. W. J. *Phytochemistry* **1985**, *24*, 1953.
(199) Legler, G.; Pohl, S. *Carbohydr. Res.* **1986**, *155*, 119.
(200) Winchester, B.; Barker, C.; Baines, S.; Jacob, G. S.; Namgoong, S. K.; Fleet, G. *Biochem. J.* **1990**, *265*, 277.
(201) Cenci di Bello, I.; Dorling, P.; Fellows, L.; Winchester, B. *FEBS Lett.* **1984**, *176*, 61.
(202) Hughes, A. B.; Rudge, A. J. *Nat. Prod. Rep.* **1994**, 135.
(203) Fromme, J. C.; Banerjee, A.; Huang, S. J.; Verdine, G. L. *Nature* **2004**, *427*, 652.
(204) Raoul, S.; Bardet, M.; Cadet, J. *Chem. Res. Toxicol.* **1995**, *8*, 924.
(205) Greenberg, M. M.; Hantosi, Z.; Wiederholt, C. J.; Rithner, C. D. *Biochemistry* **2001**, *40*, 15856.
(206) Kow, Y. W.; Wallace, S. S. *Biochemistry* **1987**, *26*, 8200.
(207) Purmal, A. A.; Rabow, L. E.; Lampman, G. W.; Cunningham, R. P.; Kow, Y. W. *Mutat. Res.* **1996**, *364*, 193.
(208) Zharkov, D. O.; Golan, G.; Gilboa, R.; Fernandes, A. S.; Gerchman, S. E.; Kycia, J. H.; Rieger, R. A.; Grollman, A. P.; Shoham, G. *EMBO J.* **2002**, *21*, 789.
(209) Williams, S. D.; David, S. S. *Biochemistry* **2000**, *39*, 10098.
(210) Burgess, S.; Jaruga, P.; Dodson, M. L.; Dizdaroglu, M.; Lloyd, R. S. *J. Biol. Chem.* **2002**, *277*, 2938.
(211) Doublie, S.; Bandaru, V.; Bond, J. P.; Wallace, S. S. *Proc. Natl. Acad. Sci. U.S.A.* **2004**, *101*, 10284.
(212) Rabow, L. E.; Kow, Y. W. *Biochemistry* **1997**, *36*, 5084.
(213) Parikh, S. S.; Mol, C. D.; Slupphaug, G.; Bharati, S.; Krokan, H. E.; Tainer, J. A. *EMBO J.* **1998**, *17*, 5214.
(214) Drohat, A. C.; Stivers, J. T. *J. Am. Chem. Soc.* **2000**, *122*, 1840.
(215) Guan, Y.; Manuel, R. C.; Arvai, A. S.; Parikh, S. S.; Mol, C. D.; Miller, J. H.; Lloyd, S.; Tainer, J. A. *Nat. Struct. Biol.* **1998**, *5*, 1058.
(216) Erion, M. D.; Takabayashi, K.; Smith, H. B.; Kessi, J.; Wagner, S.; Honger, S.; Shames, S. L.; Ealick, S. E. *Biochemistry* **1997**, *36*, 11725.
(217) O'Brien, P. J.; Ellenberger, T. *Biochemistry* **2003**, *42*, 12418.
(218) Versees, W.; Decanniere, K.; Pelle, R.; Depoorter, J.; Brosens, E.; Parkin, D. W.; Steyaert, J. *J. Mol. Biol.* **2001**, *307*, 1363.
(219) Versees, W.; Loverix, S.; Vandemeulebroucke, A.; Geerlings, P.; Steyaert, J. *J. Mol. Biol.* **2004**, *338*, 1.
(220) Desiraju, G. R. *Acc. Chem. Res.* **1996**, *29*, 441.
(221) Desiraju, G. R. *Acc. Chem. Res.* **1991**, *24*, 290.
(222) Jencks, W. P. *Adv. Enzymol. Relat. Areas Mol. Biol.* **1975**, *43*, 219.
(223) Berti, P. J.; Faerman, C. H.; Storer, A. C. *Biochemistry* **1991**, *30*, 1394.
(224) Mazzella, L. J.; Parkin, D. W.; Tyler, P. C.; Furneaux, R. H.; Schramm, V. L. *J. Am. Chem. Soc.* **1996**, *118*, 2111.
(225) Miles, R. W.; Tyler, P. C.; Evans, G. B.; Furneaux, R. H.; Parkin, D. W.; Schramm, V. L. *Biochemistry* **1999**, *38*, 13147.
(226) Basso, L. A.; Santos, D. S.; Shi, W.; Furneaux, R. H.; Tyler, P. C.; Schramm, V. L.; Blanchard, J. S. *Biochemistry* **2001**, *40*, 8196.
(227) Scharer, O. D.; Nash, H. M.; Jiricny, J.; Laval, J.; Verdine, G. L. *J. Biol. Chem.* **1998**, *273*, 8592.
(228) Deng, H.; Lewandowicz, A.; Schramm, V. L.; Callender, R. *J. Am. Chem. Soc.* **2004**, *126*, 9516.
(229) Shi, W.; Sarver, A. E.; Wang, C. C.; Tanaka, K. S. E.; Almo, S. C.; Schramm, V. L. *J. Biol. Chem.* **2002**, *277*, 39981.
(230) Vocadlo, D. J.; Davies, G. J.; Laine, R.; Withers, S. G. *Nature* **2001**, *412*, 835.
(231) Hovel, K.; Shallom, D.; Niefind, K.; Belakhov, V.; Shoham, G.; Baasov, T.; Shoham, Y.; Schomburg, D. *EMBO J.* **2003**, *22*, 4922.
(232) Guerin, D. M.; Lascombe, M. B.; Costabel, M.; Souchon, H.; Lamzin, V.; Beguin, P.; Alzari, P. M. *J. Mol. Biol.* **2002**, *316*, 1061.
(233) Varrot, A.; Macdonald, J.; Stick, R. V.; Pell, G.; Gilbert, H. J.; Davies, G. J. *Chem. Commun.* **2003**, 946.
(234) Lee, J. E.; Cornell, K. A.; Riscoe, M. K.; Howell, P. L. *J. Biol. Chem.* **2003**, *278*, 8761.
(235) Shi, W.; Schramm, V. L.; Almo, S. C. *J. Biol. Chem.* **1999**, *274*, 21114.
(236) Versees, W.; Decanniere, K.; Van Holsbeke, E.; Devroede, N.; Steyaert, J. *J. Biol. Chem.* **2002**, *277*, 15938.
(237) Lau, A. Y.; Scharer, O. D.; Samson, L.; Verdine, G. L.; Ellenberger, E. *Cell* **1998**, *95*, 249.
(238) Labahn, J.; Scharer, O. D.; Long, A.; EzazNikpay, K.; Verdine, G. L.; Ellenberger, T. E. *Cell* **1996**, *86*, 321.
(239) Lindahl, T.; Nyberg, B. *Biochemistry* **1974**, *13*, 3405.
(240) Barnes, D. E.; Lindahl, T. *Annu. Rev. Genet.* **2004**, *38*, 445.
(241) Shen, J. C.; Rideout, W. M., III.; Jones, P. A. *Nucleic Acids Res.* **1994**, *22*, 972.
(242) Cao, C.; Jiang, Y. L.; Stivers, J. T.; Song, F. *Nat. Struct. Mol. Biol.* **2004**, *11*, 1230.
(243) Ghosh, M.; Rumpal, N.; Varshney, U.; Chary, K. V. *Eur. J. Biochem.* **2002**, *269*, 1886.
(244) Ghosh, M.; Vinay, K. N.; Varshney, U.; Chary, K. V. *Nucleic Acids Res.* **2000**, *28*, 1906.
(245) Jiang, Y. L.; McDowell, L. M.; Poliks, B.; Studelska, D. R.; Cao, C.; Potter, G. S.; Schaefer, J.; Song, F.; Stivers, J. T. *Biochemistry* **2004**, *43*, 15429.
(246) Jiang, Y. L.; Stivers, J. T. *Biochemistry* **2001**, *40*, 7710.
(247) Putnam, C. D.; Shroyer, M. J.; Lundquist, A. J.; Mol, C. D.; Arvai, A. S.; Mosbaugh, D. W.; Tainer, J. A. *J. Mol. Biol.* **1999**, *287*, 331.
(248) Ravishankar, R.; Bidya, S. M.; Roy, S.; Purnapatre, K.; Handa, P.; Varshney, U.; Vijayan, M. *Nucleic Acids Res.* **1998**, *26*, 4880.
(249) Saikrishnan, K.; Bidya, S. M.; Ravishankar, R.; Roy, S.; Purnapatre, K.; Handa, P.; Varshney, U.; Vijayan, M. *Acta Crystallogr., D: Biol. Crystallogr.* **2002**, *58*, 1269.
(250) Xiao, G.; Tordova, M.; Jagadeesh, J.; Drohat, A. C.; Stivers, J. T.; Gilliland, G. L. *Proteins* **1999**, *35*, 13.
(251) Savva, R.; McAuley-Hecht, K.; Brown, T.; Pearl, L. *Nature* **1995**, *373*, 487.
(252) Jiang, Y. L.; Stivers, J. T. *Biochemistry* **2002**, *41*, 11236.
(253) Shroyer, M. J.; Bennett, S. E.; Putnam, C. D.; Tainer, J. A.; Mosbaugh, D. W. *Biochemistry* **1999**, *38*, 4834.
(254) Bellamy, S. R.; Baldwin, G. S. *Nucleic Acids Res.* **2001**, *29*, 3857.
(255) Sekino, Y.; Bruner, S. D.; Verdine, G. L. *J. Biol. Chem.* **2000**, *275*, 36506.
(256) Dinner, A. R.; Blackburn, G. M.; Karplus, M. *Nature* **2001**, *413*, 752.
(257) Luo, N.; Mehler, E.; Osman, R. *Biochemistry* **1999**, *38*, 9209.
(258) Stivers, J. T.; Drohat, A. C. *Arch. Biochem. Biophys.* **2001**, *396*, 1.
(259) Jiang, Y. L.; Ichikawa, Y.; Song, F.; Stivers, J. T. *Biochemistry* **2003**, *42*, 1922.
(260) Bennett, S. E.; Sanderson, R. J.; Mosbaugh, D. W. *Biochemistry* **1995**, *34*, 6109.
(261) Chen, C. Y.; Mosbaugh, D. W.; Bennett, S. E. *J. Biol. Chem.* **2004**, *279*, 48177.
(262) Higley, M.; Lloyd, R. S. *Mutat. Res.* **1993**, *294*, 109.
(263) Purmal, A. A.; Lampman, G. W.; Pourmal, E. I.; Melamede, R. J.; Wallace, S. S.; Kow, Y. W. *J. Biol. Chem.* **1994**, *269*, 22046.
(264) Krosky, D. J.; Schwarz, F. P.; Stivers, J. T. *Biochemistry* **2004**, *43*, 4188.
(265) Jiang, Y. L.; Kwon, K.; Stivers, J. T. *J. Biol. Chem.* **2001**, *276*, 42347.
(266) Jiang, Y. L.; Stivers, J. T.; Song, F. *Biochemistry* **2002**, *41*, 11248.
(267) Wong, I.; Lundquist, A. J.; Bernards, A. S.; Mosbaugh, D. W. *J. Biol. Chem.* **2002**, *277*, 19424.
(268) Handa, P.; Acharya, N.; Varshney, U. *Nucleic Acids Res.* **2002**, *30*, 3086.
(269) Kavli, B.; Slupphaug, G.; Mol, C. D.; Arvai, A. S.; Peterson, S. B.; Tainer, J. A.; Krokan, H. E. *EMBO J.* **1996**, *15*, 3442.
(270) Numbering is positive in the 5′-direction from the target U residue and is negative on the 3′-side.
(271) Altona, C.; Sundaralingam, M. *J. Am. Chem. Soc.* **1972**, *94*, 8205.
(272) Gelbin, A.; Schneider, B.; Clowney, L.; Hsieh, S. H.; Olson, W. K.; Berman, H. M. *J. Am. Chem. Soc.* **1996**, *118*, 519.
(273) Kojima, C.; Kawashima, E.; Sekine, T.; Ishido, Y.; Ono, A.; Kainosho, M.; Kyogoku, Y. *J. Biomol. NMR* **2001**, *19*, 19.

(274) Perrin, C. L. *Tetrahedron* **1995**, *51*, 11901.
(275) Foloppe, N.; MacKerell, A. D. *J. Phys. Chem. B* **1998**, *102*, 6669.
(276) Cloran, F.; Zhu, Y. P.; Osborn, J.; Carmichael, I.; Serianni, A. S. *J. Am. Chem. Soc.* **2000**, *122*, 6435.
(277) Slupphaug, G.; Mol, C. D.; Kavli, B.; Arvai, A. S.; Krokan, H. E.; Tainer, J. A. *Nature* **1996**, *384*, 87.
(278) Barrett, T. E.; Savva, R.; Panayotou, G.; Barlow, T.; Brown, T.; Jiricny, J.; Pearl, L. H. *Cell* **1998**, *92*, 117.
(279) Barrett, T. E.; Scharer, O. D.; Savva, R.; Brown, T.; Jiricny, J.; Verdine, G. L.; Pearl, L. H. *EMBO J.* **1999**, *18*, 6599.
(280) Wibley, J. E.; Waters, T. R.; Haushalter, K.; Verdine, G. L.; Pearl, L. H. *Mol. Cell* **2003**, *11*, 1647.
(281) Hoseki, J.; Okamoto, A.; Masui, R.; Shibata, T.; Inoue, Y.; Yokoyama, S.; Kuramitsu, S. *J. Mol. Biol.* **2003**, *333*, 515.
(282) Shaw, R. W.; Feller, J. A.; Bloom, L. B. *DNA Repair* **2004**, *3*, 1273.
(283) O'Neill, R. J.; Vorob'eva, O. V.; Shahbakhti, H.; Zmuda, E.; Bhagwat, A. S.; Baldwin, G. S. *J. Biol. Chem.* **2003**, *278*, 20526.
(284) Abu, M.; Waters, T. R. *J. Biol. Chem.* **2003**, *278*, 8739.
(285) Hardeland, U.; Bentele, M.; Jiricny, J.; Schar, P. *J. Biol. Chem.* **2000**, *275*, 33449.
(286) Kwon, K.; Jiang, Y. L.; Stivers, J. T. *Chem. Biol.* **2003**, *10*, 351.
(287) Yamataka, H.; Ando, T. *Tetrahedron Lett.* **1975**, 1059.
(288) Bender, M. L.; Hoeg, D. F. *J. Am. Chem. Soc.* **1957**, *79*, 5649.
(289) Raaen, V. F.; Juhlke, T.; Brown, F. J.; Collins, C. J. *J. Am. Chem. Soc.* **1974**, *96*, 5928.
(290) Markham, G. D.; Parkin, D. W.; Mentch, F.; Schramm, V. L. *J. Biol. Chem.* **1987**, *262*, 5609.
(291) Hegazi, M. F.; Borchardt, R. T.; Schowen, R. L. *J. Am. Chem. Soc.* **1979**, *101*, 4359.
(292) Norman, R. A.; Barry, S. T.; Bate, M.; Breed, J.; Colls, J. G.; Ernill, R. J.; Luke, R. W.; Minshull, C. A.; McAlister, M. S.; McCall, E. J.; McMiken, H. H.; Paterson, D. S.; Timms, D.; Tucker, J. A.; Pauptit, R. A. *Structure* **2004**, *12*, 75.
(293) Cole, C.; Reigan, P.; Gbaj, A.; Edwards, P. N.; Douglas, K. T.; Stratford, I. J.; Freeman, S.; Jaffar, M. *J. Med. Chem.* **2003**, *46*, 207.
(294) Mendieta, J.; Martin-Santamaria, S.; Priego, E. M.; Balzarini, J.; Camarasa, M. J.; Perez-Perez, M. J.; Gago, F. *Biochemistry* **2004**, *43*, 405.
(295) Olsnes, S.; Pihl, A. In *Molecular Action of Toxins and Viruses*; Cohen, P., van Heyningen, S., Eds.; Elsevier Biomedical: New York, 1982; p 51.
(296) Endo, Y.; Tsurugi, K. *J. Biol. Chem.* **1987**, *262*, 8128.
(297) Endo, Y.; Tsurugi, K. *J. Biol. Chem.* **1988**, *263*, 8735.
(298) Gluck, A.; Endo, Y.; Wool, I. G. *J. Mol. Biol.* **1992**, *226*, 411.
(299) Endo, Y.; Gluck, A.; Wool, I. G. *J. Mol. Biol.* **1991**, *221*, 193.
(300) Orlowski, M.; Orlowski, R.; Chang, J. C.; Wilk, E.; Lesser, M. *Mol. Cell. Biochem.* **1984**, *64*, 155.
(301) Saenger, W. *Principles of Nucleic Acid Structure*; Springer-Verlag: New York, 1984.
(302) Wolfenden, R.; Lu, X.; Young, G. *J. Am. Chem. Soc.* **1998**, *120*, 6814.
(303) Miller, D. J.; Ravikumar, K.; Shen, H.; Suh, J. K.; Kerwin, S. M.; Robertus, J. D. *J. Med. Chem.* **2002**, *45*, 90.
(304) Yan, X. J.; Hollis, T.; Svinth, M.; Day, P.; Monzingo, A. F.; Milne, G. W. A.; Robertus, J. D. *J. Mol. Biol.* **1997**, *266*, 1043.
(305) Weston, S. A.; Tucker, A. D.; Thatcher, D. R.; Derbyshire, D. J.; Pauptit, R. A. *J. Mol. Biol.* **1994**, *244*, 410.
(306) Day, P. J.; Ernst, S. R.; Frankel, A. E.; Monzingo, A. F.; Pascal, J. M.; MolinaSvinth, M. C.; Robertus, J. D. *Biochemistry* **1996**, *35*, 11098.
(307) Monzingo, A. F.; Robertus, J. D. *J. Mol. Biol.* **1992**, *227*, 1136.
(308) Parkin, D. W.; Horenstein, B. A.; Abdulah, D. R.; Estupinan, B.; Schramm, V. L. *J. Biol. Chem.* **1991**, *266*, 20658.
(309) Horenstein, B. A.; Schramm, V. L. *Biochemistry* **1993**, *32*, 7089.
(310) Horenstein, B. A.; Schramm, V. L. *Biochemistry* **1993**, *32*, 9917.
(311) Horenstein, B. A.; Zabinski, R. F.; Schramm, V. L. *Tetrahedron Lett.* **1993**, *34*, 7213.
(312) Boutellier, M.; Horenstein, B. A.; Semenyaka, A.; Schramm, V. L.; Ganem, B. *Biochemistry* **1994**, *33*, 3994.
(313) Deng, H.; Chan, A. W.-Y.; Bagdassarian, C. K.; Estupinan, B.; Ganem, B.; Callender, R. H.; Schramm, V. L. *Biochemistry* **1996**, *35*, 6037.
(314) Gopaul, D. N.; Meyer, S. L.; Degano, M.; Sacchettini, J. C.; Schramm, V. L. *Biochemistry* **1996**, *35*, 5963.
(315) Degano, M.; Gopaul, D. N.; Scapin, G.; Schramm, V. L.; Sacchettini, J. C. *Biochemistry* **1996**, *35*, 5971.
(316) Bagdassarian, C. K.; Schramm, V. L.; Schwartz, S. D. *J. Am. Chem. Soc.* **1996**, *118*, 8825.
(317) Braunheim, B. B.; Schwartz, S. D. *Methods Enzymol.* **1999**, *308*, 398.
(318) Braunheim, B. B.; Schwartz, S. D. *J. Theor. Biol.* **2000**, *206*, 27.
(319) Braunheim, B. B.; Miles, R. W.; Schramm, V. L.; Schwartz, S. D. *Biochemistry* **1999**, *38*, 16076.
(320) Mazumder, D.; Kahn, K.; Bruice, T. C. *J. Am. Chem. Soc.* **2002**, *124*, 8825.
(321) Moodie, S. L.; Thornton, J. M. *Nucleic Acids Res.* **1993**, *21*, 1369.
(322) Scapin, G.; Grubmeyer, C.; Sacchettini, J. C. *Biochemistry* **1994**, *33*, 1287.
(323) Scapin, G.; Ozturk, D. H.; Grubmeyer, C.; Sacchettini, J. C. *Biochemistry* **1995**, *34*, 10744.
(324) Althaus, F. R.; Richter, C. *Mol. Biol. Biochem. Biophys.* **1987**, *37*, 1.
(325) Wilson, B. A.; Collier, R. J. *Curr. Top. Microbiol. Immunol.* **1992**, *175*, 27.
(326) Zhang, R. G.; Westbrook, M. L.; Westbrook, E. M.; Scott, D. L.; Otwinowski, Z.; Maulik, P. R.; Reed, R. A.; Shipley, G. G. *J. Mol. Biol.* **1995**, *251*, 550.
(327) McDonald, L. J.; Wainschel, L. A.; Oppenheimer, N. J.; Moss, J. *Biochemistry* **1992**, *31*, 11881.
(328) Oppenheimer, N. J.; Bodley, J. W. *J. Biol. Chem.* **1981**, *256*, 8579.
(329) Wilson, B. A.; Reich, K. A.; Weinstein, B. R.; Collier, R. J. *Biochemistry* **1990**, *29*, 8643.
(330) Stein, P. E.; Boodhoo, A.; Armstrong, G. D.; Cockle, S. A.; Klein, M. H.; Read, R. J. *Structure* **1994**, *2*, 45.
(331) Antoine, R.; Tallett, A.; van Heyningen, S.; Locht, C. *J. Biol. Chem.* **1993**, *268*, 24149.
(332) Zharkov, D. O.; Shoham, G.; Grollman, A. P. *DNA Repair* **2003**, *2*, 839.
(333) Eisen, J. A.; Hanawalt, P. C. *Mutat. Res.* **1999**, *435*, 171.
(334) Thayer, M. M.; Ahern, H.; Xing, D.; Cunningham, R. P.; Tainer, J. A. *EMBO J.* **1995**, *14*, 4108.
(335) Wallace, S. S.; Bandaru, V.; Kathe, S. D.; Bond, J. P. *DNA Repair* **2003**, *2*, 441.
(336) Denver, D. R.; Swenson, S. L.; Lynch, M. *Mol. Biol. Evol.* **2003**, *20*, 1603.
(337) Pearl, L. H. *Mutat. Res.* **2000**, *460*, 165.
(338) Aravind, L.; Koonin, E. V. *Genome Biol.* **2000**, *1*, RESEARCH0007.
(339) Baba, D.; Maita, N.; Jee, J. G.; Uchimura, Y.; Saitoh, H.; Sugasawa, K.; Hanaoka, F.; Tochio, H.; Hiroaki, H.; Shirakawa, M. *Nature* **2005**, *435*, 979.
(340) Sartori, A. A.; Fitz-Gibbon, S.; Yang, H.; Miller, J. H.; Jiricny, J. *EMBO J.* **2002**, *21*, 3182.
(341) Neuberger, M. S.; Di Noia, J. M.; Beale, R. C.; Williams, G. T.; Yang, Z.; Rada, C. *Nat. Rev. Immunol.* **2005**, *5*, 171.
(342) Neddermann, P.; Gallinari, P.; Lettieri, T.; Schmid, D.; Truong, O.; Hsuan, J. J.; Wiebauer, K.; Jiricny, J. *J. Biol. Chem.* **1996**, *271*, 12767.
(343) Sibghat, U.; Gallinari, P.; Xu, Y. Z.; Goodman, M. F.; Bloom, L. B.; Jiricny, J.; Day, R. S., III. *Biochemistry* **1996**, *35*, 12926.
(344) Scharer, O. D.; Kawate, T.; Gallinari, P.; Jiricny, J.; Verdine, G. L. *Proc. Natl. Acad. Sci. U.S.A.* **1997**, *94*, 4878.
(345) Liu, P.; Burdzy, A.; Sowers, L. C. *Chem. Res. Toxicol.* **2002**, *15*, 1001.
(346) Saparbaev, M.; Laval, J. *Proc. Natl. Acad. Sci. U.S.A.* **1998**, *95*, 8508.
(347) Waters, T. R.; Gallinari, P.; Jiricny, J.; Swann, P. F. *J. Biol. Chem.* **1999**, *274*, 67.
(348) Matsubara, M.; Masaoka, A.; Tanaka, T.; Miyano, T.; Kato, N.; Terato, H.; Ohyama, Y.; Iwai, S.; Ide, H. *Biochemistry* **2003**, *42*, 4993.
(349) Nilsen, H.; Haushalter, K. A.; Robins, P.; Barnes, D. E.; Verdine, G. L.; Lindahl, T. *EMBO J.* **2001**, *20*, 4278.
(350) Nilsen, H.; Rosewell, I.; Robins, P.; Skjelbred, C. F.; Andersen, S.; Slupphaug, G.; Daly, G.; Krokan, H. E.; Lindahl, T.; Barnes, D. E. *Mol. Cell* **2000**, *5*, 1059.
(351) Matsubara, M.; Tanaka, T.; Terato, H.; Ohmae, E.; Izumi, S.; Katayanagi, K.; Ide, H. *Nucleic Acids Res.* **2004**, *32*, 5291.
(352) Haushalter, K. A.; Todd Stukenberg, M. W.; Kirschner, M. W.; Verdine, G. L. *Curr. Biol.* **1999**, *9*, 174.
(353) Masaoka, A.; Matsubara, M.; Hasegawa, R.; Tanaka, T.; Kurisu, S.; Terato, H.; Ohyama, Y.; Karino, N.; Matsuda, A.; Ide, H. *Biochemistry* **2003**, *42*, 5003.
(354) Hinks, J. A.; Evans, M. C.; De Miguel, Y.; Sartori, A. A.; Jiricny, J.; Pearl, L. H. *J. Biol. Chem.* **2002**, *277*, 16936.
(355) Sartori, A. A.; Jiricny, J. *J. Biol. Chem.* **2003**, *278*, 24563.
(356) Sandigursky, M.; Franklin, W. A. *Curr. Biol.* **1999**, *9*, 531.
(357) Sandigursky, M.; Faje, A.; Franklin, W. A. *Mutat. Res.* **2001**, *485*, 187.
(358) Lukianova, O. A.; David, S. S. *Curr. Opin. Chem. Biol.* **2005**, *9*, 145.
(359) Boal, A. K.; Yavin, E.; Lukianova, O. A.; O'Shea V, L.; David, S. S.; Barton, J. K. *Biochemistry* **2005**, *44*, 8397.
(360) Chepanoske, C. L.; Lukianova, O. A.; Lombard, M.; Golinelli-Cohen, M. P.; David, S. S. *Biochemistry* **2004**, *43*, 651.
(361) Doherty, A. J.; Serpell, L. C.; Ponting, C. P. *Nucleic Acids Res.* **1996**, *24*, 2488.
(362) Mol, C. D.; Arvai, A. S.; Begley, T. J.; Cunningham, R. P.; Tainer, J. A. *J. Mol. Biol.* **2002**, *315*, 373.

(363) Williams, S. D.; David, S. S. *Nucleic Acids Res.* **1998**, *26*, 5123.
(364) Parker, A. R.; Eshleman, J. R. *Cell Mol. Life Sci.* **2003**, *60*, 2064.
(365) Klaunig, J. E.; Kamendulis, L. M. *Annu. Rev. Pharmacol.* **2004**, *44*, 239.
(366) Pouget, J. P.; Frelon, S.; Ravanat, J. L.; Testard, I.; Odin, F.; Cadet, J. *Radiat. Res.* **2002**, *157*, 589.
(367) Wallace, S. S. *Radiat. Res.* **1998**, *150*, S60.
(368) European Standards Committee on Oxidative DNA Damage. *Carcinogenesis* **2002**, *23*, 2129.
(369) Kouchakdjian, M.; Bodepudi, V.; Shibutani, S.; Eisenberg, M.; Johnson, F.; Grollman, A. P.; Patel, D. J. *Biochemistry* **1991**, *30*, 1403.
(370) McAuley-Hecht, K. E.; Leonard, G. A.; Gibson, N. J.; Thomson, J. B.; Watson, W. P.; Hunter, W. N.; Brown, T. *Biochemistry* **1994**, *33*, 10266.
(371) Grollman, A. P.; Moriya, M. *Trends Genet.* **1993**, *9*, 246.
(372) Al-Tassan, N.; Chmiel, N. H.; Maynard, J.; Fleming, N.; Livingston, A. L.; Williams, G. T.; Hodges, A. K.; Davies, D. R.; David, S. S.; Sampson, J. R.; Cheadle, J. P. *Nat. Genet.* **2002**, *30*, 227.
(373) Cheadle, J. P.; Sampson, J. R. *Hum. Mol. Genet.* **2003**, *12*, R159.
(374) Chow, E.; Thirlwell, C.; Macrae, F.; Lipton, L. *Lancet Oncol.* **2004**, *5*, 600.
(375) Lipton, L.; Tomlinson, I. *Clin. Gastroenterol. Hepatol.* **2004**, *2*, 633.
(376) Lu, A. L.; Fawcett, W. P. *J. Biol. Chem.* **1998**, *273*, 25098.
(377) Pope, M. A.; David, S. S. *DNA Repair* **2005**, *4*, 91.
(378) Ma, H.; Lee, H. M.; Englander, E. W. *Nucleic Acids Res.* **2004**, *32*, 4332.
(379) Bai, H. B.; Jones, S.; Guan, X.; Wilson, T. M.; Sampson, J. R.; Cheadle, J. P.; Lu, A. L. *Nucleic Acids Res.* **2005**, *33*, 597.
(380) Wooden, S. H.; Bassett, H. M.; Wood, T. G.; McCullough, A. K. *Cancer Lett.* **2004**, *205*, 89.
(381) Manuel, R. C.; Hitomi, K.; Arvai, A. S.; House, P. G.; Kurtz, A. J.; Dodson, M. L.; McCullough, A. K.; Tainer, J. A.; Lloyd, R. S. *J. Biol. Chem.* **2004**, *279*, 46930.
(382) Volk, D. E.; House, P. G.; Thiviyanathan, V.; Luxon, B. A.; Zhang, S.; Lloyd, R. S.; Gorenstein, D. G. *Biochemistry* **2000**, *39*, 7331.
(383) Gogos, A.; Cillo, J.; Clarke, N. D.; Lu, A. L. *Biochemistry* **1996**, *35*, 16665.
(384) Chmiel, N. H.; Golinelli, M. P.; Francis, A. W.; David, S. S. *Nucleic Acids Res.* **2001**, *29*, 553.
(385) Li, X.; Wright, P. M.; Lu, A. L. *J. Biol. Chem.* **2000**, *275*, 8448.
(386) Manuel, R. C.; Lloyd, R. S. *Biochemistry* **1997**, *36*, 11140.
(387) Bernards, A. S.; Miller, J. K.; Bao, K. K.; Wong, I. *J. Biol. Chem.* **2002**, *277*, 20960.
(388) Lu, A. L.; Tsai-Wu, J. J.; Cillo, J. *J. Biol. Chem.* **1995**, *270*, 23582.
(389) Hollis, T.; Ichikawa, Y.; Ellenberger, T. *EMBO J.* **2000**, *19*, 758.
(390) Lingaraju, G. M.; Sartori, A. A.; Kostrewa, D.; Prota, A. E.; Jiricny, J.; Winkler, F. K. *Structure* **2005**, *13*, 87.
(391) Yang, H.; Clendenin, W. M.; Wong, D.; Demple, B.; Slupska, M. M.; Chiang, J. H.; Miller, J. H. *Nucleic Acids Res.* **2001**, *29*, 743.
(392) McCann, J. A. B.; Berti, P. J. *J. Biol. Chem.* **2003**, *278*, 29587.
(393) Pope, M. A.; Chmiel, N. H.; David, S. S. *DNA Repair* **2005**, *4*, 315.
(394) Pope, M. A.; Porello, S. L.; David, S. S. *J. Biol. Chem.* **2002**, *277*, 22605.
(395) Porello, S. L.; Leyes, A. E.; David, S. S. *Biochemistry* **1998**, *37*, 14756.
(396) Michaels, M. L.; Cruz, C.; Grollman, A. P.; Miller, J. H. *Proc. Natl. Acad. Sci. U.S.A.* **1992**, *89*, 7022.
(397) Radicella, J. P.; Clark, E. A.; Fox, M. S. *Proc. Natl. Acad. Sci. U.S.A.* **1988**, *85*, 9674.
(398) Tsai-Wu, J. J.; Liu, H. F.; Lu, A. L. *Proc. Natl. Acad. Sci. U.S.A.* **1992**, *89*, 8779.
(399) Sanchez, A. M.; Volk, D. E.; Gorenstein, D. G.; Lloyd, R. S. *DNA Repair* **2003**, *2*, 863.
(400) Francis, A. W.; David, S. S. *Biochemistry* **2003**, *42*, 801.
(401) Boon, E. M.; Pope, M. A.; Williams, S. D.; David, S. S.; Barton, J. K. *Biochemistry* **2002**, *41*, 8464.
(402) Leroy, J. L.; Charretier, E.; Kochoyan, M.; Gueron, M. *Biochemistry* **1988**, *27*, 8894.
(403) Leroy, J. L.; Kochoyan, M.; Huynhdinh, T.; Gueron, M. *J. Mol. Biol.* **1988**, *200*, 223.
(404) Coman, D.; Russu, I. M. *J. Biol. Chem.* **2005**, *280*, 20216.
(405) Bulychev, N. V.; Varaprasad, C. V.; Dorman, G.; Miller, J. H.; Eisenberg, M.; Grollman, A. P.; Johnson, F. *Biochemistry* **1996**, *35*, 13147.
(406) O'Shea, V. L.; Francis, A. S.; David, S. S. (University of Utah), personal communication.
(407) Francis, A. W.; Helquist, S. A.; Kool, E. T.; David, S. S. *J. Am. Chem. Soc.* **2003**, *125*, 16235.
(408) Sponer, J.; Leszczynski, J.; Hobza, P. *Biopolymers* **2001**, *61*, 3.
(409) Begley, T. J.; Haas, B. J.; Morales, J. C.; Kool, E. T.; Cunningham, R. P. *DNA Repair* **2003**, *2*, 107.
(410) Begley, T. J.; Cunningham, R. P. *Protein Eng.* **1999**, *12*, 333.
(411) Begley, T. J.; Haas, B. J.; Noel, J.; Shekhtman, A.; Williams, W. A.; Cunningham, R. P. *Curr. Biol.* **1999**, *9*, 653.
(412) Fondufe-Mittendorf, Y. N.; Harer, C.; Kramer, W.; Fritz, H. J. *Nucleic Acids Res.* **2002**, *30*, 614.
(413) Yang, H. J.; Fitz-Gibbon, S.; Marcotte, E. M.; Tai, J. H.; Hyman, E. C.; Miller, J. H. *J. Bacteriol.* **2000**, *182*, 1272.
(414) Hendrich, B.; Hardeland, U.; Ng, H. H.; Jiricny, J.; Bird, A. *Nature* **1999**, *401*, 301.
(415) Petronzelli, F.; Riccio, A.; Markham, G. D.; Seeholzer, S. H.; Stoerker, J.; Genuardi, M.; Yeung, A. T.; Matsumoto, Y.; Bellacosa, A. *J. Biol. Chem.* **2000**, *275*, 32422.
(416) Petronzelli, F.; Riccio, A.; Markham, G. D.; Seeholzer, S. H.; Genuardi, M.; Karbowski, M.; Yeung, A. T.; Matsumoto, Y.; Bellacosa, A. *J. Cell Physiol.* **2000**, *185*, 473.
(417) Wu, P. Y.; Qiu, C.; Sohail, A.; Zhang, X.; Bhagwat, A. S.; Cheng, X. D. *J. Biol. Chem.* **2003**, *278*, 5285.
(418) O'Rourke, E. J.; Chevalier, C.; Boiteux, S.; Labigne, A.; Ielpi, L.; Radicella, J. P. *J. Biol. Chem.* **2000**, *275*, 20077.
(419) Eichman, B. F.; O'Rourke, E. J.; Radicella, J. P.; Ellenberger, T. *EMBO J.* **2003**, *22*, 4898.
(420) Cao, C. Y.; Kwon, K.; Jiang, Y. L.; Drohat, A. C.; Stivers, J. T. *J. Biol. Chem.* **2003**, *278*, 48012.
(421) Bjelland, S.; Bjoras, M.; Seeberg, E. *Nucleic Acids Res.* **1993**, *21*, 2045.
(422) Alseth, I.; Osman, F.; Korvald, H.; Tsaneva, I.; Whitby, M. C.; Seeberg, E.; Bjoras, M. *Nucleic Acids Res.* **2005**, *33*, 1123.
(423) Habraken, Y.; Ludlum, D. B. *Carcinogenesis* **1989**, *10*, 489.
(424) Bjelland, S.; Seeberg, E. *Nucleic Acids Res.* **1987**, *15*, 2787.
(425) Bjelland, S.; Seeberg, E. *FEBS Lett.* **1996**, *397*, 127.
(426) Riazuddin, S.; Lindahl, T. *Biochemistry* **1978**, *17*, 2110.
(427) Thomas, L.; Yang, C. H.; Goldthwait, D. A. *Biochemistry* **1982**, *21*, 1162.
(428) Drohat, A. C.; Kwon, K.; Krosky, D. J.; Stivers, J. T. *Nat. Struct. Biol.* **2002**, *9*, 659.
(429) Tudek, B.; VanZeeland, A. A.; Kusmierek, J. T.; Laval, J. *Mutat. Res.—DNA Repair* **1998**, *407*, 169.
(430) Mattes, W. B.; Lee, C. S.; Laval, J.; O'Connor, T. R. *Carcinogenesis* **1996**, *17*, 643.
(431) Terato, H.; Masaoka, A.; Asagoshi, K.; Honsho, A.; Ohyama, Y.; Suzuki, T.; Yamada, M.; Makino, K.; Yamamoto, K.; Ide, H. *Nucleic Acids Res.* **2002**, *30*, 4975.
(432) Gasparutto, D.; Dherin, C.; Boiteux, S.; Cadet, J. *DNA Repair* **2002**, *1*, 437.
(433) Bjelland, S.; Birkeland, N. K.; Benneche, T.; Volden, G.; Seeberg, E. *J. Biol. Chem.* **1994**, *269*, 30489.
(434) Privezentzev, C. V.; Saparbaev, M.; Sambandam, A.; Greenberg, M. M.; Laval, J. *Biochemistry* **2000**, *39*, 14263.
(435) Masaoka, A.; Terato, H.; Kobayashi, M.; Honsho, A.; Ohyama, Y.; Ide, H. *J. Biol. Chem.* **1999**, *274*, 25136.
(436) Berdal, K. G.; Johansen, R. F.; Seeberg, E. *EMBO J.* **1998**, *17*, 363.
(437) Scharer, O. D.; Ortholand, J. Y.; Ganesan, A.; Ezaznikpay, K.; Verdine, G. L. *J. Am. Chem. Soc.* **1995**, *117*, 6623.
(438) Yamagata, Y.; Kato, M.; Odawara, K.; Tokuno, Y.; Nakashima, Y.; Matsushima, N.; Yasumura, K.; Tomita, K.; Ihara, K.; Fujii, Y.; Nakabeppu, Y.; Sekiguchi, M.; Fujii, S. *Cell* **1996**, *86*, 311.
(439) Minowa, O.; Arai, T.; Hirano, M.; Monden, Y.; Nakai, S.; Fukuda, M.; Itoh, M.; Takano, H.; Hippou, Y.; Aburatani, H.; Masumura, K.; Nohmi, T.; Nishimura, S.; Noda, T. *Proc. Natl. Acad. Sci. U.S.A.* **2000**, *97*, 4156.
(440) Bjoras, M.; Luna, L.; Johnsen, B.; Hoff, E.; Haug, T.; Rognes, T.; Seeberg, E. *EMBO J.* **1997**, *16*, 6314.
(441) Girard, P. M.; D'Ham, C.; Cadet, J.; Boiteux, S. *Carcinogenesis* **1998**, *19*, 1299.
(442) Nash, H. M.; Lu, R.; Lane, W. S.; Verdine, G. L. *Chem. Biol.* **1997**, *4*, 693.
(443) Leipold, M. D.; Muller, J. G.; Burrows, C. J.; David, S. S. *Biochemistry* **2000**, *39*, 14984.
(444) Nash, H. M.; Bruner, S. D.; Scharer, O. D.; Kawate, T.; Addona, T. A.; Sponner, E.; Lane, W. S.; Verdine, G. L. *Curr. Biol.* **1996**, *6*, 968.
(445) van der Kemp, P. A.; Thomas, D.; Barbey, R.; de Oliveira, R.; Boiteux, S. *Proc. Natl. Acad. Sci. U.S.A.* **1996**, *93*, 5197.
(446) Bruner, S. D.; Nash, H. M.; Lane, W. S.; Verdine, G. L. *Curr. Biol.* **1998**, *8*, 393.
(447) de Oliveira, R.; van der Kemp, P. A.; Thomas, D.; Geiger, A.; Nehls, P.; Boiteux, S. *Nucleic Acids Res.* **1994**, *22*, 3760.
(448) Senturker, S.; Auffret van der Kemp, P.; You, H. J.; Doetsch, P. W.; Dizdaroglu, M.; Boiteux, S. *Nucleic Acids Res.* **1998**, *26*, 5270.
(449) Eide, L.; Bjoras, M.; Pirovano, M.; Alseth, I.; Berdal, K. G.; Seeberg, E. *Proc. Natl. Acad. Sci. U.S.A.* **1996**, *93*, 10735.
(450) You, H. J.; Swanson, R. L.; Doetsch, P. W. *Biochemistry* **1998**, *37*, 6033.

(451) Hazra, T. K.; Izumi, T.; Maidt, L.; Floyd, R. A.; Mitra, S. *Nucleic Acids Res.* **1998**, *26*, 5116.
(452) Sartori, A. A.; Lingaraju, G. M.; Hunziker, P.; Winkler, F. K.; Jiricny, J. *Nucleic Acids Res.* **2004**, *32*, 6531.
(453) Bjoras, M.; Seeberg, E.; Luna, L.; Pearl, L. H.; Barrett, T. E. *J. Mol. Biol.* **2002**, *317*, 171.
(454) Banerjee, A.; Yang, W.; Karplus, M.; Verdine, G. L. *Nature* **2005**, *434*, 612.
(455) Bruner, S. D.; Norman, D. P.; Verdine, G. L. *Nature* **2000**, *403*, 859.
(456) Norman, D. P. G.; Bruner, S. D.; Verdine, G. L. *J. Am. Chem. Soc.* **2001**, *123*, 359.
(457) Chung, S. J.; Verdine, G. L. *Chem. Biol.* **2004**, *11*, 1643.
(458) Warner, H. R.; Demple, B. F.; Deutsch, W. A.; Kane, C. M.; Linn, S. *Proc. Natl. Acad. Sci. U.S.A.* **1980**, *77*, 4602.
(459) Katcher, H. L.; Wallace, S. S. *Biochemistry* **1983**, *22*, 4071.
(460) Fromme, J. C.; Verdine, G. L. *EMBO J.* **2003**, *22*, 3461.
(461) Katafuchi, A.; Nakano, T.; Masaoka, A.; Terato, H.; Iwai, S.; Hanaoka, F.; Ide, H. *J. Biol. Chem.* **2004**, *279*, 14464.
(462) Ali, M. M.; Hazra, T. K.; Hong, D.; Kow, Y. W. *DNA Repair* **2005**, *4*, 679.
(463) Aspinwall, R.; Rothwell, D. G.; Roldan-Arjona, T.; Anselmino, C.; Ward, C. J.; Cheadle, J. P.; Sampson, J. R.; Lindahl, T.; Harris, P. C.; Hickson, I. D. *Proc. Natl. Acad. Sci. U.S.A.* **1997**, *94*, 109.
(464) Miller, H.; Fernandes, A. S.; Zaika, E.; McTigue, M. M.; Torres, M. C.; Wente, M.; Iden, C. R.; Grollman, A. P. *Nucleic Acids Res.* **2004**, *32*, 338.
(465) Roldan-Arjona, T.; Anselmino, C.; Lindahl, T. *Nucleic Acids Res.* **1996**, *24*, 3307.
(466) Dizdaroglu, M.; Laval, J.; Boiteux, S. *Biochemistry* **1993**, *32*, 12105.
(467) Liu, X.; Roy, R. *J. Mol. Biol.* **2002**, *321*, 265.
(468) Hazra, T. K.; Muller, J. G.; Manuel, R. C.; Burrows, C. J.; Lloyd, R. S.; Mitra, S. *Nucleic Acids Res.* **2001**, *29*, 1967.
(469) Ikeda, S.; Biswas, T.; Roy, R.; Izumi, T.; Boldogh, I.; Kurosky, A.; Sarker, A. H.; Seki, S.; Mitra, S. *J. Biol. Chem.* **1998**, *273*, 21585.
(470) Dizdaroglu, M.; Karahalil, B.; Senturker, S.; Buckley, T. J.; Roldan-Arjona, T. *Biochemistry* **1999**, *38*, 243.
(471) Kuo, C. F.; McRee, D. E.; Fisher, C. L.; O'Handley, S. F.; Cunningham, R. P.; Tainer, J. A. *Science* **1992**, *258*, 434.
(472) Mazumder, A.; Gerlt, J. A.; Absalon, M. J.; Stubbe, J.; Cunningham, R. P.; Withka, J.; Bolton, P. H. *Biochemistry* **1991**, *30*, 1119.
(473) Miller, N.; Cerutti, P. *Proc. Natl. Acad. Sci. U.S.A.* **1968**, *59*, 34.
(474) Sugahara, M.; Mikawa, T.; Kumasaka, T.; Yamamoto, M.; Kato, R.; Fukuyama, K.; Inoue, Y.; Kuramitsu, S. *EMBO J.* **2000**, *19*, 3857.
(475) Sun, B.; Latham, K. A.; Dodson, M. L.; Lloyd, R. S. *J. Biol. Chem.* **1995**, *270*, 19501.
(476) Chetsanga, C. J.; Lindahl, T. *Nucleic Acids Res.* **1979**, *6*, 3673.
(477) Chetsanga, C. J.; Lozon, M.; Makaroff, C.; Savage, L. *Biochemistry* **1981**, *20*, 5201.
(478) Chung, M. H.; Kasai, H.; Jones, D. S.; Inoue, H.; Ishikawa, H.; Ohtsuka, E.; Nishimura, S. *Mutat. Res.* **1991**, *254*, 1.
(479) Tchou, J.; Kasai, H.; Shibutani, S.; Chung, M. H.; Laval, J.; Grollman, A. P.; Nishimura, S. *Proc. Natl. Acad. Sci. U.S.A.* **1991**, *88*, 4690.
(480) Hatahet, Z.; Kow, Y. W.; Purmal, A. A.; Cunningham, R. P.; Wallace, S. S. *J. Biol. Chem.* **1994**, *269*, 18814.
(481) Tchou, J.; Bodepudi, V.; Shibutani, S.; Antoshechkin, I.; Miller, J.; Grollman, A. P.; Johnson, F. *J. Biol. Chem.* **1994**, *269*, 15318.
(482) Boiteux, S.; Gajewski, E.; Laval, J.; Dizdaroglu, M. *Biochemistry* **1992**, *31*, 106.
(483) Castaing, B.; Boiteux, S.; Zelwer, C. *Nucleic Acids Res.* **1992**, *20*, 389.
(484) Asagoshi, K.; Yamada, T.; Terato, H.; Ohyama, Y.; Monden, Y.; Arai, T.; Nishimura, S.; Aburatani, H.; Lindahl, T.; Ide, H. *J. Biol. Chem.* **2000**, *275*, 4956.
(485) Zaika, E. I.; Perlow, R. A.; Matz, E.; Broyde, S.; Gilboa, R.; Grollman, A. P.; Zharkov, D. O. *J. Biol. Chem.* **2004**, *279*, 4849.
(486) Perlow-Poehnelt, R. A.; Zharkov, D. O.; Grollman, A. P.; Broyde, S. *Biochemistry* **2004**, *43*, 16092.
(487) Fedorova, O. S.; Nevinsky, G. A.; Koval, V. V.; Ishchenko, A. A.; Vasilenko, N. L.; Douglas, K. T. *Biochemistry* **2002**, *41*, 1520.
(488) Ishchenko, A. A.; Vasilenko, N. L.; Sinitsina, O. I.; Yamkovoy, V. I.; Fedorova, O. S.; Douglas, K. T.; Nevinsky, G. A. *Biochemistry* **2002**, *41*, 7540.
(489) Serre, L.; Pereira de Jesus, K.; Boiteux, S.; Zelwer, C.; Castaing, B. *EMBO J.* **2002**, *21*, 2854.
(490) Forsyth, W. R.; Antosiewicz, J. M.; Robertson, A. D. *Proteins* **2002**, *48*, 388.
(491) Fuxreiter, M.; Warshel, A.; Osman, R. *Biochemistry* **1999**, *38*, 9577.
(492) Dizdaroglu, M.; Burgess, S. M.; Jaruga, P.; Hazra, T. K.; Rodriguez, H.; Lloyd, R. S. *Biochemistry* **2001**, *40*, 12150.
(493) Bandaru, V.; Sunkara, S.; Wallace, S. S.; Bond, J. P. *DNA Repair* **2002**, *1*, 517.
(494) Hazra, T. K.; Kow, Y. W.; Hatahet, Z.; Imhoff, B.; Boldogh, I.; Mokkapati, S. K.; Mitra, S.; Izumi, T. *J. Biol. Chem.* **2002**, *277*, 30417.
(495) Rosenquist, T. A.; Zaika, E.; Fernandes, A. S.; Zharkov, D. O.; Miller, H.; Grollman, A. P. *DNA Repair* **2003**, *2*, 581.
(496) Hazra, T. K.; Izumi, T.; Venkataraman, R.; Kow, Y. W.; Dizdaroglu, M.; Mitra, S. *J. Biol. Chem.* **2000**, *275*, 27762.
(497) Golan, G.; Zharkov, D. O.; Fernandes, A. S.; Zaika, E.; Kycia, J. H.; Wawrzak, Z.; Grollman, A. P.; Shoham, G. *Acta Crystallogr., D: Biol. Crystallogr.* **2004**, *60*, 1476.
(498) Hollis, T.; Lau, A.; Ellenberger, T. *Mutat. Res.* **2000**, *460*, 201.
(499) O'Brien, P. J.; Ellenberger, T. *J. Biol. Chem.* **2004**, *279*, 9750.
(500) Saparbaev, M.; Laval, J. *Proc. Natl. Acad. Sci. U.S.A.* **1994**, *91*, 5873.
(501) Hitchcock, T. M.; Dong, L.; Connor, E. E.; Meira, L. B.; Samson, L. D.; Wyatt, M. D.; Cao, W. G. *J. Biol. Chem.* **2004**, *279*, 38177.
(502) Gros, L.; Maksimenko, A. V.; Privezentzev, C. V.; Laval, J.; Saparbaev, M. K. *J. Biol. Chem.* **2004**, *279*, 17723.
(503) Guliaev, A. B.; Hang, B.; Singer, B. *Nucleic Acids Res.* **2002**, *30*, 3778.
(504) Vallur, A. C.; Feller, J. A.; Abner, C. W.; Tran, R. K.; Bloom, L. B. *J. Biol. Chem.* **2002**, *277*, 31673.
(505) Xia, L. Q.; Zheng, L.; Lee, H. W.; Bates, S. E.; Federico, L.; Shen, B. H.; O'Connor, T. R. *J. Mol. Biol.* **2005**, *346*, 1259.
(506) Scharer, O. D.; Nash, H. M.; Jiricny, J.; Laval, J.; Verdine, G. L. *J. Biol. Chem.* **1998**, *273*, 8592.
(507) Lloyd, R. S. *Mutat. Res.*, in press.
(508) Dodson, M. L.; Michaels, M. L.; Lloyd, R. S. *J. Biol. Chem.* **1994**, *269*, 32709.
(509) Lloyd, R. S. *Mutat. Res.—DNA Repair* **1998**, *408*, 159.
(510) Morikawa, K.; Matsumoto, O.; Tsujimoto, M.; Katayanagi, K.; Ariyoshi, M.; Doi, T.; Ikehara, M.; Inaoka, T.; Ohtsuka, E. *Science* **1992**, *256*, 523.
(511) Vassylyev, D. G.; Kashiwagi, T.; Mikami, Y.; Ariyoshi, M.; Iwai, S.; Ohtsuka, E.; Morikawa, K. *Cell* **1995**, *83*, 773.
(512) McCullough, A. K.; Romberg, M. T.; Nyaga, S.; Wei, Y. F.; Wood, T. G.; Taylor, J. S.; Van Etten, J. L.; Dodson, M. L.; Lloyd, R. S. *J. Biol. Chem.* **1998**, *273*, 13136.
(513) Garvish, J. F.; Lloyd, R. S. *J. Biol. Chem.* **1999**, *274*, 9786.
(514) Smith, C. A.; Taylor, J. S. *J. Biol. Chem.* **1993**, *268*, 11143.
(515) Dizdaroglu, M.; Zastawny, T. H.; Carmical, J. R.; Lloyd, R. S. *Mutat. Res.—DNA Repair* **1996**, *362*, 1.
(516) Doi, T.; Recktenwald, A.; Karaki, Y.; Kikuchi, M.; Morikawa, K.; Ikehara, M.; Inaoka, T.; Hori, N.; Ohtsuka, E. *Proc. Natl. Acad. Sci. U.S.A.* **1992**, *89*, 9420.
(517) Nyaga, S. G.; Dodson, M. L.; Lloyd, R. S. *Biochemistry* **1997**, *36*, 4080.
(518) Hori, N.; Doi, T.; Karaki, Y.; Kikuchi, M.; Ikehara, M.; Ohtsuka, E. *Nucleic Acids Res.* **1992**, *20*, 4761.
(519) Iwai, S.; Maeda, M.; Shirai, M.; Shimada, Y.; Osafune, T.; Murata, T.; Ohtsuka, E. *Biochemistry* **1995**, *34*, 4601.
(520) Chepanoske, C. L.; Porello, S. L.; Fujiwara, T.; Sugiyama, H.; David, S. S. *Nucleic Acids Res.* **1999**, *27*, 3197.
(521) Stivers, J. T.; Pankiewicz, K. W.; Watanabe, K. A. *Biochemistry* **1999**, *38*, 952.
(522) Schrock, R. D., 3rd; Lloyd, R. S. *J. Biol. Chem.* **1991**, *266*, 17631.
(523) Meador, M. G.; Rajagopalan, L.; Lloyd, R. S.; Dodson, M. L. *J. Biol. Chem.* **2004**, *279*, 3348.
(524) Morikawa, K.; Ariyoshi, M.; Vassylyev, D. G.; Matsumoto, O.; Katayanagi, K.; Ohtsuka, E. *J. Mol. Biol.* **1995**, *249*, 360.
(525) Vassylyev, D. G.; Kashiwagi, T.; Mikami, Y.; Ariyoshi, M.; Iwai, S.; Ohtsuka, E.; Morikawa, K. *Protein Eng.* **1995**, *8*, 64.
(526) Manuel, R. C.; Latham, K. A.; Dodson, M. L.; Lloyd, R. S. *J. Biol. Chem.* **1995**, *270*, 2652.
(527) McCullough, A. K.; Scharer, O.; Verdine, G. L.; Lloyd, R. S. *J. Biol. Chem.* **1996**, *271*, 32147.

CR040461T